

ARGONNE NATIONAL LABORATORY
9700 South Cass Avenue
Argonne, Illinois 60439

VENUS: A Two-dimensional Coupled
Neutronics-Hydrodynamics Computer Program for
Fast-reactor Power Excursions

by

W. T. Sha* and T. H. Hughes**

Reactor Analysis and Safety Division

October 1970

*Now with Materials Science Division.

**Applied Mathematics Division.

ARGONNE NATIONAL LABORATORY
9700 South Cass Avenue
Argonne, Illinois 60439

VENUS: A Two-dimensional Coupled
Neutronics-Hydrodynamics Computer Program for
Fast-reactor Power Excursions

by

W. T. Sha* and T. H. Hughes**

Reactor Analysis and Safety Division

October 1970

*Now with Materials Science Division.

**Applied Mathematics Division.

THE NATIONAL LABORATORY
OF THE UNITED STATES
DEPARTMENT OF AGRICULTURE

RESEARCH REPORT NO. 100
BY J. H. HARRIS AND T. H. HARRIS

WASHINGTON, D. C.

1915

1915

U. S. GOVERNMENT PRINTING OFFICE
1915

TABLE OF CONTENTS

	<u>Page</u>
ABSTRACT	9
I. INTRODUCTION	9
II. MATHEMATICAL MODEL	10
A. Basic Assumptions	10
B. Neutronics	11
C. Hydrodynamics	13
1. Governing Equations	13
2. Derivation of Finite-difference Equations	14
3. Viscous Pressure	18
4. Numerical Stability	18
D. Energy Balance	19
E. Reactivity Attributes	19
1. Programmed Neutron-multiplication-factor Change	19
2. Doppler Broadening Feedback	20
3. Neutron-multiplication-factor Change due to Motion of Reactor Material	20
F. Equation of State	21
1. Equations of State for a Medium with Heat Source	23
2. Equations of State for a Medium without Heat Source	31
III. COMPARISON BETWEEN VENUS AND THE EXISTING METHODS	32
A. VENUS versus AX-1	32
B. VENUS versus Bethe-Tait-type Calculations	32
IV. DESCRIPTION OF COMPUTER PROGRAM	34
A. Curve Fitting for Material Reactivity Worth	34
B. Control of Time Step	35
C. Output Control Options	36
D. Options to Terminate the Program	36
E. Problem-size Limitations and Core-storage Requirements	37
F. Simplified Flow Diagram	38

TABLE OF CONTENTS

	<u>Page</u>
V. NUMERICAL RESULTS	39
A. Time-step Size and Mesh Setup	41
1. To Estimate the Time-step Size for a Given Mesh Setup	42
2. Effect of Mesh Size for a Given Time Step.	43
3. Variable Mesh Setup	46
B. Fundamental Difference between Energy-dependent and Energy-density-dependent Equations of State	47
C. Iteration between Power and Reactivity Feedbacks	47
VI. DISCUSSION AND CONCLUSIONS	48
APPENDIXES	
A. Energy- (or Temperature-) density-dependent Equation of State Developed by BNWL	51
1. Sodium Out or Incompressible Sodium	51
2. Compressible Sodium	54
B. Input Format	57
C. Sample Problems	66
1. Typical Input	66
2. Typical Output	77
ACKNOWLEDGMENT	111
REFERENCES	112

LIST OF FIGURES

<u>No.</u>	<u>Title</u>	<u>Page</u>
1.	Setup for Finite-difference Mesh.	15
2.	Calculated and Measured Vapor-pressure Curves.	24
3.	Temperature vs Vapor Pressure for EOS1 through EOS4. . . .	26
4.	Temperature vs Internal Energy for EOS1, EOS2, and EOS5. .	27
5.	Pressure vs Internal Energy for EOS5	27
6.	Pressure vs Internal Energy for EOS6	28
7.	Temperature vs Internal Energy for EOS6.	28
8.	Comparison of Energy Yield Obtained from MARS and VENUS	33
9.	Simplified Flow Diagram of VENUS Program.	39
10.	Geometrical Configuration and Power-density Distribution of Reactor I.	40
11.	Geometrical Configuration and Power-density Distribution of Reactor II	40
12.	Pressure vs Time at Core Center of Reactor I for Sodium-out Case.	42
13.	Pressure vs Time at Core Center of Reactor I for Sodium-in Case	42
14.	Various Mesh Setups Used in VENUS Calculation.	44
15.	Pressure vs Time at Core Center of Reactor II for Sodium-out Case.	44
16.	Pressure vs Time at Core Center of Reactor II for Sodium-in Case	44
17.	Pressure vs Time at Location 1 of Reactor II for Sodium-out Case.	44
18.	Pressure vs Time at Location 1 of Reactor II for Sodium-in Case	45
19.	Comparison between the "Extrapolation Technique" and the "Direct Iteration"	48
A.1.	Liquid Density of UO_2	52
A.2.	Pressure-Temperature Relationship for Sodium-in Case. . . .	53
A.3.	Schematic of Computational Procedure Used to Evaluate Slope of P-T Curve for Compressible Sodium	55

LIST OF FIGURES

<u>No.</u>	<u>Title</u>	<u>Page</u>
B.1.	Procedure to Input Feedback Reactivities	61
B.2.	Arrangement of Regionwise Coordinates	62
C.1.	Energy Release vs Time	109
C.2.	Effective Neutron Multiplication vs Time	109
C.3.	Reactivity Feedbacks due to Doppler and Material Motion vs Time	109
C.4.	Three-dimensional Pictorial Pressure Distribution at $t = 0$ sec.	110
C.5.	Distant-deformed Mesh Configuration at $t = 0.608$ msec	110

LIST OF TABLES

<u>No.</u>	<u>Title</u>	<u>Page</u>
I.	Critical Constants of UO_2	22
II.	Material Reactivity Worth for Reactor II	40
III.	Core Characteristics of Reactors I and II	41
IV.	Total Energy Yield and Excursion Time for Various Time-step Sizes	43
V.	Total Energy Yield and Excursion Time for Various Mesh Sizes	45
VI.	Comparison of Total Energy Yield and Excursion Time between Regular and Variable Mesh Setup	46

TABLE OF CONTENTS

1	1. Introduction
2	2. Objectives of the Study
3	3. Literature Review
4	4. Methodology
5	5. Results and Discussion
6	6. Conclusion
7	7. References
8	8. Appendix
9	9. Bibliography
10	10. Glossary
11	11. Index
12	12. Summary
13	13. Acknowledgments
14	14. Appendix A
15	15. Appendix B
16	16. Appendix C
17	17. Appendix D
18	18. Appendix E
19	19. Appendix F
20	20. Appendix G
21	21. Appendix H
22	22. Appendix I
23	23. Appendix J
24	24. Appendix K
25	25. Appendix L
26	26. Appendix M
27	27. Appendix N
28	28. Appendix O
29	29. Appendix P
30	30. Appendix Q
31	31. Appendix R
32	32. Appendix S
33	33. Appendix T
34	34. Appendix U
35	35. Appendix V
36	36. Appendix W
37	37. Appendix X
38	38. Appendix Y
39	39. Appendix Z
40	40. Appendix AA
41	41. Appendix AB
42	42. Appendix AC
43	43. Appendix AD
44	44. Appendix AE
45	45. Appendix AF
46	46. Appendix AG
47	47. Appendix AH
48	48. Appendix AI
49	49. Appendix AJ
50	50. Appendix AK
51	51. Appendix AL
52	52. Appendix AM
53	53. Appendix AN
54	54. Appendix AO
55	55. Appendix AP
56	56. Appendix AQ
57	57. Appendix AR
58	58. Appendix AS
59	59. Appendix AT
60	60. Appendix AU
61	61. Appendix AV
62	62. Appendix AW
63	63. Appendix AX
64	64. Appendix AY
65	65. Appendix AZ
66	66. Appendix BA
67	67. Appendix BB
68	68. Appendix BC
69	69. Appendix BD
70	70. Appendix BE
71	71. Appendix BF
72	72. Appendix BG
73	73. Appendix BH
74	74. Appendix BI
75	75. Appendix BJ
76	76. Appendix BK
77	77. Appendix BL
78	78. Appendix BM
79	79. Appendix BN
80	80. Appendix BO
81	81. Appendix BP
82	82. Appendix BQ
83	83. Appendix BR
84	84. Appendix BS
85	85. Appendix BT
86	86. Appendix BU
87	87. Appendix BV
88	88. Appendix BW
89	89. Appendix BX
90	90. Appendix BY
91	91. Appendix BZ
92	92. Appendix CA
93	93. Appendix CB
94	94. Appendix CC
95	95. Appendix CD
96	96. Appendix CE
97	97. Appendix CF
98	98. Appendix CG
99	99. Appendix CH
100	100. Appendix CI

VENUS: A Two-dimensional Coupled
Neutronics-Hydrodynamics Computer Program for
Fast-reactor Power Excursions

by

W. T. Sha and T. H. Hughes

ABSTRACT

A new computational model for fast-reactor disassembly analyses is presented. The model utilizes the space-independent neutronics, two-dimensional (RZ) Lagrangian hydrodynamics, and an energy-density-dependent equation of state. The reactivity feedbacks due to Doppler broadening and material motion are explicitly taken into account. This model can analyze both high- and low-density systems in contrast with the modified Bethe-Tait methods, which are valid only for the low-density systems. A unique feature of this model is its pointwise description of core material contents so that an appropriate equation of state corresponding to sodium-in and sodium-out conditions can be assigned. Another is its rigorous treatment of implosion effects at any arbitrary boundary surface, such as a void region surrounded by a nonvoid region or at the interface of two regions of a zoned core. The total energy release during a nuclear excursion calculated from this model is much lower (except for a completely voided core) than the values obtained from the modified Bethe-Tait methods.

I. INTRODUCTION

Evaluation of the safety of large fast breeder reactors has been the primary motivation for extensive theoretical investigation of power excursions. Although it is a major concern of the fast-reactor designer to prevent such an excursion under any adverse circumstance, it is nevertheless desirable to know the consequences of a power excursion. This report presents a method for estimating the magnitude of the energy released by a reactor undergoing a power excursion.

In general, there are three approaches to the analysis of reactor power excursions. The first uses space-independent reactor kinetics with a preassigned feedback reactivity to estimate the energy release. The second technique, known as Bethe-Tait analysis,¹ is analytical in nature,

and has been used to derive scaling laws and check numerical procedures. The following three major assumptions are made in Bethe-Tait analyses: (1) reactivity changes can be calculated by first-order perturbation theory; (2) the duration of the excursion is so short that expansion is negligible, thus permitting the time behavior of the pressure to be calculated by ignoring any change in the density; (3) the effects of wave propagation can be neglected. The third approach is to solve the system of governing time-space-dependent partial differential equations numerically by using a high-speed computer.²

The first method is the simplest. However, the feedback reactivity is not an "a priori" known function; therefore, the validity of this approach is very much in doubt. As for the second technique, a number of significant modifications³⁻⁶ have been made since Bethe and Tait's original paper appeared. The modified Bethe-Tait analysis is to date the most widely used method for reactor-disassembly study. However, the validity of this method is subject to the assumptions listed above. The third approach provides a much more accurate and complete model. However, obtaining a solution of the complete time-space-dependent coupled neutronic-hydrodynamic equations is no easy task. Experience with multigroup, time-space-dependent, two dimensional neutron-diffusion-theory calculations indicate that the direct numerical approach is very expensive and perhaps, at present, impractical for the "production-line" type of calculation. Recently, very active research has been launched to develop approximations⁷⁻¹³ to the exact time-space neutronic solution with much less computational effort. It is believed that until a very general and efficient approximating method is found, the third approach will not be extensively used in the analyses of severe power excursions.

The computational method presented in this report and used in the VENUS computer program is a compromise between the second and third approaches. It consists of space-independent neutronics and time-space-dependent Lagrangian hydrodynamics (RZ cylindrical geometry). The feedback due to Doppler broadening and reactor material motion (or disassembly) are explicitly taken into account. Thus, the computer time required for a typical power-excursion analysis is kept within a practical range (of the order of 10 min with an IBM-360 Model 75) and the reactivity-feedback mechanisms are treated with reasonable accuracy during the excursion. In short, it retains simplicity and yet provides essential information with reasonable accuracy.

II. MATHEMATICAL MODEL

A. Basic Assumptions

1. The power associated with each Lagrangian cell is assumed to be given by its original location in the mesh, a time-independent power distribution, and a space-independent time function calculated from the point-kinetics equations.

2. The material-reactivity worth of the Lagrangian cell is assumed to be given by its instantaneous location with respect to a time-independent distribution of reactivity worth. The reactivity changes are calculated from first-order perturbation theory based on the original configuration.

3. The adiabatic approximation is employed, i.e., no heat transfer is allowed between the fuel and nonfuel materials during the power excursion.

4. The finite-difference representation of the Lagrangian hydrodynamic equations, i.e., conservation of mass and momentum, will introduce a truncation error. As the Lagrangian mesh becomes severely distorted, this truncation error is greatly amplified. Thus, in order for the finite-difference representation to be valid, the extent of the mesh distortion must not be excessively large.

It is to be noted that assumptions 1, 2, and 3 are also employed in the modified Bethe-Tait calculations.⁵ The imposition of the assumptions 1 and 2 is mainly due to mathematical simplification and computational expedience, and they are justified by the argument that the gross movement of the core material is small. Assumption 3 is based upon the short duration of the disassembly power excursion. The last assumption is an inherent difficulty of the finite-difference formulation.

B. Neutronics

A one-energy-group, space-independent model is used to describe the neutron kinetics of the reactor. It is assumed that the reactor power distribution $Q(r, z, t)$ can be expressed as

$$Q(r(t), z(t), t) = n(t) \psi(r(0), z(0)),$$

where the power density $\psi(r, z)$ assigned to the Lagrangian mesh is assumed independent of time and is normalized initially such that

$\int_{\text{Volume}} \psi(r(0), z(0)) dV = 1$. The total power $n(t)$ is the solution of the following equations:

$$\frac{dn}{dt} = \frac{\rho^* - \beta}{\ell} n + \sum_{i=1}^I \lambda_i C_i; \quad (1)$$

$$\frac{dC_i}{dt} = \frac{\beta_i n}{\ell} - \lambda_i C_i, \quad (i = 1, 2, \dots, I), \quad (2)$$

where

ρ^* is the reactivity,

n is the neutron level which is proportional to the reactor power,

ℓ is the prompt-neutron generation time,

β_i is the delayed-neutron fraction of group i ,

C_i is the concentration of delayed-neutron precursor group i ,

λ_i is the decay time constant of the delayed-neutron precursor group i ,

and

I is the total number of delayed-neutron groups.

In most step-by-step integration methods for solving Eqs. 1 and 2 the previously calculated values of n are used to obtain the next value. Thus, to compute n^{k+1} , knowledge of n^k , n^{k-1} , and n^{k-2} is required, where superscripts k and $k+1$ denote the time-step sequence. These methods have the disadvantage that several initial values of n are needed in order to start the calculation. These initial values must be obtained by an auxiliary calculation. This disadvantage can be bypassed by using one of the Runge-Kutta procedures. However, the time step required by this method to yield accurate solutions is often found very restrictive.

The method used here for the solution of Eqs. 1 and 2 was formulated by Kaganove.¹⁴ It has the advantage of being self-starting and is numerically stable for relatively large time intervals. Kaganove's method is briefly described below.

Combining Eqs. 1 and 2 gives

$$\frac{dn}{dt} = \frac{\rho^*}{\ell} n - \sum_{i=1}^I \frac{dC_i}{dt}. \quad (3)$$

Integrating Eq. 3 over the time interval τ yields

$$n(\tau) - n^k = \int_{t^k}^{t^{k+\tau}} \frac{\rho^* n}{\ell} dt - \sum_{i=1}^I [C_i(\tau) - C_i^k], \quad (4)$$

where n^k and C_i^k are $n(t^k)$ and $C_i(t^k)$, respectively. Upon making the linear transformation $t' = t - t^k$, Eq. 4 becomes

$$n(\tau) - n^k = \int_0^{\tau} \frac{\rho^* n}{\ell} dt' - \sum_{i=1}^I [C_i(\tau) - C_i^k], \quad (5)$$

where $n(0) = n^k$ and $C_i(0) = C_i^k$.

The solution of Eq. 2 is

$$C_i(\tau) - C_i^k = -C_i^k(1 - e^{-\lambda_i \tau}) + \frac{\beta_i}{\ell} \int_0^\tau e^{-\lambda_i(\tau-t')} n \, dt'. \quad (6)$$

Substituting Eq. 6 into Eq. 5 yields

$$n(\tau) - n^k = \int_0^\tau \frac{\rho^* n}{\ell} dt' - \sum_{i=1}^I \frac{\beta_i}{\ell} \int_0^\tau e^{-\lambda_i(\tau-t')} n \, dt' + \sum_{i=1}^I C_i^k(1 - e^{-\lambda_i \tau}). \quad (7)$$

During the time interval under consideration, let n be represented by a second-order polynomial:

$$n = n^k + n_1 t' + n_2 (t')^2. \quad (8)$$

Substituting Eq. 8 into 7, with the condition that Eq. 7 be satisfied both at $\tau = \Delta t^{k+1}$ and at $\tau = \Delta t^{k+1}/2$, yields two linear equations with two unknowns n_1 and n_2 . Substituting values of n_1 and n_2 into Eq. 8 gives $n(t)$ for this time interval.

The reactivity ρ^* is the sum of the programmed reactivity and the reactivity feedbacks due to the Doppler broadening and the motion of the reactor material. A detailed discussion of reactivity will be presented in Sect. II.E.

C. Hydrodynamics

1. Governing Equations

The motion of the reactor materials is assumed to satisfy the equations of motion of a compressible, nonviscous fluid. In this report we consider the case of a cylindrical reactor with axial symmetry, that is, we assume that there is no motion in the azimuthal direction ϕ and that none of the properties of the system depend upon ϕ . Let the distance along the axis of symmetry from some fixed point be denoted by z , and let r denote the radial distance from the axis. Denote the Lagrangian coordinates by R and Z , and define the Lagrangian coordinates to be the position of the material at $t = 0$. The actual position of the materials at a later time are two of the dependent variables for which we must solve. The properties of the reactor motion are characterized by the density $\rho(R, Z, t)$, the pressure $P(R, Z, t)$, the temperature $T(R, Z, t)$, and the material velocities in radial, $u(R, Z, t)$, and axial direction, $v(R, Z, t)$.

If $\overline{\Delta V}$ denotes the volume of a fixed mass of material (small enough that it can be reasonably assumed to have uniform density), then conservation of mass states that

$$\rho = \rho_0 \frac{\Delta \bar{V}_0}{\Delta \bar{V}}, \quad (9)$$

where ρ_0 and $\Delta \bar{V}_0$ are the values of ρ and $\Delta \bar{V}$ at time $t = 0$. Thus, given a method of computing the volume of a Lagrangian mass from the displacements of its boundary, we can use the equation above to compute the density ρ . If (\cdot) denotes partial differentiation with respect to t with R and Z fixed, then the two equations of conservation of momentum are

$$\dot{u} \equiv \ddot{r} = -\frac{1}{\rho} \frac{\partial P}{\partial r}; \quad (10)$$

$$\dot{v} \equiv \ddot{z} = -\frac{1}{\rho} \frac{\partial P}{\partial z}, \quad (11)$$

where $P = p + q$, with p and q the pressure calculated from the equation of state and the pseudoviscosity pressure, respectively. The pseudoviscosity pressure will be discussed in Sect. II.C.3.

The boundary conditions used in the VENUS program are:

- a. Material on the axis of cylindrical symmetry is constrained to move only along the axis, but not away from the axis;
- b. The pressure at all the external reactor surfaces is assumed to be zero throughout the excursion (free surface boundary conditions).

2. Derivation of Finite-difference Equations

One of the principle difficulties in hydrodynamic calculations is the selection of a finite-difference representation of the spatial derivatives in the momentum equation. A number¹⁵⁻²⁰ of different expressions have appeared in the literature, each claiming certain advantages over the others. Herrmann²¹ evaluated the relative merits of many of the finite-difference representations and concluded that no one finite-difference method is clearly superior to the other. Accordingly, the selection of the finite-difference representation for this study was based upon minimizing the amount of computation.

Quantities are considered only at a finite number of locations in space, initially at distances ΔR and ΔZ apart. The initial R coordinate after the I th increment ΔR is denoted as R_I , and the initial Z coordinate after the J th increment ΔZ is denoted as Z_J . In effect, the material is covered by a finite coordinate grid which deforms with the material (see Fig. 1). Coordinates r and z at time t for the point R_I, Z_J are denoted $r_{I,J}$ and $z_{I,J}$.

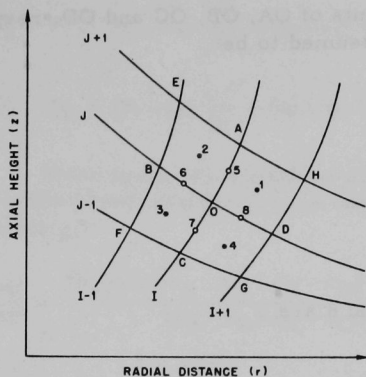


Fig. 1
Setup for Finite-difference Mesh

Although positions, velocities, and accelerations are considered only at the vertices of the finite-difference grid, densities and pressures are considered as an average over the cell and denoted by $\rho_{I+\frac{1}{2}, J+\frac{1}{2}}$, etc.

In developing the finite-difference equations it is considerably more convenient to use the notation shown in Fig. 1. The equations can later be translated into indicial notation.

The finite-difference representation of conservation of mass will be derived for the cell AHDO shown in Fig. 1. The current area of AHDO may be approximated by

$$A = \frac{1}{2} \{ (z_H - z_O)(r_D - r_A) + (r_H - r_O)(z_A - z_D) \}, \quad (12)$$

and the original area A_0 at time $t = 0$ is obtained from the same equation by replacing r and z by R and Z , respectively. For moderate distortions, the radius of the centroid of cell AHDO can be approximated by

$$\bar{r} = \frac{1}{4}(r_H + r_D + r_O + r_A), \quad (13)$$

and the initial centroid \bar{r}_0 can be found similarly. Thus the equation for conservation of mass can be written

$$\rho_{I+\frac{1}{2}, J+\frac{1}{2}} = \frac{\rho_{O, I+\frac{1}{2}, J+\frac{1}{2}} A_{O, I+\frac{1}{2}, J+\frac{1}{2}} \bar{r}_{O, I+\frac{1}{2}, J+\frac{1}{2}}}{A_{I+\frac{1}{2}, J+\frac{1}{2}} \bar{r}_{I+\frac{1}{2}, J+\frac{1}{2}}} \quad (14)$$

As was pointed out before, the finite-difference representation of the pressure-gradient terms in the momentum equations is the most difficult part of the numerical calculations in the hydrodynamics. The pressures are known at discrete points 1, 2, 3, and 4 surrounding point O (see Fig. 1). The pressure gradients at point O are to be evaluated.

Points 5, 6, 7, and 8 are the midpoints of OA, OB, OC and OD, respectively; the corresponding pressures are assumed to be

$$\begin{aligned}
 P_5 &= \frac{1}{2}(P_1 + P_2); \\
 P_6 &= \frac{1}{2}(P_2 + P_3); \\
 P_7 &= \frac{1}{2}(P_3 + P_4); \\
 P_8 &= \frac{1}{2}(P_4 + P_1).
 \end{aligned} \tag{15}$$

The coordinates of points 5, 6, 7, and 8 are

$$\begin{aligned}
 r_5 &= \frac{1}{2}(r_A + r_O); \\
 r_6 &= \frac{1}{2}(r_B + r_O); \\
 r_7 &= \frac{1}{2}(r_C + r_O); \\
 r_8 &= \frac{1}{2}(r_D + r_O); \\
 z_5 &= \frac{1}{2}(z_A + z_O); \\
 z_6 &= \frac{1}{2}(z_B + z_O); \\
 z_7 &= \frac{1}{2}(z_C + z_O); \\
 z_8 &= \frac{1}{2}(z_D + z_O).
 \end{aligned} \tag{16}$$

A Taylor's expansion between points O and 5, O and 6, O and 7, and O and 8 gives the following equations:

$$\begin{aligned}
 P_5 &= P_O + (r_5 - r_O) \frac{\partial P}{\partial r} + (z_5 - z_O) \frac{\partial P}{\partial z} + \dots; \\
 P_6 &= P_O + (r_6 - r_O) \frac{\partial P}{\partial r} + (z_6 - z_O) \frac{\partial P}{\partial z} + \dots; \\
 P_7 &= P_O + (r_7 - r_O) \frac{\partial P}{\partial r} + (z_7 - z_O) \frac{\partial P}{\partial z} + \dots; \\
 P_8 &= P_O + (r_8 - r_O) \frac{\partial P}{\partial r} + (z_8 - z_O) \frac{\partial P}{\partial z} + \dots.
 \end{aligned} \tag{17}$$

By neglecting the second- and higher-order terms in the above equations, and making a few algebraic operations, the following are obtained:

$$P_5 - P_7 = (r_5 - r_7) \frac{\partial P}{\partial r} + (z_5 - z_7) \frac{\partial P}{\partial z}; \quad (18)$$

$$P_6 - P_8 = (r_6 - r_8) \frac{\partial P}{\partial r} + (z_6 - z_8) \frac{\partial P}{\partial z}. \quad (19)$$

When these two equations are solved for $\partial P/\partial r$ and $\partial P/\partial z$, and the approximate expressions for the coordinates of the points 5, 6, 7, and 8 are used, we get

$$\frac{\partial P}{\partial r} = \frac{(P_1 - P_3)(z_A - z_C + z_B - z_D) - (P_2 - P_4)(z_A - z_C - z_B + z_D)}{(z_B - z_D)(r_A - r_C) - (z_A - z_C)(r_B - r_D)}; \quad (20)$$

similarly,

$$\frac{\partial P}{\partial z} = \frac{(P_1 - P_3)(r_A - r_C + r_B - r_D) - (P_2 - P_4)(r_A - r_C - r_B + r_D)}{(z_A - z_C)(r_B - r_D) - (z_B - z_D)(r_A - r_C)}. \quad (21)$$

Correspondingly, the finite-difference approximation of the momentum equations are

$$\begin{aligned} (\ddot{r})_{I,J} = & - \left\{ 4 / \left(\rho_{I+\frac{1}{2},J+\frac{1}{2}} + \rho_{I+\frac{1}{2},J-\frac{1}{2}} + \rho_{I-\frac{1}{2},J-\frac{1}{2}} + \rho_{I-\frac{1}{2},J+\frac{1}{2}} \right) \right\} \\ & \cdot \left\{ \left(P_{I+\frac{1}{2},J+\frac{1}{2}} - P_{I-\frac{1}{2},J-\frac{1}{2}} \right) \left(z_{I,J+1} - z_{I,J-1} + z_{I-1,J} - z_{I+1,J} \right) \right. \\ & - \left. \left(P_{I-\frac{1}{2},J+\frac{1}{2}} - P_{I+\frac{1}{2},J-\frac{1}{2}} \right) \left(z_{I,J+1} - z_{I,J-1} - z_{I-1,J} + z_{I+1,J} \right) \right\} / \\ & \left\{ \left(z_{I-1,J} - z_{I+1,J} \right) \left(r_{I,J+1} - r_{I,J-1} \right) - \left(z_{I,J+1} - z_{I,J-1} \right) \left(r_{I-1,J} - r_{I+1,J} \right) \right\}; \end{aligned} \quad (22)$$

$$\begin{aligned} (\ddot{z})_{I,J} = & - \left\{ 4 / \left(\rho_{I+\frac{1}{2},J+\frac{1}{2}} + \rho_{I-\frac{1}{2},J+\frac{1}{2}} + \rho_{I+\frac{1}{2},J-\frac{1}{2}} + \rho_{I-\frac{1}{2},J-\frac{1}{2}} \right) \right\} \\ & \cdot \left\{ \left(P_{I+\frac{1}{2},J+\frac{1}{2}} - P_{I-\frac{1}{2},J-\frac{1}{2}} \right) \left(r_{I,J+1} - r_{I,J-1} + r_{I-1,J} - r_{I+1,J} \right) \right. \\ & - \left. \left(P_{I-\frac{1}{2},J+\frac{1}{2}} - P_{I+\frac{1}{2},J-\frac{1}{2}} \right) \left(r_{I,J+1} - r_{I,J-1} - r_{I-1,J} + r_{I+1,J} \right) \right\} / \\ & \left\{ \left(r_{I-1,J} - r_{I+1,J} \right) \left(z_{I,J+1} - z_{I,J-1} \right) - \left(r_{I,J+1} - r_{I,J-1} \right) \left(z_{I-1,J} - z_{I+1,J} \right) \right\}. \end{aligned} \quad (23)$$

3. Viscous Pressure

Although shocks may not occur during a weak excursion, they can occur in severe excursions in which there is a large and rapid pressure buildup. A shock is a surface across which the pressure, density, internal energy, and velocity are all discontinuous.

In this study, shocks are handled by an approximation technique developed by von Neumann and Richtmyer.²² This technique, called "shock smearing," adds a dissipative term to the differential equations. The dissipative term may be regarded as representing viscosity. The "shock smearing" technique has only been proved physically valid when applied to problems of one-dimensional plane shock waves. Nevertheless, this technique has been employed successfully in two-dimensional hydrodynamics. The pressure in the VENUS program is the sum of the pressure calculated from the equation of state and the viscous pressure given by

$$q = \begin{cases} 1.44A\rho^3\left(\frac{\partial v}{\partial t}\right)^2 & \text{if } \frac{\partial v}{\partial t} < 0 \\ 0 & \text{if } \frac{\partial v}{\partial t} \geq 0, \end{cases} \quad (24)$$

where

A is the area of the cell;

v is the specific volume.

4. Numerical Stability

Because of the nonlinearity of the governing equations, a rigorous discussion of stability of the finite-difference equations cannot be carried out. The concept of space-dependent time-step selection, similar to the HAST1 program,²³ has been adopted in this study.

An extensively used stability index for equations of the type solved by VENUS has the form:²³

$$\left(\frac{\bar{W}}{1.2}\right)^2 = \frac{c^2}{A} \left(\frac{\Delta t}{1.2}\right)^2 + 4|\rho\Delta V|, \quad (25)$$

where \bar{W} is the "white" stability number, c is the velocity of sound, and ΔV is the change in the specific volume during the previous time step.

The time step size, Δt , is adjusted during the calculation so that the maximum value of $(\bar{W}/1.2)^2$ calculated for all the mesh cells remains within preset limits. The speed of sound is estimated for the equation of state being used at a given mesh position. The details of implementing this criterion are given in Ref. 24.

No time step during the excursion is allowed to be larger than the maximum and less than the minimum specified in the input.

D. Energy Balance

If $\Delta E(r, z, t)$ denotes the change in internal energy per unit volume of a fluid particle during the time interval Δt and $\Delta v(r, z, t)$ denotes its change in specific volume ($v = 1/\rho$) during Δt , the energy-balance equation is

$$\Delta E(r, z, t) = -P(r, z, t)\rho(r, z, t)\Delta v(r, z, t) + \Delta Q(r, z, t), \quad (26)$$

where $\Delta Q(r, z, t)$ is the nuclear energy gained during Δt .

E. Reactivity Attributes

Reactivity at any time is defined as follows:

$$\rho^*(t) = [\delta k_1(t) + \delta k_2(t) + \delta k_3(t)] / [1 + \delta k_1(t) + \delta k_2(t) + \delta k_3(t)], \quad (27)$$

where δk_1 is the programmed neutron-multiplication-factor change, δk_2 is the neutron-multiplication-factor change due to Doppler broadening, and δk_3 is the neutron-multiplication-factor change due to motion of reactor materials.

1. Programmed Neutron-multiplication-factor Change

The programmed multiplication-factor change is assumed to obey the following function of time:

$$\delta k_1(t) = \delta k_0 + At + Bt^2 \quad (0 \leq t \leq t_{\text{stop}});$$

$$\delta k_1(t) = \delta k_0 + At_{\text{stop}} + Bt_{\text{stop}}^2 = \text{constant} \quad (t > t_{\text{stop}}),$$

where

δk_0 is the initial change in neutron-multiplication factor;

A and B are coefficients of programmed multiplication-factor change;

and

t_{stop} designates the time when the neutron-multiplication-factor change stops.

The term proportional to t^2 and t_{stop}^2 can be used to account for the gravity collapse.

2. Doppler Broadening Feedback

The neutron-multiplication-factor change with respect to change of fuel temperature is given by

$$\frac{dk_2(t)}{dT} = aT^{-3/2}(t) + bT^{-1}(t) + \frac{c}{T^{1-m}(t)}, \quad (28)$$

where

a , b , and c are parameters known from experiments or other reactor calculations;

T is the core-averaged fuel temperature in $^{\circ}\text{K}$;

m is an integer.

In integrated form the above equation is

$$k_2(t) = -2aT^{-1/2}(t) + b \ln T(t) + (c/m)T^m(t) + \text{constant}. \quad (29)$$

In order to simplify the calculation, the fuel temperature is averaged regionwise, and $\delta k_2(t)$ becomes

$$\delta k_2(t) = \sum_{\text{region } i} \left(k_{2,i}(t) - k_{2,(\text{at } t=0),i} \right) W_i^*, \quad (30)$$

where

i designates the region;

W_i^* is the regional weighting factor for the Doppler effect. It accounts for the relative volume, and real and adjoint flux levels of the region.

3. Neutron-multiplication-factor Change due to Motion of Reactor Material

According to assumptions A and B in Sect. II.1, the material-reactivity-worth distribution (W) is independent of time, and the reactivity change due to motion of reactor material can be calculated by first-order perturbation theory. Therefore, upon making a Taylor's expansion, the worth of material after displacement Δr and Δz from its initial position can be written as

$$W(r,z) = W_0(r,z) + \frac{\partial W_0(r,z)}{\partial r} \Delta r + \frac{\partial W_0(r,z)}{\partial z} \Delta z + \dots, \quad (31)$$

where $W_0(r,z)$ is the initial material-reactivity-worth distribution.

If we can neglect the high-order terms in Eq. 31, the local change of reactivity per unit density is

$$W(r,z) - W_0(r,z) = \frac{\partial W_0}{\partial r} \Delta r + \frac{\partial W_0}{\partial z} \Delta z = \nabla W_0 \cdot \Delta X. \quad (32)$$

The total change of neutron-multiplication-factor due to the material motion over the reactor volume is

$$\delta k_3(t) = \int_V \rho(r,z,t) \nabla W_0(r,z) \cdot \Delta X(r,z,t) dV, \quad (33)$$

where

$W(r,z)$ is the material reactivity worth per unit density,

$\rho(r,z,t)$ is the material density,

ΔX is the material displacement vector at point r and z calculated by hydrodynamics, and its components are Δr and Δz ,

and

V designates reactor volume.

F. Equation of State

There is currently a great lack of quantitative knowledge about the equations of state of reactor materials and a wide diversity of opinion about the best way to approximate this information. As a result, it is not possible to provide in VENUS a single equation of state (or even a single general form for the equation of state with input parameters) that would be useful and acceptable to all users. As different applications of the code have arisen, equations of state suitable to those applications have been added and retained in the code. This is relatively easy to do, and it is anticipated that in many cases the user will delete the existing ones to make room for ones of his own choice. The following gives the general description of the equations of state in the code at present and some brief background on their origin.

The equation of state plays an important role in estimating the energy release of a fast reactor power excursion. It serves as a bridge between the neutronics and the hydrodynamics. Up to now, very little experimental data on reactor fuel materials are available to aid in establishing the functional

dependence of pressure, energy (or temperature), and material density in the range of interest encountered in reactor-disassembly analyses. It has been common practice to estimate the physical properties of the fuel by extrapolating from experimental data available either at very low or very high temperatures.

The principle of corresponding states²⁵ is the most widely used method to estimate functional dependence of pressure, energy (or temperature), and density. This principle states that substances are characterized by their thermodynamic critical properties: critical pressure (p_c), critical temperature (T_c), and critical volume (V_c), and that materials at the same reduced pressure, temperature, and volume will have similar behavior. The reduced pressure, temperature, and volume are defined as the ratio of the actual pressure, temperature, and volume to the critical pressure, temperature, and volume, respectively. It has been shown²⁶ that several substances deviate significantly from this principle. However, in view of the lack of any better method, the procedure will provide at least an estimate of the quantities desired.

The choice of critical constants can appreciably alter the equation of state derived from the corresponding-states principle. Both Miller²⁷ and Robbins²⁸ have investigated the possible ranges of constants and obtained quite large limits of their values. Values of critical constants for UO_2 as suggested by different investigators are listed in Table I.

TABLE I. Critical Constants of UO_2

	Menzies ²⁹	Miller ²⁷	Meyer ³⁰
Critical pressure, atm	2000	1230	1915
Critical temperature, °K	8000	9115	7300
Critical volume, cm^3/mol	90	170	85

In this report the only fuel material considered is UO_2 or a mixture with PuO_2 . Since a relatively small amount of PuO_2 will be present in the mixed-oxide fuel and no experimental data are available, the physical properties of PuO_2 are assumed to be the same as UO_2 .

If sodium and other nonfuel constituents are considered as inert materials, their presence and absence are assumed to influence the pressure only because they occupy space that is thereby unavailable for fuel expansion. These nonfuel materials can be treated as either compressible or noncompressible. In general, the equation of state of core materials may be written in the following three coupled equations:

$$p(t) = f_1(E(t), \rho_f(t)) = f_2(T(t), \rho_f(t)); \quad (34)$$

$$\rho_i(t) = \rho_{i,0} \left[\frac{p(t)B'}{B_0} + 1 \right] \frac{1}{B'} \approx \rho_{i,0} \exp[\alpha_i(p(t) - p_0)]; \quad (35)$$

$$\rho_f(t) = \frac{M_f}{V_T(t) - \sum_i \frac{M_i}{\rho_i(t)}} \quad (36)$$

where

p and T are the pressure and temperature;

ρ_i , M_i , and α_i are the densities, masses, and compressibilities of the nonfuel materials,

ρ_f and M_f are the density and mass of the fuel;

p_0 and $\rho_{i,0}$ are the initial pressure and initial density of the nonfuel materials, respectively;

B_0 is the bulk modulus at zero pressure;

B' is $\partial B / \partial p$,

V_T is the total mesh volume enclosing constants M_i and M_f in the Lagrangian coordinates.

The spatial variables have been suppressed in Eqs. 34-36.

For brevity, the equations of state employed in the reactor-disassembly analysis may be classified into two categories; one is that for the medium with heat source, and the other is for the medium without heat source. The former refers to core regions and the latter to blankets* or reflectors. All the equations of state can be described in terms of Eqs. 34-36.

1. Equations of State for a Medium with Heat Source

Equations of state for the medium with heat source may further be generalized into two broad classes: energy-dependent and energy-density-dependent. A number of equations of state have been incorporated into the VENUS computer program, and each is described below.

a. Energy-dependent Equation of State. The energy-dependent equation of state gives an equilibrium vapor pressure as a function of temperature at constant volume. In general such an equation is of the form

$$p(r, z, t) = A \exp \left[B + \frac{C}{T(r, z, t)} + D \ln T(r, z, t) \right], \quad (37)$$

*Heat generation per unit volume in the reactor blanket is much smaller than in the core.

where A, B, C, and D are fitting parameters. Ackermann's³¹ and Ohse's³² vapor-pressure measurements are widely used in evaluating these parameters.

Vapor-pressure curves, using the reduced vapor-pressure equation of Riedel,²⁵ are presented in Fig. 2, for the Menzies²⁹ and Miller²⁷ critical constants (the Meyer³⁰ constants yielded values approximately the same to those of Menzies) and also the analytic fit to the data of Ackermann³¹ and Ohse.³² As can be seen from Fig. 2, the vapor pressure with Menzies' constants agrees reasonably well with the experiment whereas Miller's constants yield lower values.

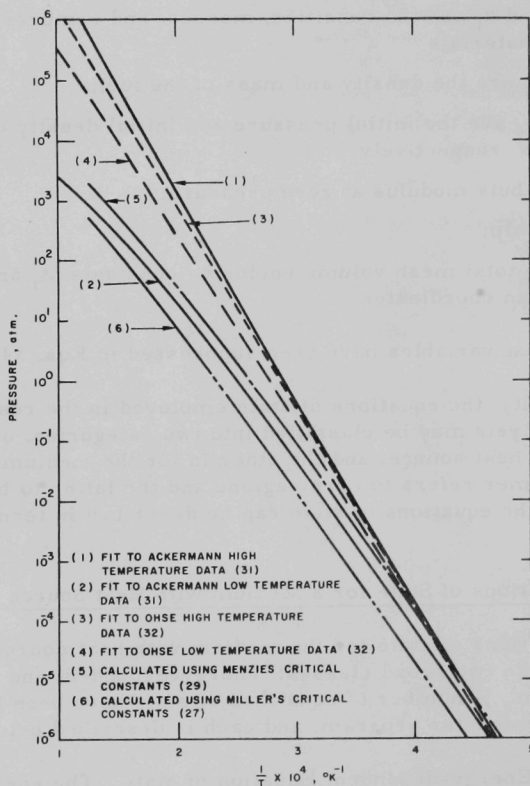


Fig. 2. Calculated and Measured Vapor-pressure Curves

All energy-dependent equations of state assume that the fuel density remains constant throughout an excursion, i.e., $\rho_f(r,z,t) = \rho_f(r,z,0)$, and only Eq. 34 is used. It is to be noted that Eq. 37 is a special

case of Eq. 34. The following five energy-dependent equations have been programmed into VENUS; they are designated in this report by EOSN, where N = 1, 2, ... :

$$\text{EOS1}^{29} \quad p = \exp[69.979 - (76800/T) - 4.34 \ln T]$$

$$\text{EOS2}^{33,34} \quad p = 10^6 \exp[55.455 - (7884/T) - 4.2808 \ln T]$$

$$\text{EOS3}^{35} \quad p = 4.398 \times 10^{14} \exp(-7118/T)$$

$$\text{EOS4}^{35} \quad p = 2.1925 \times 10^{11} \exp(-43957/T)$$

$$\text{EOS5}^{36} \quad p_1 = 10^9 \exp[2.1 + 1.054\rho_f^{2/3} - (5.3 \times 10^5/U)]$$

$$p_2 = 2.7 \times 10^{11} \exp(-7.7 \times 10^5/U)$$

$$p_3 = 5.7 \times 10^8 \exp\{-[8.12 + 2.56(\rho_f - 2.5) - 0.11(\rho_f - 2.5)^2]$$

$$[(10^5/U) - 0.8]\}$$

$$\text{a. If } \rho_f < 2.5 \text{ and } p_1 < p_2: p = p_1$$

$$\text{b. If } \rho_f < 2.5 \text{ and } p_1 \geq p_2: p = p_2$$

$$\text{c. If } \rho_f \geq 2.5 \text{ and } U < 1.25 \times 10^5: p = p_2$$

$$\text{d. If } \rho_f > 2.5 \text{ and } 1.25 \times 10^5 \leq U < 1.667 \times 10^5: p = \text{Min}(p_1, p_3)$$

$$\text{e. If } \rho_f \geq 2.5 \text{ and } U \geq 1.667 \times 10^5: p = p_1$$

$$\text{If } T < T_{\text{melt}}: T = T_0 + (U/26)$$

$$\text{If } T \geq T_{\text{melt}} \text{ and } U \leq 1.43 \times 10^5: T = \text{Max}(T_{\text{melt}}, T_1)$$

$$\text{If } T > T_{\text{melt}} \text{ and } U > 1.43 \times 10^5: T = (U/14) - 5290,$$

where

$$T_1 = 455 + (U/32), \quad U_0 = 27T_0 - H_{\text{fuse}},$$

$$T_{\text{melt}} = \text{Fuel-melting temperature,}$$

$$\rho_f = \rho_{f,0}.$$

All pressures and temperatures are in dynes/cm² and °K, respectively, and U is the internal energy in cal/g-mol.

EOS1 was developed by United Kingdom Atomic Energy Authority (UKAEA), using the Menzies critical constants. EOS2 originated at Battelle Northwest Laboratory and utilizes Christensen's³⁴ temperature-density relationship. The detailed description of this equation of state can be found in Appendix A. Both EOS3 and EOS4 were specifically designed for the FFTF disassembly analysis by Westinghouse Advanced Reactor Division (WARD); accordingly, their application is limited to reactors with characteristics similar to those of the FFTF core. EOS5 was originally developed by APDA. Recently R. B. Nicholson and J. F. Jackson have refitted the data

used in Ref. 36 so that the new fit will give accurate results over the range of fuel densities from ~ 1.5 to 5 g/cc and energy up to about 7×10^5 cal/g-mol. The APDA data were calculated from corresponding states using initial constants estimated from Miller and Ackermann's high-temperature measurements.

Figure 3 presents temperature-versus-vapor-pressure relationships for EOS1 through EOS4. For a given temperature, EOS1 yields higher pressure than EOS2; in general, EOS3 and EOS4 give upper and lower bounds of pressure among all these equations of state in the high-temperature range. Plots of internal energy versus temperature are shown in Fig. 4 for EOS1, EOS2, and EOS5. The latter gives a much higher temperature than the others at high internal energies. Figure 5 presents the functional dependence of pressure, energy, and reduced volume for EOS5, which uses a critical density of 3.47 g/cc, whereas a value of 3.0 g/cc is used in the others. The curves with reduced specific volumes $V_r = 0.694$ and $V_r = 1.1567$ in Fig. 5 correspond to the same fuel temperature as those with $V_r = 0.6$ and $V_r = 1.0$ in Figs. 6 and 7 (see below).

The internal-energy scale in Figs. 4 and 5 is normalized to $U = 0$ at 0°C . The heat of fusion used for all the cases was 0.28 kJ/g.

b. Energy-density-dependent Equation of State. Most core-disassembly calculations to date assume that the core is completely voided

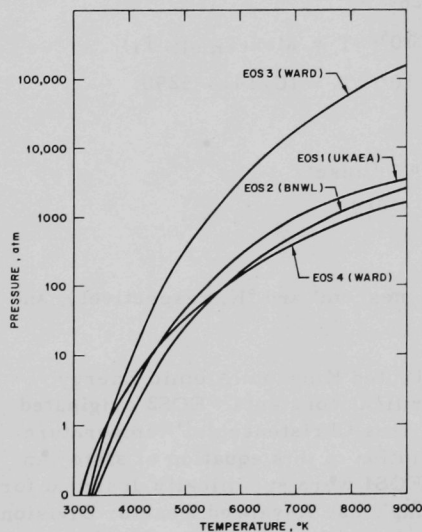


Fig. 3. Temperature vs Vapor Pressure for EOS1 through EOS4

of sodium. The justification of this assumption, of course, is to be conservative (i.e., more energy yield). A more acceptable assumption is that the core is partially voided, at least, at the initiation of a disassembly accident. The presence of sodium coolant as well as structural steel during the disassembly phase can significantly decrease the volume available to the fuel. Thus, as the energy (or temperature) of the system increases, the liquid-phase fuel expands to fill all available volume. Any additional energy increase can result in a very high pressure. The functional relationship between the pressure, energy, and reduced volume as calculated by Menzies is presented in Figs. 6 and 7, which are reproduced here directly from Ref. 29.

All the energy-density-dependent equations of state use

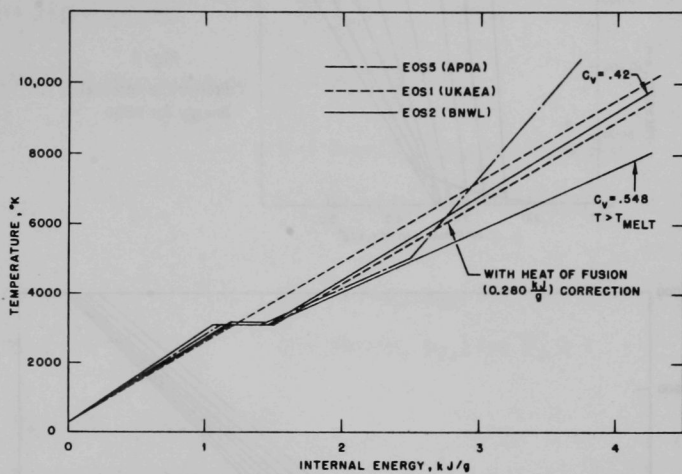


Fig. 4. Temperature vs Internal Energy for EOS1, EOS2, and EOS5

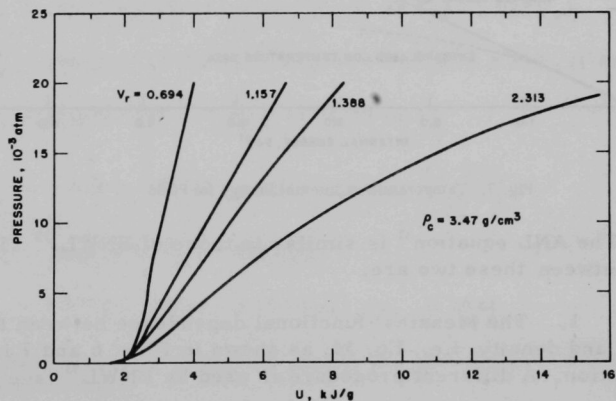


Fig. 5. Pressure vs Internal Energy for EOS5

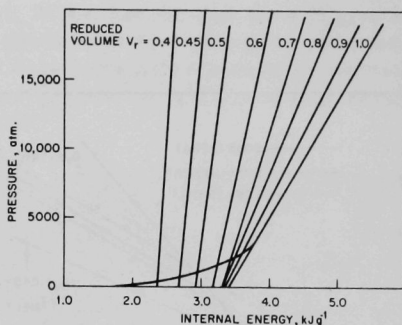


Fig. 6
Pressure vs Internal
Energy for EOS6

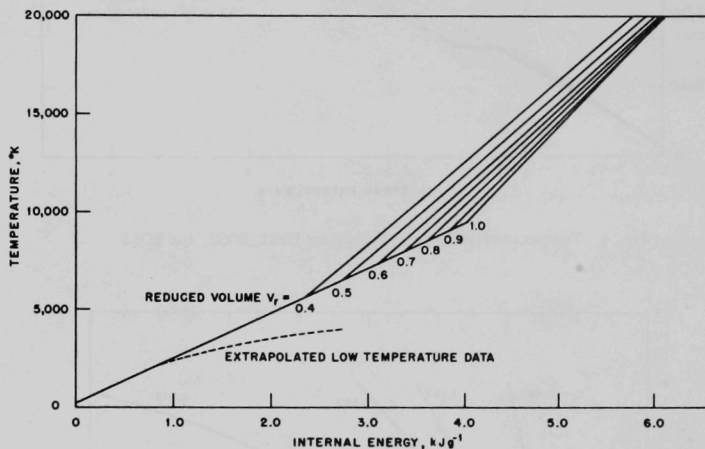


Fig. 7. Temperature vs Internal Energy for EOS6

Eqs. 34-36. The ANL equation³⁷ is similar to those of BNWL.³³ The basic differences between these two are:

1. The Menzies' functional dependence between the pressure, energy, and density, i.e., Eq. 34, as shown in Figs. 6 and 7 is used in ANL's equation. A different procedure is used by BNWL³³ (see Appendix A).
2. All nonfuel materials are considered to be compressible; in BNWL's version only sodium is considered compressible.
3. An iterative solution of Eqs. 34-36 is obtained in ANL's equation. An approximate solution to avoid iteration is used by BNWL (see Appendix A).

The ANL and the BNWL energy-density-dependent equations are designated as EOS6 and EOS7, respectively. A brief description of each is given below.

$$\text{EOS6 (ANL) At } l\text{th time step } U = U_0 + \sum_{i=1}^I \Delta U_i \quad (38)$$

$$T = \text{Max}(T_v, T_{\ell 1}) \text{ for } V_r \leq 0.6$$

$$T = \text{Max}[T_v, \text{Min}(T_{\ell 1}, T_{\ell 2})] \quad (39)$$

$$\text{for } V_r > 0.6$$

$$p = \text{Max}(p_v, p_{\ell 1}) \text{ for } V_r \leq 1$$

$$p = \text{Max}(p_v, p_{\ell 2}) \text{ for } V_r > 1 \quad (40)$$

where

$$U_0 = (T_0 - 273)/(2287);$$

$$T_0 = \text{Initial temperature};$$

$$T_v = 273 + 2287U;$$

$$T_{\ell 1} = (4272.5 - 1003V_r + 1699V_r^2)(U - 0.237 - 1.882V_r);$$

$$T_{\ell 2} = [4272.5 - (1003 \times 0.6) + (1699 \times 0.6^2)][U - 0.237 - (1.882 \times 0.6)];$$

$$p_v = \text{Exp}[69.979 - (76800/T) - 4.34 \ln T];$$

$$p_{\ell 1} = 1.554 \times 10^{12} \left(U - 3.59 + 0.119V_r + \frac{0.0767}{V_r^3} \right)$$

$$\exp(-9.67V_r + 4.445V_r^2);$$

$$p_{\ell 2} = 10^{10}(U - 3.2213 - 0.173V_r)(1.9V_r - 0.704).$$

The subscripts v and ℓ designate fuel in the two-phase and single-phase regions, respectively.

Equations 38-40 are analytical fits (due to R. B. Nicholson and J. F. Jackson) to the corresponding state of Menzies as shown in Figs. 6 and 7. These expressions adequately fit his data throughout its entire range of reduced specific volumes from 0.4 to 1.0. They appear to be reasonably acceptable for extrapolation to reduced volumes slightly below 0.4 and slightly larger than 1.0. It is to be noted that these analytical fits have a much wider range of applicability than the original Menzies' fit.

If the Murnaghan equation is used to compute the densities of sodium and stainless steel as function of pressure, the parameters associated with Eq. 35 must be defined. We chose the following values:³⁸

$$B'_{Na} = 3.59;$$

$$B_{0,Na} = 74.8 - 0.050T_{Na} + 9.71 \times 10^{-6} T_{Na}^2;$$

$$B'_{ss} = 5.0;$$

$$B_{0,ss} = 508 + 4.3T_{ss} - 5.53 \times 10^{-3} T_{ss}^2,$$

where subscripts Na and ss designate sodium and stainless steel.

Equations 38-40 coupled with Eqs. 35 and 36 form a set of equations which are solved at each time step and spatial mesh position by a direct iterative scheme.

Results from MELT-II-VENUS^{39,40} indicate that a significant portion of the core is below the melting temperature at the initiation of a disassembly calculation; therefore, the heat of fusion must be included in calculations for a power transient. Since the heat of fusion was not accounted for in the original Menzies corresponding-state calculations, the following modifications were made.

If $T < T_{melt}$, the same procedure is used as outlined before without any modifications to the heat of fusion.

If $T \geq T_{melt}$ and $U_{melt} \leq U \leq U_{melt} + H_{fusion}$, then $T = T_{melt}$; $U = U_{melt} = (T_{melt} - 273)/2287$ and $p = \text{Max}(p_v, p_{\ell 1})$ for $V_r \leq 1$ and $p = \text{Max}(p_v, p_{\ell 2})$ for $V_r > 1$.

Both T_{melt} and U_{melt} values are used for the pressure calculations, where U_{melt} and H_{fusion} are defined as the internal energy required to raise the temperature to the melting point and the heat of fusion, respectively.

If $T > T_{melt}$ and $U > U_{melt} + H_{fusion}$, an adjustment in energy scale is made, i.e., $U' = U - H_{fusion}$. The calculation then proceeds using the shifted internal energy U' in place of U in the temperature and pressure equations.

For a description of EOS7, see Appendix A.

It is to be noted that both EOS5 and EOS6 have built-in energy-temperature relationships. However, this caloric dependence can be adjusted through the input of specific heat when using the other equations of state.

2. Equations of State for a Medium without Heat Source

All the equations of state that have been discussed so far are limited to the core regions in which significant internal heat generation occurs. In regions such as blankets or reflectors, there is a smaller amount of heat generation or no heat generation, and a somewhat different approach is employed in computing the pressures. It is assumed that the pressures generated in these regions are due to the compression resulting from the mesh distortion or the propagation of shock waves. The equation of state for the blanket or the reflector used here is essentially Eq. 35, and it may be simplified to the following form:

$$p(t) = \text{Max}(p_1(t), 0), \quad (41)$$

where

$$p_1(t) = p_0 + \frac{1}{\bar{\alpha}} \frac{\rho(t) - \rho_0}{\rho_0},$$

with

$$\bar{\alpha} = \sum_i \frac{\delta V_i}{\rho(t)_i C_i^2};$$

δV_i the volume fraction of i th material;

ρ_i the density of i th material;

C_i the velocity of sound in i th material.

The presence of void space in the blanket or reflector is not considered in the above formulation. A provision has been made to account for this in the following manner:

$$\text{If } \frac{\rho(t) - \rho_0}{\rho_0} \leq \epsilon, \text{ then } p = 0.$$

$$\text{If } \frac{\rho(t) - \rho_0}{\rho_0} > \epsilon, \text{ then } p(t) = \text{Max}(p_1(t), 0), \quad (42)$$

where ϵ is the void fraction in blanket or reflector, and

$$p_1(t) = p_0 + \frac{1}{\bar{\alpha}} \left(\frac{\rho(t) - \rho_0}{\rho_0} - \epsilon \right).$$

III. COMPARISON BETWEEN VENUS AND THE EXISTING METHODS

A. VENUS versus AX-1 (Ref. 2)

The following are three principal differences between the VENUS and the AX-1 programs:

1. VENUS is two-dimensional and AX-1 is one-dimensional.
2. VENUS accounts for the Doppler-reactivity feedback.
3. In VENUS neutronics, the reactivity changes due to material motion are calculated from perturbation theory, whereas in AX-1 the reactivity is periodically recalculated for the distorted core by using neutron-transport theory as the disassembly progresses.

B. VENUS versus Bethe-Tait-type Calculations³⁻⁶

As pointed out before, the most widely used method for estimating the total energy generation during a disassembly accident is the Bethe-Tait type of calculation. The method presented in this report has the following three distinct advantages over the Bethe-Tait and the modified Bethe-Tait analyses:

1. The Bethe-Tait and the modified Bethe-Tait analysis methods fail to account for the effect on pressure of changes in fuel density during the excursion. Pressure can rise and fall extremely rapidly with small changes in density when the fuel density is high, as for "sodium-in" accident conditions, or if the core is assumed collapsed with high density following meltdown. Also in zoned core systems there can be large local density changes near a zone boundary during the course of the excursion. If the reactor accident under analysis should require this type of density-dependent pressure relation, the Bethe-Tait method cannot perform a meaningful disassembly calculation. That VENUS has overcome this limitation represents a major improvement in the ability to make calculations for severe disassemblies.

VENUS also computes the development of momentum as a function of position. This information can be used to estimate conversion of nuclear energy to reactor damage including missile damage.

2. Since the density is computed explicitly as a function of time, an energy- (or temperature-) density-dependent equation of state can readily be employed.

3. Another advantage is that the use of Lagrangian coordinates in the VENUS program provides detailed information on the motion of the

reactor materials during the excursion. This information is essential to the basic understanding of the mechanics of the accident and is vital to the assessment of possible damage to the surrounding structures.

As a consequence of the advantages mentioned above, the method presented in this report is applicable to relatively slow excursion problems and high-density systems. In particular, two unique features are provided by the VENUS program. One is the pointwise description of core material contents and temperature. Thus, an appropriate equation of state can be assigned accordingly (such as sodium-in and sodium-out equations of state). Another is its treatment of implosion at any arbitrary boundary surface (such as the voided region surrounded by the nonvoided region).

Figure 8 presents the core configuration and the predicted energy yields during two excursions as obtained from the MARS⁵ (Bethe-Tait-type model) and the VENUS programs. As is expected, the agreement is good for the low-density system ($\rho = 3.496 \text{ g/cm}^3$).

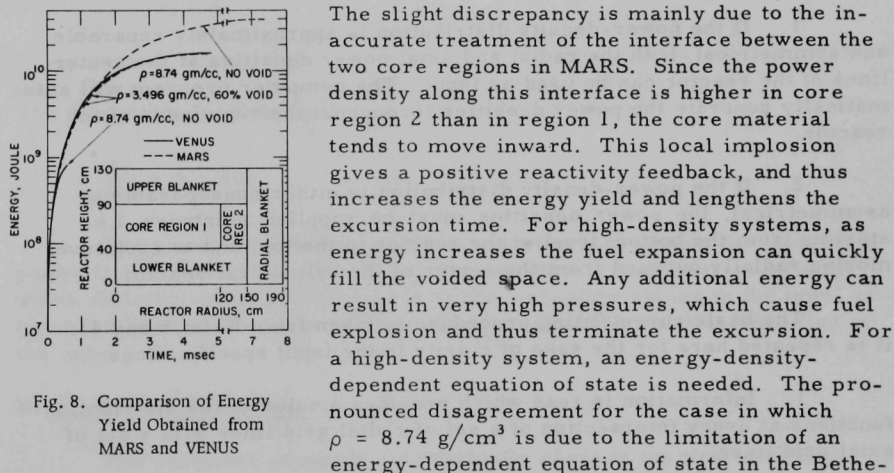


Fig. 8. Comparison of Energy Yield Obtained from MARS and VENUS

The slight discrepancy is mainly due to the inaccurate treatment of the interface between the two core regions in MARS. Since the power density along this interface is higher in core region 2 than in region 1, the core material tends to move inward. This local implosion gives a positive reactivity feedback, and thus increases the energy yield and lengthens the excursion time. For high-density systems, as energy increases the fuel expansion can quickly fill the voided space. Any additional energy can result in very high pressures, which cause fuel explosion and thus terminate the excursion. For a high-density system, an energy-density-dependent equation of state is needed. The pronounced disagreement for the case in which $\rho = 8.74 \text{ g/cm}^3$ is due to the limitation of an energy-dependent equation of state in the Bethe-Tait-type model used in MARS. In high-density systems, as energy is added the solid and liquid fuel expansion can fill the void space and produce high pressures before there is a significant fuel vapor pressure. The equation of state then becomes strongly density dependent. In the case $\rho = 8.74 \text{ g/cm}^3$ in Fig. 8, the MARS calculation was done using the saturated vapor pressure. This resulted in the pronounced disagreement evident in the figure. It should be noted that one could have altered the constants in the expression for the saturated vapor pressure or revised the equation of state in MARS to give a better approximation to the pressure at $\rho = 8.74 \text{ g/cm}^3$. If this is done, a significant improvement in estimating of the energy release for high-density systems calculated by MARS is expected.

IV. DESCRIPTION OF COMPUTER PROGRAM

Because the computer time required for a typical reactor-excursion problem is reasonable (approximately 10 min) with the IBM-360 Model 75 and core storage is manageable, not much efforts were given to optimizing the computer time and conserving storage by using shortcuts or clever programming. Consequently, there may be instances where the program is somewhat inefficient in these respects.

A. Curve Fitting for Material Reactivity Worth

Both the power-density and material-reactivity-worth distributions are obtained either from experimental data or from nuclear calculations. These values are required by the program and are not necessarily equally spaced. The power-density distribution can be specified in one of the following two ways:

1. If the power-density distribution is approximately separable and symmetrical, both the radial and axial power densities at the center lines of the reactor can be used as input. The computer program will automatically generate the power densities throughout the remainder of the reactor.

2. If the power-density distribution is either nonseparable or asymmetrical, the power densities must be supplied pointwise, i.e., starting from the bottom level of the reactor to the top, and at each level moving radially outward from the center of the cylindrical reactor.

The basic curve-fitting procedure is taken from Refs. 5 and 41. It is repeated here for the sake of clarity in the input specifications.

1. Information is read which provides a value of the distribution functions at every intersection of a set of radial grid lines with a set of axial grid lines.

2. Each triplet of adjacent points on every axial grid line is fitted with a second-degree polynomial function of z . These polynomials are used to evaluate the distribution function at the intersection points of the uniformly spaced set of radial mesh lines with the axial grid lines.

3. This "new" distribution is fitted as a quadratic function of R along each of these newly defined radial lines. These polynomials are used to produce values of the distribution function at the intersection of the uniformly spaced radial lines with the uniformly spaced set of axial lines which is to be used in the numerical integration.

4. The final values of the derived distribution are fitted once more to a quadratic function of Z . The algorithm used to compute the quadratic functions is the following:

The triplet of adjacent points is fitted to a polynomial of the form

$$y = a + bx + cx^2,$$

where the coefficients a , b , and c are given by substituting the values of three adjacent points (x_i, y_i) $i = 1, 2$, and 3 .

$$c = \frac{y_1 - y_3 - \frac{(y_1 - y_2)(x_1 - x_3)}{x_1 - x_2}}{(x_1 - x_3)(x_3 - x_2)};$$

$$b = \frac{y_1 - y_2}{x_1 - x_2} - c(x_1 + x_2);$$

$$a = y_1 - bx_1 - cx_1^2.$$

The derivative is given by

$$\frac{dy}{dx} = b + 2cx.$$

The power-density distribution is normalized so that the integrated power in the reactor is unity at $t = 0$; however, the material-reactivity-worth distribution must either have correct absolute values in the input or be normalized to the regionwise total material worth which is specified in the input.

B. Control of Time Step

The computer program automatically changes the time step size (within the limitation of the maximum and minimum time step specified by input) according to the numerical stability criterion discussed in Section II.C.4. The step size can also be altered during a calculation by preset amounts specified in the input data. In addition, the time step is halved whenever the following conditions are met:

$$\frac{|\text{Power}_t - \text{Power}_{t-\Delta t}|}{\text{Power}_t} > 1/3 \text{ for decreasing power} \quad (43)$$

or

$$\frac{|\text{Power}_t - \text{Power}_{t-\Delta t}|}{\text{Power}_{t-\Delta t}} > \eta_4 \text{ for increasing power,} \quad (44)$$

where η_3 and η_4 are specified in the input.

Whenever the power either increases or decreases very rapidly, numerical instability has been observed. This numerical instability can be eliminated by placing restrictions on the maximum allowable power change in a given time interval. The values of η_3 and η_4 depend on the characteristics of the power excursion under investigation.

Experience with the typical fast reactor power-excursion analyses indicates that there is no numerical instability with time steps of the order of 10 or 2 μsec for energy-dependent and energy-density-dependent equations of state, respectively.

C. Output Control Options

It is useful to print the two-dimensional temperature, pressure, density, displacement, and velocity distributions in the reactor at specified times during the excursion. This option has been incorporated in the VENUS program. These distributions will be printed out every Nth time step, N being specified by the user.

One of the output features in the VENUS program is the utilization of the IBM 2280, which produces 35-mm pictures of a cathode-ray-tube (CRT). The user can request a picture of the deformed mesh configuration after every K time steps. Again K is specified in the input and is not necessarily the same as N. Another output feature is the three-dimensional (r-z-p) pictorial plot⁴² of pressure distribution, which is also available to the user upon request.

The user has the option of selecting a particular location (or locations) in the reactor at which either the pressure or temperature at that location as a function of time is to be plotted. The curve of energy release versus time can also be plotted upon request.

D. Options to Terminate the Program

The VENUS program will be terminated if any one of the following conditions is met:

1. The effective neutron-multiplication factor (k_{eff}) is less than the minimum value ($k_{\text{eff min}}$) specified in the input.

2. The reactor power becomes smaller than the minimum or greater than the maximum specified in the input.
3. Time exceeds the maximum value specified in the input.
4. Distortion of the initial Lagrangian mesh exceeds the value specified in the input.
5. The number of cycles of calculation exceeds a predetermined limit. A cycle of calculation is defined as the completion of a combined neutronics, hydrodynamics, and reactivity-feedback time step.
6. If W_{\max} exceeds a preset value such as 0.14.²³

E. Problem-size Limitations and Core-storage Requirements

There are three classes of data-storage arrays in VENUS that largely determine the maximum problem size and total core-storage requirements. The first class is a series of variable-dimensioned arrays that store data required at each spatial mesh position. These include such data as densities, volume fractions, mesh point positions, temperatures, and pressures. If these arrays are dimensioned in the main program to a given size, say D1, then the maximum number of mesh intervals (zones) is constrained such that

$$(IMAX + 3) \cdot (JMAX + 3) \leq D1.$$

Here IMAX and JMAX are the total number of mesh intervals in the radial and axial directions (see input-data description in Appendix B).

Arrays of this type constitute a large fraction of the total core-storage requirement. For example, a D1 = 1500 necessitates about 360,000 bytes* on the IBM-360 computer.

*Four bytes of storage are required to store a single-precision number.

The second type of arrays are those used to store regionwise information. This includes such data as Doppler-feedback coefficients, region-averaged temperatures, and regionwise densities and volume fractions. The size D2 of these one-dimensional arrays again limits the total number of regions that can be used.

Since the number of regions is naturally much smaller than the number of mesh points (zones), the storage requirement for arrays of this second type is relatively small.

The base version of the code has dimensions of $D1 = 1500$ and $D2 = 20$. It is the smallest dimension, however, that sets the size restriction on the problem specification. The above version of the code requires a core-region size of approximately 600,000 bytes to execute on an IBM 360.

For many problems of interest, the total core requirements can be lowered considerably by decreasing the array-size dimensions to fit more closely the needs of a given problem. Indeed, the core size of a given computer dictates how large the array dimensions can become. As an example, a version of the code that has been applied to certain FFTF calculations allows about 700 mesh points, 20 regions, and 26 intervals per region. This version requires about 375,000 bytes of core.

A decrease in the storage requirements can be obtained most readily by lowering the total number of mesh points allowed (D1). Significant decreases can also be effected by lowering D2.

One reason for the large storage requirements in VENUS is that all the floating-point data are stored in double precision (eight bytes per number stored). If core storage were a problem, it is probable that some of the large data arrays could be stored in single precision without significantly affecting the results of the calculation. Further, if the code is being run on a computer with a more accurate single-precision word size than an IBM 360, it might be possible to go entirely to single precision with a subsequent decrease in the storage requirements of nearly 40%.

F. Simplified Flow Diagram

Figure 9 is a simplified diagram showing the overall logic and the sequence of computations performed by the program.

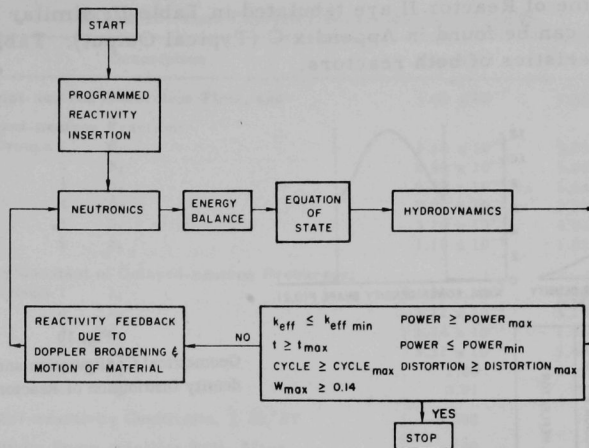


Fig. 9. Simplified Flow Diagram of VENUS Program

V. NUMERICAL RESULTS

The system of equations used in the VENUS program is a set of mixed nonlinear ordinary and partial differential equations; therefore, one cannot derive an analytical stability criteria for the time-step size. Furthermore, the energy-density-dependent equation of state is believed to be used here for the first time in two-dimensional disassembly analysis. The characteristics of this type of equation of state have not been well explored. For these reasons, a number of numerical experiments were performed. The primary purposes for these numerical experiments were as follows:

1. To establish empirical rules for selecting both time-step size and mesh setup for the range of parameters of interest in disassembly analyses;
2. To investigate the fundamental differences between the energy-dependent and the energy-density-dependent equations of state;
3. To examine the validity of the "extrapolation technique" used to avoid "direct iteration" between the power and the reactivity feedbacks at each time step.

Two representative reactor problems, designated Reactors I and II, were investigated. Figures 10 and 11 present their geometric configuration and power-density shape. The material-reactivity-worth distributions

per unit volume of Reactor II are tabulated in Table II; similar information for Reactor I can be found in Appendix C (Typical Output). Table III lists core characteristics of both reactors.

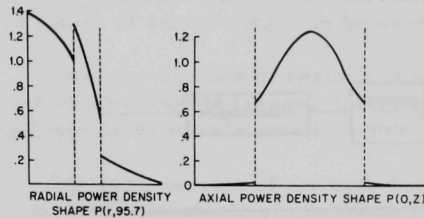


Fig. 10
Geometrical Configuration and Power-density Distribution of Reactor I

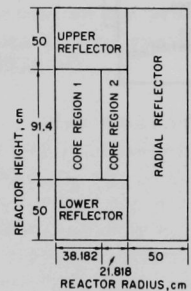


Fig. 11
Geometrical Configuration and Power-density Distribution of Reactor II

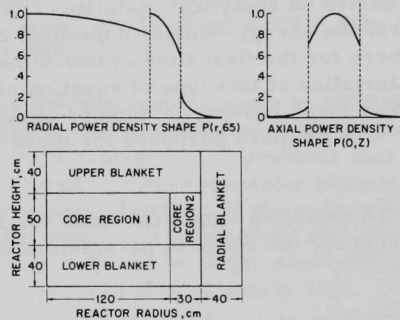


TABLE II. Material Reactivity Worth for Reactor II

$\frac{Z}{R}$	Core Region 1				Core Region 2			
	0	40	80	120	120	130	140	150
90	0.315×10^{-6}	0.289×10^{-6}	0.225×10^{-6}	0.125×10^{-6}	0.194×10^{-6}	0.155×10^{-6}	0.110×10^{-6}	0.600×10^{-7}
73.33	0.360×10^{-6}	0.331×10^{-6}	0.246×10^{-6}	0.145×10^{-6}	0.224×10^{-6}	0.179×10^{-6}	0.128×10^{-6}	0.700×10^{-7}
56.67	0.360×10^{-6}	0.331×10^{-6}	0.246×10^{-6}	0.145×10^{-6}	0.224×10^{-6}	0.179×10^{-6}	0.128×10^{-6}	0.700×10^{-7}
40	0.315×10^{-6}	0.289×10^{-6}	0.225×10^{-6}	0.125×10^{-6}	0.194×10^{-6}	0.155×10^{-6}	0.110×10^{-6}	0.600×10^{-7}

TABLE III. Core Characteristics of Reactors I and II

Description		Reactor I	Reactor II
Prompt-neutron Generation Time, sec		3.50×10^{-7}	5.00×10^{-7}
Delayed-neutron Fraction:			
Groups 1	β_1	1.10×10^{-4}	7.59×10^{-5}
2	β_2	8.40×10^{-4}	6.26×10^{-4}
3	β_3	6.50×10^{-4}	5.64×10^{-4}
4	β_4	9.90×10^{-4}	1.70×10^{-3}
5	β_5	3.10×10^{-4}	4.89×10^{-4}
6	β_6	1.10×10^{-4}	1.63×10^{-4}
Decay Constant of Delayed-neutron Precursor:			
Groups 1	λ_1	1.29×10^{-2}	1.30×10^{-2}
2	λ_2	3.11×10^{-2}	3.14×10^{-2}
3	λ_3	1.34×10^{-1}	1.36×10^{-1}
4	λ_4	3.31×10^{-1}	3.40×10^{-1}
5	λ_5	1.26	1.32
6	λ_6	3.21	3.50
Doppler-reactivity Coefficient, $T \partial k / \partial T$		-0.002	-0.002
Reactivity Ramp-insertion Rate, $\$/\text{sec}$		100	100
Initial Reactor Power, W		1.524×10^{12}	1×10^{12}
Initial Average Reactor Temperature, $^{\circ}\text{K}$		^a	1200 ^b
Core Volume Fractions:			
Fuel ($\text{PuO}_2\text{-UO}_2$)		0.37	0.40
Sodium		0.33	0.40
Structure Steel		0.25	0.20
Void		0.05	0
Density of Fuel ($\text{PuO}_2\text{-UO}_2$), g/cm^3		8.74	8.74
Density of Sodium, g/cc		0.80	0.80
Density of Structure Steel, g/cm^3		8.00	8.00

^aPointwise temperature-input option is chosen for actual temperature distribution; see Appendix C.

^bTemperature is assumed proportional to the local power density and normalized to the reactor average temperature. The peak temperature in the core is $\sim 5700^{\circ}\text{K}$.

The present chapter summarizes some of the numerical results for these two reactors, namely, the FFTF-type core (Reactor I) and the Pancake-type core (Reactor II). These numerical problems were originally tackled at various times over a year and one-half, and as a result there was considerable variation in the reactor parameters used in the calculations. It is believed that the most significant conclusions will remain true for a substantial range of parameter values corresponding to the current sodium-cooled fast breeder reactors.

A. Time-step Size and Mesh Setup

In this section, three problems are investigated. The first is to estimate an appropriate time-step size for a given mesh setup (or mesh size). The second problem is opposite to the first one, i.e., for a given time step what is the effect of the mesh setup. The last is to examine the

possibility of using variable mesh size so that the computer running time can be shortened without impairing the accuracy of the results. It is important to note that all the conclusions reached in this section are empirical in nature and merely provide guidance to the user.

1. To Estimate the Time-step Size for a Given Mesh Setup

The criterion for estimating an appropriate time-step size for a given mesh setup is as follows; the time-step size is decreased sequentially, until at two consecutive time steps the results closely agree both in local and integral quantities. The pressure, temperature, density, etc., are considered as local quantities; the total energy yield and the excursion time represent integral quantities.

Figures 12 and 13 present the pressure distribution as a function of time at the central nodal point of Reactor I for the sodium-out and sodium-in cases, respectively. For the sodium-out case, energy-dependent equation of state is used, and for the sodium-in case, energy-density-dependent equation of state is used. The mesh setup used in these calculations can be found in Appendix C (Typical Input). Table IV lists the total energy yield and the excursion time for both sodium-in and sodium-out cases. The reason for presenting the pressure among all the local quantities is that the pressure is the most sensitive to the time-step variation.

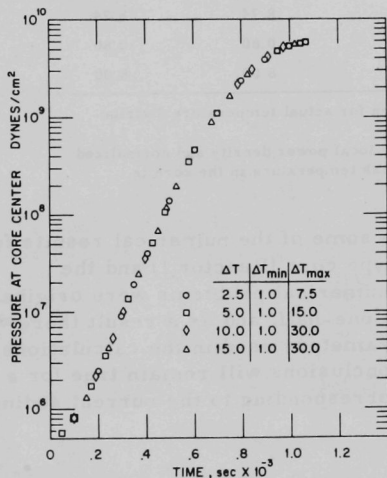


Fig. 12. Pressure vs Time at Core Center of Reactor I for Sodium-out Case

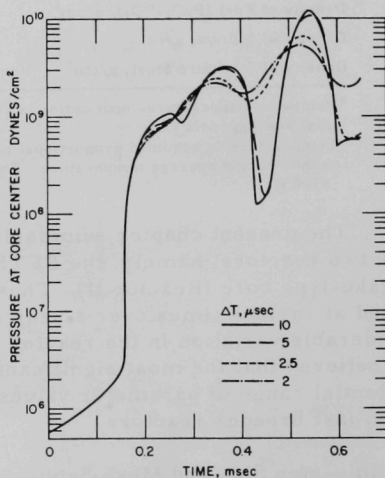


Fig. 13. Pressure vs Time at Core Center of Reactor I for Sodium-in Case

TABLE IV. Total Energy Yield and Excursion Time
for Various Time-step Sizes

	Time Steps, μsec			Total Energy Yield, 10^9 J	Excursion Time, msec
	ΔT	$\Delta T \text{ min}$	$\Delta T \text{ max}$		
<u>Sodium-out</u>					
EOS2 ^a	2.5	1.0	7.5	8.72	1.070
EOS2	5.0	1.0	15.0	8.71	1.067
EOS2	10.0	1.0	30.0	8.73	1.070
EOS2	15.0	1.0	30.0	8.73	1.071
<u>Sodium-in</u>					
EOS7	1.0 ^b	1.0	2.0	3.74	0.647
EOS7	2.0	1.0	4.0	3.74	0.646
EOS7	2.5	1.0	7.5	3.72	0.642
EOS7	5.0	1.0	15.0	3.69	0.636
EOS7	10.0	1.0	30.0	3.70	0.639

^aEOS = Equation of state.

^bThe pressure distribution as a function of time for this case was not presented in Fig. 13 because it follows closely to the case $\Delta T = 2 \mu\text{sec}$.

From the results presented in Figs. 12 and 13 and Table IV, it is concluded that

a. The local pressure distribution is not sensitive when the energy-dependent equation of state is employed (see Fig. 12). However, when the energy-density-dependent equation of state is used, the local pressure distribution becomes very sensitive to the size of the time step used (see Fig. 13).

b. The integral quantities (i.e., the total energy yield and the excursion time) are not very sensitive to the time-step sizes, at least in the range of time-step sizes investigated in this study (see Table IV).

c. A time-step size of approximately 10 and 2 sec were found adequate for the sodium-out (energy-dependent equation) and the sodium-in (energy-density-dependent equation) cases, respectively. When an energy-density-dependent equation is used, the selection of the time-step size is strongly influenced by such factors as the initial power-density (or temperature) distribution, the range of material densities encountered during an excursion, the compressibility of the nonfuel core constituents, and the inherent characteristics of the equation of state.

2. Effect of Mesh Size for a Given Time Step

A similar approach is employed in estimating the effect of the spatial mesh size for a given time step. The time-step sizes used here are the values recommended in the previous section. The number of mesh points describing a reactor is increased sequentially until using two consecutive mesh sizes yields nearly the same results in both local quantities.

A somewhat arbitrary criterion is adapted here in checking the local quantities such as pressure. The pressure in a particular zone of the coarse-mesh setup is compared to an average pressure of many zones in the corresponding volume occupied by the fine-mesh setup. Because of the limitations of the fast core capacity and running time of the computer it is not feasible to run a problem with as many mesh points as would be desired. The results presented here are based on the three different mesh sizes which are designated as Problems 1, 2, and 3, and shown in Fig. 14. All power-density distributions of Reactor II (shown in Fig. 11) are expressed in analytical form so as to minimize the errors due to the interpolation or extrapolation. Figures 15 and 16 show the pressure distribution of Problems 1, 2, and 3 at the central nodal point of Reactor II for sodium-out and sodium-in cases, respectively. Similar information can be found in Figs. 17 and 18 at location marked 1 in Fig. 14. Table V lists the total energy yield and excursion time for all cases.

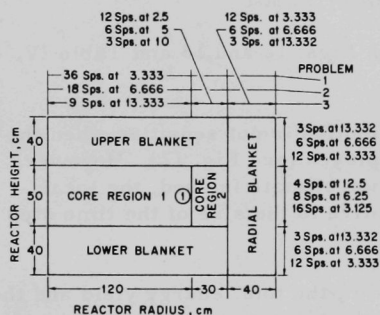


Fig. 14. Various Mesh Setups Used in VENUS Calculation

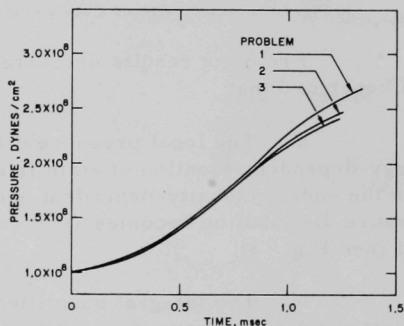


Fig. 15. Pressure vs Time at Core Center of Reactor II for Sodium-out Case

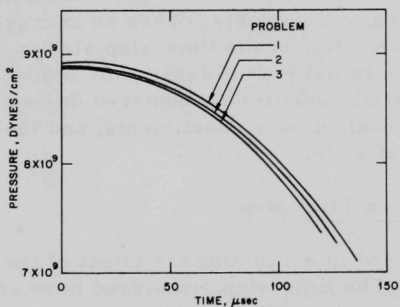


Fig. 16. Pressure vs Time at Core Center of Reactor II for Sodium-in Case

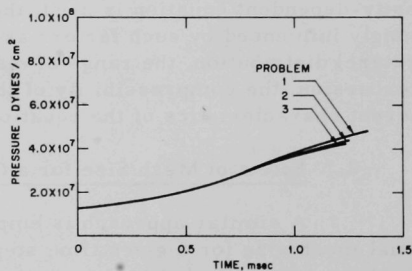


Fig. 17. Pressure vs Time at Location 1 of Reactor II for Sodium-out Case

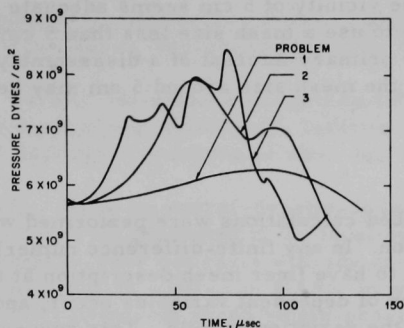


Fig. 18

Pressure vs Time at Location 1 of
Reactor II for Sodium-in Case

TABLE V. Total Energy Yield and Excursion Time for Various Mesh Sizes

Description	Equation of State	Time Steps, μsec			Total Energy Yield, J	Excursion Time, msec
		ΔT	ΔT min	ΔT max		
<u>Sodium-out</u>						
Prob. 1	EOS2	10	1	30	4.02×10^9	1.340
Prob. 2	EOS2	10	1	30	3.68×10^9	1.250
Prob. 3	EOS2	10	1	30	3.57×10^9	1.220
<u>Sodium-in</u>						
Prob. 1	EOS7	2	1	5	1.84×10^8	0.137
Prob. 2	EOS7	2	1	5	1.67×10^8	0.127
Prob. 3	EOS7	2	1	5	1.56×10^8	0.120

Based on the results shown in Figs. 15-18, and in Table V, it is concluded that:

a. The local pressure distribution is not very sensitive when the energy-dependent equation of state is used (see Figs. 15 and 17). However, when the energy-density-dependent equation is employed, the local pressure distribution becomes very sensitive to the variations of mesh size, and there is little resemblance among the results (see Fig. 18). It is believed that additional mesh points (and a smaller time-step size) may be needed in order to reproduce the local pressure distribution. This probably will cause excessive computer running time and exceed fast core-storage capacity.

b. The total energy yield and excursion time are more sensitive to the different mesh sizes than to time-step variations (see Tables IV and V). The maximum variation in total energy yield between Problems 1 and 3 are approximately 11 and 15% for sodium-in and sodium-out cases, respectively; the corresponding differences between Problems 2 and 3 are reduced to 3 and 6%. As will be shown later for Problem 2, these differences can be further reduced by using variable mesh setup with few additional mesh points.

c. A mesh size in the vicinity of 5 cm seems adequate for sodium-out cases. It is desirable to use a mesh size less than 5 cm for sodium-in cases. However, if the primary interest of a disassembly analysis is the total energy yield, the mesh size around 5 cm may be sufficient.

3. Variable Mesh Setup

The previously described calculations were performed with an equally spaced mesh within a region. In any finite-difference numerical calculation, it is always desirable to have finer mesh description at the locations where the sharp variation of dependent variables occur, and coarser mesh may be used where the variation is mild. This suggests a variable mesh setup is most economical since the computer running time is roughly proportional to the square of total mesh points. To demonstrate this point we reran Problem 2 with an additional cell on each side at every interface between two regions. These runs are designated as Problem 2A, and their results are presented in Table VI along with Problems 1, 2, and 3 for comparison.

TABLE VI. Comparison of Total Energy Yield and Excursion Time between Regular and Variable Mesh Setup

Description	Equation of State	Problem 1	Problem 2	Problem 2A	Problem 3
<u>Sodium-out</u>					
Total energy yield, 10^9 J	EOS2	4.02	3.68	3.61	3.57
Excursion time, msec	EOS2	1.34	1.25	1.235	1.220
Complete running time, min	EOS2	2.10	4.80	5.56	18.07
<u>Sodium-in</u>					
Total energy yield, 10^8 J	EOS7	1.84	1.67	1.61	1.56
Excursion time, msec	EOS7	0.137	0.127	0.124	0.120
Complete running time, min	EOS7	1.85	3.11	6.77	17.27

We concluded from these results that

a. conclusion a in 2 still holds;

b. the differences in total energy yield between Problems 2A and 3 are approximately 1 and 3% for sodium-out and sodium-in cases, respectively, a significant reduction when compared to the corresponding differences of 3 and 6% between Problems 2 and 3. This suggests that the accuracy in results from Problem 2A is comparable to Problem 3, at least in integral quantities, and yet the saving on computer time is a factor of three. Therefore, the variable mesh setup as shown in Problem 2A is recommended for all disassembly analyses.

B. Fundamental Differences between Energy-dependent and Energy-density-dependent Equations of State

Careful examination of the results presented in Sect. V.A suggest that the fundamental differences between the energy-dependent and energy-density-dependent equations of state can be stated as follows:

1. When an energy-density-dependent equation is used, very high pressures can be generated if the local system states fall into the single-phase region. This contrasts with the calculations employing the energy-dependent equation such as in MARS, in which the local system states cannot be correctly predicted in the single-phase region.

2. For either high-density or high-energy-density systems, the local pressures can exhibit oscillating characteristics when the energy-density-dependent equation is used. This is because very little density change (or volumetric compression or expansion) can cause local pressure oscillations between the single-phase and two-phase regions.

In general, high pressures are generated much earlier during the sodium-in cases as compared to the sodium-out cases. Therefore, it is expected that for sodium-in cases the excursion will be terminated earlier and, accordingly, decrease the total energy yield.

C. Iteration between Power and Reactivity Feedbacks

In theory an iterative scheme must be employed between the power- and the reactivity-feedback calculations at each time step during a transient. Practically, this requires twice the computer storage space and perhaps the computer running time is lengthened by a factor of two or more. In view of the size of the VENUS program and the limited capacity of the computer fast core, it was decided to use an "extrapolation technique" similar to that used in MARS. The "extrapolation technique" is carried out as follows:

1. Express each component of change in neutron multiplication factor (such as the Doppler feedback) in quadratic form:

$$\delta k_i = a_0 + a_1 t + a_2 t^2; \quad i = 2, 3, \quad (45)$$

where a_0 , a_1 , and a_2 are coefficients which are evaluated by knowing the feedback multiplication factor changes at the previous three time steps.

2. Extrapolating the current feedback multiplication factor changes by using Eq. 45 along with the programmed change in neutron multiplication factor. Perform the cyclic computation as shown in Fig. 9, i.e., Neutronic-Energy Balance--Equation of State--Hydrodynamic--Feedback Reactivity Calculation. With these new feedback multiplication factor changes the coefficients in Eq. 45 is updated.

3. Increment the time step, and repeat the calculations as outlined in 1 and 2 until the transient is terminated.

One of the shortcomings of the above procedure is the lack of information needed to evaluate the coefficients in Eq. 45 at the initiation of the calculation. This shortcoming has been overcome by dividing the first time step (ΔT) into three equal sub-time steps: at $t = 0$, $\Delta T_1/3$, and $2\Delta T/3$, and the system equation is solved iteratively at these time steps. Thus, the coefficients in Eq. 45 can be evaluated. Once these coefficients are known, calculations can proceed by using the "extrapolation technique" outlined above.

The results of a comparison was made between the "extrapolation technique" and the "direct iteration" presented in Fig. 19. It is concluded that the agreement in both feedback neutron multiplication factor changes and energy yield is good.

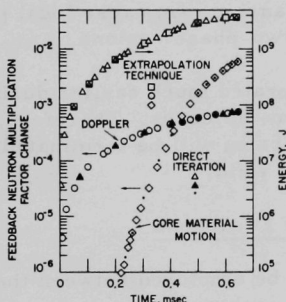


Fig. 19

Comparison between the "Extrapolation Technique" and the "Direct Iteration"

VI. DISCUSSION AND CONCLUSIONS

1. In the course of developing the VENUS computer program, the paramount objective was simplicity in calculation with reasonable accuracy in describing the physical situation during a power excursion. It is believed this objective is satisfactorily fulfilled.

2. Because of the lack of experimental data on the functional dependence of pressure, energy (or temperature), and density in the range of interest, the validity of the equations of state used in this study is questionable. The user must be aware of the uncertainty involved in the equation of state and the resultant uncertainty in the results obtained from the VENUS program. It is hoped that more research effort will be channeled into this area, so that a better understanding of the behavior of the reactor fuel at high temperatures and pressures will eventually provide a sound and valid equation of state.

3. The finite-difference scheme used in the hydrodynamics is a modified version of Kolsky's¹⁵ method. This scheme is called the Midpoint method.¹⁶ Amurud and Orr¹⁶ have observed that Kolsky's method led to reversal of signs of the accelerations when the mesh became sufficiently distorted. The Midpoint method tends to correct this deficiency. Hermann²¹ investigated a number of finite-difference schemes and has concluded that no one finite-difference scheme is clearly superior to the others. None of the schemes give correct results when the mesh deformation becomes very large. Accordingly, we conclude that the VENUS calculation is meaningful only if the distorted mesh does not deviate excessively from the original. No work has been done to investigate what is an excessive mesh distortion. However, experience with VENUS for normal analyses of disassembly accidents indicates no difficulty due to this problem. In any event, this problem can be removed by "rezoning."⁴³

4. The effect of the blanket on the total energy yield, pressure distribution, etc., has not as yet been examined thoroughly. Two problems are often associated with the blanket. One is to specify an equation of state in the blanket which has a complex structure. The other is the propagation of pressure waves and subsequent treatment of the external boundary conditions. The current treatment of the blanket in the VENUS calculation is simply to relate the pressure and local compression linearly. A threshold in the compression is provided in order to take account of the void space. It is further assumed that the blanket is a homogeneous mixture of the various materials. This model is very crude, and more effort is needed in this area.

5. In order to estimate the total energy generation accurately, a time-space-dependent neutronics formulation is needed. It is believed that the limitations in both computer speed and storage space prohibit the massive calculations necessary to generate the solutions of two- (or three-) dimensional, time-space dependent, multigroup diffusion-theory problems by a direct numerical method. Our current effort¹³ is directed toward the development of a fast and reasonably accurate method to replace the direct numerical approach in time-space-dependent neutronics calculations.

6. The second-order polynomial curve fitting for the material-reactivity-worth distribution is found, in certain cases, to be very restrictive. In order to avoid this unnecessary restriction, a higher-order (>2) polynomial curve fitting routine is suggested.

7. The current version of VENUS is written specifically for IBM-360 Model 75. Several output options such as the IBM-2280, CALCOMP PLOT 780 etc., are system-dependent. Therefore, it is suggested to delete these options if one wants to convert VENUS program applicability to other computers such as CDC 6600 or UNIVAC 1108.

8. One of the serious difficulties in reactor-explosion studies is to postulate the possible events which will lead to superprompt critical power excursions. It is even more difficult to pinpoint the reactor state prior to an explosive accident (i.e., to describe the input data to the VENUS program). In order to bypass these difficulties and to compute systematically the reactor accident sequence, joint effort between BNWL and ANL to develop a computational system--MELT-II-VENUS, i.e., coupling MELT-II and VENUS programs--has been successfully completed. Parallel efforts at ANL to develop the SASIB program has been initiated, and VENUS will become a segment of SASIB. It is believed that the MELT-II-VENUS program is the first attempt in two-dimensional analysis to predict the history of an accident as well as to predict the events that will lead to a severe power excursion.

9. The complexity of coupled neutronics-hydrodynamics excursion analysis always leaves plenty of room for further improvements. Several modifications of the VENUS program are being carried out, and much more time will be needed to complete these. Because a number of people have expressed interest in the VENUS-type analyses for weak-explosion studies, the authors have released the VENUS computer program in this early form.

APPENDIX A

Energy- (or Temperature-) density-dependent Equation
of State Developed by BNWL

Alan E. Waltar

Knowledge of the fuel vapor pressure as a function of temperature is not sufficient to characterize the driving pressures in a core-disassembly accident once the fuel has expanded to the point where all available voids are filled. Should a region of the core contain a sizable portion of the original sodium inventory, all voids can be filled early in the transient, and pressures beyond that point become characteristic of a heated, confined liquid. The large pressures which then ensue quickly force fuel toward lower-pressure regions, and the resultant decrease in local fuel density can allow the return of the two-phase (liquid-vapor) regime. Hence, it is important to allow for an explicit density dependence in the fuel equation of state.

The present appendix contains a summary of a particular formulation derived for use in early FFTF studies. The approach is outlined in two phases, the first being applicable to dry-core (sodium-out) cases or for sodium-in cases where sodium compressibility is ignored, and the second includes the complications arising when sodium compressibility is included.

1. Sodium Out or Incompressible Sodium

Two types of pressure formulations are necessary in specifying a temperature-density-dependent equation of state. One accounts for fuel vapor pressure when the system is comprised of the liquid and vapor phases, and the other is required to estimate the pressure of the heated, confined liquid.

A numerical fit to the vapor pressures of Ackerman's low-temperature data³¹ is

$$p_v = \exp \left\{ 55.455 - \frac{78847}{T} - 4.2808 \ln T \right\}. \quad (\text{A.1})$$

The pressure-versus-temperature curve of Eq. A.1 can be found in Fig. 3, labeled EOS2.

Estimates for the pressure existing in the purely liquid state have been made using fuel density versus temperature data to determine the point of departure (that is, the departure temperature) from the saturated-vapor line and corresponding states to determine the P-T slopes in the liquid

phase. Christensen³⁴ found that the melting temperature, liquid density at the melting point, and linear coefficient of expansion at the melting point of UO_2 were 3070°K, 8.74 g/cm³, and $3.5 \times 10^{-5} \text{ }^\circ\text{K}^{-1}$, respectively. From these data, it was estimated that the volumetric coefficient of expansion (α) was about $1.05 \times 10^{-4} \text{ }^\circ\text{K}^{-1}$. Disregarding any pressure dependence, the liquid density was then estimated to be

$$\begin{aligned}\rho &= \rho_0[1 - \alpha(T - T_0)] \\ &= 8.74[1 - 1.05 \times 10^{-4}(T - 3070)] \text{ g/cm}^3.\end{aligned}\quad (\text{A.2})$$

This equation can be used to determine the departure temperature for a given fuel system by letting ρ equal the density of the fuel in its available volume. Thus,

$$\begin{aligned}T_d &= \left(1 - \frac{\rho}{\rho_0}\right) \frac{1}{\alpha} + T_0 \\ &= \left(1 - \frac{\rho}{8.74}\right) \frac{1}{1.05 \times 10^{-4}} + 3070^\circ\text{K}.\end{aligned}\quad (\text{A.3})$$

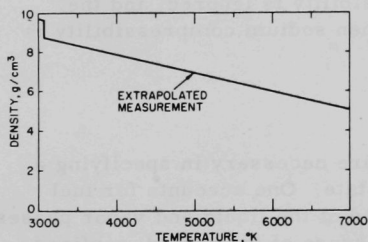


Fig. A.1. Liquid Density of UO_2

The temperature dependence of the density of liquid UO_2 , as described above, is shown in Fig. A.1. The extrapolated-data relationship is shown as a straight line even though it should curve downward (at least near the critical point). Miller²⁷ utilized Christensen's data and the "law of rectilinear diameters" to construct a temperature-density relationship up to the critical point. From his plot it was estimated that a linear temperature-density relationship was quite adequate over the temperature range of interest. In any event, any downward curvature in the relationship would cause departure to occur at lower temperatures, so that the linear relationship is a conservative choice.

Once the fuel system is purely liquid, it is assumed that the slope of the pressure-temperature curve is a constant for a given fuel density:

$$\left(\frac{\partial p}{\partial T}\right)_\rho = f(\rho).$$

An estimate of $f(\rho)$ was obtained from the corresponding-states tables of Hough *et al.*²⁵ The plot (for an assumed critical compressibility of 0.27) in Fig. A.2 indicates that the straight-line approximation is quite adequate. The vapor pressure plotted in the curve is a fit to the high-temperature data of Ackermann.³¹ An analytic fit to this figure is

$$\left. \frac{\partial p_r}{\partial T_r} \right)_{\rho_r} = \rho_r \exp[2.0958 + 0.430(\rho_r - 0.832)^2], \quad (\text{A.4})$$

where

p_r = reduced pressure;

T_r = reduced temperature;

ρ_r = reduced density,

or,

$$\left. \frac{\partial p}{\partial T} \right)_{\rho} = \frac{R\rho}{M} 0.27 \exp[2.0958 + 0.430(\rho_r - 0.832)^2], \quad (\text{A.5})$$

where

p = pressure;

T = temperature;

ρ = density;

M = molecular weight of fuel;

R = gas constant.

If a critical density (ρ_c) of 3.0 g/cm^3 , as obtained from Menzies,²⁹ is assumed,

$$\left. \frac{\partial p}{\partial T} \right)_{\rho} = \rho 0.666 \exp[0.048(\rho - 2.5)^2]. \quad (\text{A.6})$$

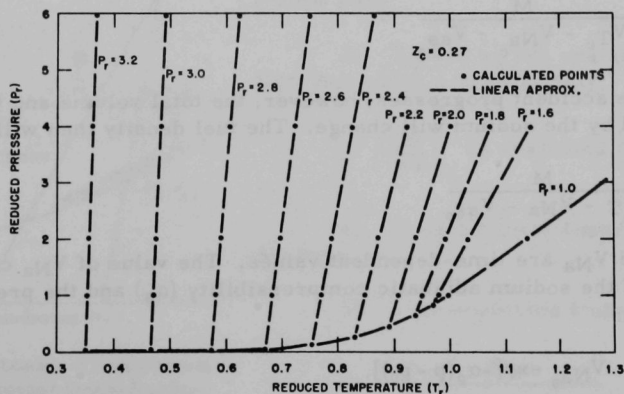


Fig. A.2. Pressure-Temperature Relationship for Sodium-in Case

The pressure-temperature relationship in the liquid fuel region can thus be written as

$$p = \left. \frac{\partial p}{\partial T} \right|_{\rho} (T - T_d) + p_d, \quad (\text{A.7})$$

where

$$\left. \frac{\partial p}{\partial T} \right|_{\rho} \text{ is given by Eq. A.6;}$$

$$T_d \text{ is given by Eq. A.3;}$$

$$p_d \text{ is the pressure of the fuel vapor at the temperature } T_d.$$

This formulation appears reasonable for analyzing dry cores (ρ is fuel density in its available volume and is relatively low if no sodium is present) and for wet core cases if sodium compressibility is ignored.

2. Compressible Sodium

If sodium is assumed to be incompressible, Eq. A.7 can be evaluated explicitly for any temperature-density condition. However, in considering the effects of sodium compressibility, the problem becomes significantly more complicated. To include this effect, consider a small core volume element initially containing M grams of fuel, V_{Na_0} cm³ of sodium, and V_{ss_0} cm³ of the inert material. The inert material (i.e., stainless steel) is assumed to be incompressible. If the initial volume of the element is V_{T_0} , the initial density of the fuel in its available volume is

$$\rho_0 = \frac{M}{V_{T_0} - V_{Na_0} - V_{ss_0}}. \quad (\text{A.8})$$

As the accident progresses, however, the total volume and the volume occupied by the sodium will change. The fuel density then will be

$$\rho = \frac{M}{V_T - V_{Na} - V_{ss_0}}. \quad (\text{A.9})$$

where V_T and V_{Na} are time-dependent values. The value of V_{Na} can be determined if the sodium adiabatic compressibility (α_s) and the pressure (p) are known:

$$V_{Na} = V_{Na_0} \exp[-\alpha_s(p - p_0)]. \quad (\text{A.10})$$

In a code using a Lagrangian coordinate system, such as VENUS, the mass of material in each nodal element remains constant during the transient, and the current nodal volume and fuel temperature are monitored. The volume occupied by the sodium is not calculated explicitly and therefore, must be inherent in the equation of state of the fuel material. If the sodium has a finite compressibility, Eq. A.9 becomes a function of pressure and Eq. A.7 can only be solved for pressure by iteration. In order to avoid iterations in the disassembly code, it would be desirable to have an equation similar to Eq. A.7 in which $\left(\frac{\partial p}{\partial T}\right)_\rho$ is replaced by $\left(\frac{\partial p}{\partial T}\right)_{V_T}$, and $\left(\frac{\partial p}{\partial T}\right)_{V_T}$, T_d , and p_d become functions only of the current volume occupied by the volume element (V_T). The resulting equation, if it can be found, would, of course, be a function not only of the fuel properties, but also of the reactor composition and adiabatic compressibility of sodium.

In BNWL-760 Supplement 1,³³ iterative solutions to Eqs. A.7, A.9, and A.10 have been obtained, and the feasibility of assuming $\left(\frac{\partial p}{\partial T}\right)_{V_T}$ to be a function only of V_T has been demonstrated. The details will not be repeated here. Since the total nodal volume V_T is always monitored in VENUS, the approach discussed above, i.e., avoiding iterations on pressure, can be utilized at a great saving in computation time.

In order to get $\left(\frac{\partial p}{\partial T}\right)_{V_T}$, as suggested above, a rather lengthy (but straightforward) scheme is used. Figure A.3 illustrates the sequence used:

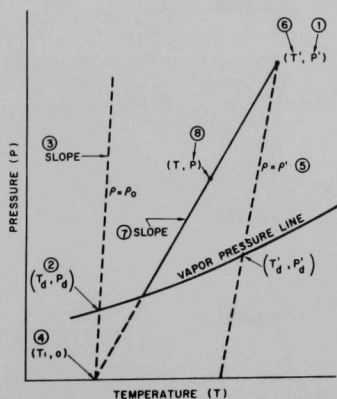


Fig. A.3. Schematic of Computational Procedure Used to Evaluate Slope of P-T Curve for Compressible Sodium

- 1) p' is selected to be some large pressure near the upper range of interest (~2000 atm);
- 2) T_d and p_d are evaluated from Eqs. A.3 and A.1 respectively;
- 3) $\left(\frac{\partial p}{\partial T}\right)_{\rho_0}$ is evaluated from Eq. A.6;
- 4) T_1 is obtained knowing 2) and 3) above;
- 5) ρ' is evaluated from the equation

$$\rho' = \frac{\rho f_0}{\frac{\rho f_0}{\rho_f} - f_0 e^{-\alpha_s \rho'} - g_0}$$

where

ρ_f = current fuel smeared density;

ρ_{f0} = initial fuel smeared density;

f_0 = initial volume fraction sodium;

g_0 = initial volume fraction structure;

α_s = adiabatic sodium compressibility;

6) T' is evaluated by assuming sodium always had the volume it occupies at pressure p' , i.e., T'_d , p'_d , and $\left(\frac{\partial p}{\partial T}\right)_{\rho'}$ are evaluated by Eqs. A.3, A.1, and A.6, respectively;

7) $\left(\frac{\partial p}{\partial T}\right)_{V_T}$ is then evaluated since p' , T' , and T_1 are known. Hence, p can be evaluated directly.

Although this appears cumbersome, the method avoids iteration on pressure, allows ease of changing core compositions, and is believed to be reasonably accurate.

APPENDIX B

Input Format

<u>Card No.</u>	<u>Format</u>	<u>Parameter and Description</u>
1	(10A8)	Title Card - Any alphanumeric information may be entered in Column 1 to 80.
2	(12I6)	IMAX = Number of radial zones (mesh intervals). JMAX = Number of axial zones (mesh intervals). NOTE: $(IMAX^{+3}) \cdot (JMAX^{+3}) \leq 700$.
3	(12I6)	INDEX = 1 Input Maximum number of cycles (MCYCLE). = 2 Input Maximum distortion (DISTOM). NOTE: A cycle is defined as one complete calculation of the neutronic-hydrodynamic-reactivity feedback sequence. IOUTA = 0 No detailed full-accuracy printout. = 1 Detailed full-accuracy printout requested. ICYCLA = Frequency of this type of printout. INUMBA = Total number of this type printout. IOUTB = 0 No limited-accuracy display printout. = 1 Limited-accuracy display printout requested. ICYCLB = Frequency of this type of printout. IOTCRT = 0 No CRT plot, i.e., linked-mesh point pictures. = 1 CRT plot requested. ICYCLT = Frequency of this type printout. IFLPWR = 1 Input power densities at reactor centerlines. = 2 Input power densities pointwise. IFLTHT = 1 Input temperatures regionwise. = 2 Input temperatures pointwise. = 3 Input reactor average temperature (AVTEMP). = 4 Input temperatures pointwise for core regions and regionwise for blankets (or reflectors). = 5 Temperatures in core regions are proportional to power densities and normalized to the reactor average temperature; temperatures in blankets are inputted regionwise. IFLKT = 1 Input Equation of State index regionwise. = 2 Input Equation of State index pointwise. = 3 Input Equation of State index pointwise for core regions and regionwise for blankets. IFLVF = 1 Input volume fractions of reactor materials regionwise. = 2 Input volume fractions pointwise. = 3 Input volume fractions pointwise for core regions and regionwise for blankets.

*Recommended value.

**Using as many cards as needed.

Card No.	Format	Parameter and Description
4	(12I6)	<p>ISTEP2 = 1 Second-step calculation requested. = 2 No second-step calculation.</p> <p>NOTE: The second-step calculation is essentially a plot routine. It stores data from the first-step calculation, then plots these data, such as energy yield versus time, after the completion of the first-step calculation.</p> <p>IFLTMP = 1 Temperature-versus-time plot at a particular location requested. / 1 No temperature-versus-time plot.</p> <p>IFLPRS = 1 Pressure-versus-time plot at a particular location requested. / 1 No pressure-versus-time plot.</p> <p>NTMPPT = Number of locations of temperature-versus-time plot requested. (NTMPPT = 1).*</p> <p>NPRSPT = Number of locations of pressure-versus-time plot requested. (NPRSPT = 1).*</p> <p>KTVAPP = 1 Using MARS-type vapor-pressure equation of state (EOS3 and EOS4). = 2 Using Menzies vapor-pressure equation of state (EOS1). = 3 Using BNWL vapor-pressure equation of state (EOS2). = 4 Using APDA equation of state (EOS5).</p> <p>NOTE: KTVAPP is used only if KT = 1.</p> <p>IFLC = 1 Initial delayed-neutron-precursor concentrations obtained from steady-state conditions. = 2 Initial delayed-neutron-precursor concentrations obtained to be read in.</p> <p>IFLXKF = 1 Initial reactivity-feedback coefficients calculated by SUBROUTINE ITERAT, i.e., VENUS calculation starts from the steady-state condition. = 2 Initial reactivity-feedback coefficients evaluated by input feedback reactivities and corresponding time steps of predisassembly phase. (See Card No. 18), i.e., VENUS calculation starts from the transient condition.</p> <p>IFL3DP = 1 3-D plot, i.e., three-dimensional pressure distribution, requested. = 2 No 3-D plot.</p> <p>IFLDOP = 1 Volume-weighted, regionwise temperature is calculated. = 2 Fuel-mass-weighted, regionwise temperature is calculated.</p>
5**	(12I6)	<p>ITMPPT(I) = Ith radial location for temperature-versus-time plot.</p> <p>JTMPPT(I) = Ith axial location for temperature-versus-time plot.</p> <p>NOTE: ((ITMPPT(I), JTMPPT(I)), I = 1, NTMPPT). Delete this card if IFLTMP / 1.</p>

Card No.	Format	Parameter and Description
6	(12I6)	<p>IPRSPT(I) = Ith radial location for pressure-versus-time plot.</p> <p>JPRSPT(I) = Ith axial location for pressure-versus-time plot.</p> <p>NOTE: ((IPRSPT(I), JPRSPT(I)), I = 1, NPRSPT). Delete this card if IFLPRS \neq 1.</p>
7	(6E12.5)	<p>VALUE = Maximum number of cycles if INDEX = 1 (VALUE = 500).*</p> <p>= Maximum distortion allowed if INDEX = 2 (VALUE = 1000).*</p> <p>DELT = Time-step size in sec.</p> <p>DELTMX = Maximum time-step size in sec.</p> <p>DELTMIN = Minimum time-step size in sec.</p> <p>TSTOP = Reactivity or insertion stops when time reaches TSTOP, in sec.</p> <p>TMAX = Maximum allowed excursion time.</p>
8**	(6E12.5)	<p>R(I,J) = Initial radii in cm of the IMAX radial zones from the center of reactor (I = 2) to the outermost boundary (I = IMAX + 2) at a given height such as J = 2.</p> <p>NOTE: (R(I,2), I = 2, IMAX + 2).</p>
9**	(6E12.5)	<p>Z(I,J) = Initial axial distances of the JMAX axial zones from the bottom of reactor (J = 2) to the top (J = JMAX + 2) at a given radial distance such as I = 2.</p> <p>NOTE: (Z(2,J), j = 2, JMAX + 2).</p>
10**	(6E12.5)	<p>H(I,J) = Pointwise power densities; start at lower left-hand corner (2,2) of the input mesh, proceed radially outward up to the outermost boundary (IMAX + 2,2) then move up to the next level (I,3). Repeat the procedure as outlined above until upper right-hand corner of the input mesh is reached.</p> <p>NOTE: H(I,J) represents the power density at the center of zone (I,J), which is bounded by r-coordinates I and I + 1 and z-coordinates J and J + 1, ((H(I,J), I = 2, IMAX + 1), J = 2, JMAX + 1). Delete this card if IFLPWR \neq 2.</p>
11**	(6E12.5)	<p>RADPSP(I) = Radial power densities at the midplane of core height, start at center of a reactor, proceed radially outward up to the outermost boundary.</p> <p>NOTE: RADPSP(I) represents the power density at the mid-point of r-coordinates I and I + 1, (RADPSP(I), I = 2, IMAX + 2). Delete this card if IFLPWR \neq 1.</p>
12**	(6E12.5)	<p>AXPSHP(J) = Axial power densities at axial centerline from bottom of reactor to top.</p> <p>NOTE: AXPSHP(J) represents the power density at the mid-point of z-coordinates J and J + 1, (AXPSHP(J), J = 2, JMAX + 2). Delete this card if IFLPWR \neq 1.</p>

Card No.	Format	Parameter and Description	
13	(12I6)	NOREG	= Number of regions (≤ 20).
		NDELAY	= Number of delayed-neutron groups. (NDELAY = 6).*
		ISP(1)	= Time-step number for first ΔT modification.
		ISP(2)	= Time-step number for second ΔT modification.
		ISP(3)	= Parameters used in ANL EOS pressure iterations are to be overridden.
		NOTE:	ISP(1) = 0. No time-step modification, and IPS(3) = 0. Default values are used for pressure-iteration parameter (SP(3) = 0.5) and pressure-convergency criterion (SP(4) = 0.01). See card No. 17.
14	(6E12.5)	BETA(I)	= Delayed-neutron fraction of Ith group.
		ALAM(I)	= Decay constant of Ith delayed-neutron-precursor group, 1/sec.
		C(I)	= Precursor concentration of Ith group; delete this information if IFLC = 1.
		NOTE:	Repeat the above information I times, where I = 1, NDELAY, and each time a new card is started.
15	(6E12.5)	DELKO	= Initial excess neutron multiplication factor.
		AK BK	= } Coefficients of change in neutron multiplication factor.
		NOTE:	$\delta k_1^* = \text{DELKO} + (\text{AK})t + (\text{BK})t^2$.
		EL	= Neutron lifetime in seconds.
		XKLIM	= Lower limit of effective neutron multiplication factor to terminate calculation.
16	(6E12.5)	PPSUP	= Upper limit of reactor power in watts to terminate calculation.
		PZERO	= Initial reactor power in watts (P_0).
		PFINAL	= Lower limit of reactor power in watts to terminate calculation.
		RHOCRT	= Critical fuel density in g/cm ³ .
		SP(1)	= Set ΔT to SP(1) at cycle ISP(1).
		SP(2)	= Set ΔT to SP(2) at cycle ISP(2).
		NOTE:	If ISP(1) = 0, Ignore SP(1) and SP(2).
17	(6E12.5)	EPS1 EPS2	= } Convergence criteria used in neutron kinetics. (EPS1 = EPS2 = 0).*
		EPS3 EPS4	= } Power convergence criteria. See Eqs. 43 and 44. (EPS3 = EPS4 = 0.05).*
		SP(3)	= Pressure-iteration parameter used in ANL EOS.
		SP(4)	= Pressure-convergency criterion used in ANL EOS.
		NOTE:	If ISP(3) = 0, Ignore SP(3) and SP(4).

Card	Format	Parameter and Description
18**	(6E12.5)	$\left. \begin{array}{l} TM(1) \\ TM(2) \\ TM(3) \end{array} \right\} = \left. \begin{array}{l} \text{Last three time steps in} \\ \text{predisassembly phase.} \end{array} \right\} \begin{array}{l} (TM(1) = -\Delta T_2)^* \\ (TM(2) = -\Delta T_1)^* \\ (TM(3) = 0)^* \end{array}$ $\left. \begin{array}{l} XKDIS(1) \\ XKDIS(2) \\ XKDIS(3) \end{array} \right\} = \left. \begin{array}{l} \text{Feedback multiplication factor} \\ \text{change due to material motion cor-} \\ \text{responding to above time steps.} \end{array} \right\} \begin{array}{l} (XKDIS(1) = k_2)^* \\ (XKDIS(2) = k_1)^* \\ (XKDIS(3) = 0)^* \end{array}$ $\left. \begin{array}{l} XKDOP(1) \\ XKDOP(2) \\ XKDOP(3) \end{array} \right\} = \left. \begin{array}{l} \text{Feedback multiplication factor} \\ \text{change due to Doppler broadening} \\ \text{corresponding to above time steps.} \end{array} \right\} \begin{array}{l} (XKDOP(1) = k_4)^* \\ (XKDOP(2) = k_3)^* \\ (XKDOP(3) = 0)^* \end{array}$

NOTE: Figure B.1 shows the procedure to obtain the above input data. Delete this card if IFLXKF = 1.

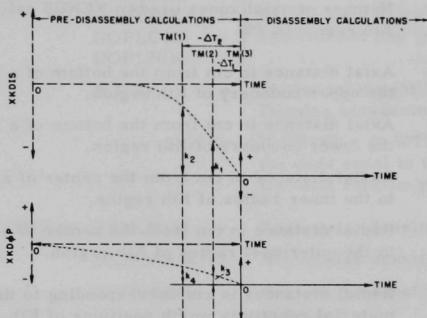


Fig. B.1

Procedure to Input Feed-
back Reactivities

Card No.	Format	Parameter and Description
BEGINNING OF REGIONWISE INPUT		
19	(12I6)	$\left. \begin{array}{l} I1(K) \\ J1(K) \\ I2(K) \\ J2(K) \\ I3(K) \\ J3(K) \\ I4(K) \\ J4(K) \end{array} \right\} = \left. \begin{array}{l} \\ \\ \\ \\ \\ \\ \\ \end{array} \right\} \text{Coordinates of Kth region as shown in Fig. B.2.}$ $IREGKT(K) = \left. \begin{array}{l} \text{Regionwise equation of state index in Kth region.} \\ \text{1 Vapor pressure expressions according to} \\ \text{KT VAPP.} \\ \text{2 Straton's equation of state.} \\ \text{3 ANL equation of state.} \\ \text{4 Blanket (or reflector) equation of state.} \\ \text{5 BNWL--Sodium-out equation of state.} \\ \text{6 BNWL--Incompressible-sodium equation of state.} \\ \text{7 BNWL--Compressible-sodium equation of state.} \end{array} \right\}$
20	(12I6)	$NRIN = \text{Number of radial zones of input material reactivity worth of Kth region } (3 \leq NRIN \leq 26).$ $NZIN = \text{Number of axial zones of input material reactivity worth of Kth region } (3 \leq NZIN \leq 26).$ $NR = \text{Number of radial zones used in VENUS calculation of Kth region } (\leq 25).$

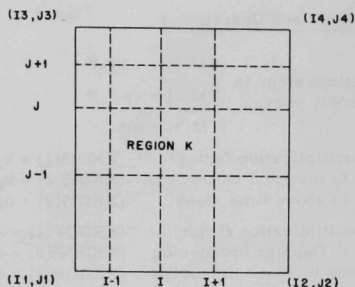


Fig. B.2
Arrangement of Regionwise Coordinates

Card No.	Format	Parameter and Description	
20 (Contd.)	(12I6) (Contd.)	NZ	= Number of axial zones used in VENUS calculation of Kth region (≤ 25).
21	(6E12.5)	ZUP	= Axial distance in cm from the bottom of a reactor to the upper boundary of Kth region.
		ZDN	= Axial distance in cm from the bottom of a reactor to the lower boundary of Kth region.
		RINB	= Radial distance in cm from the center of a reactor to the inner radius of Kth region.
		ROUT	= Radial distance in cm from the center of a reactor to the outermost radius of Kth region.
22**	(6E12.5)	RIN(J)	= Radial distances in cm corresponding to the input material reactivity worth positions of Kth region.
		NOTE:	(RIN(I), I = 1, NRIN).
23**	(6E12.5)	ZIN(I)	= Axial distances in cm corresponding to the input material reactivity worth positions of Kth region.
		NOTE:	(ZIN(I), I = 1, NZIN).
24**	(6E12.5)	WORTH(I,J)	= Pointwise material reactivity worth distribution in Kth region; start at lower left corner, proceed radially outward up to the outermost boundary of Kth region, then move to the next level up and start with a <u>new card</u> . Repeat the procedure until the upper right corner of this region is reached.
		NOTE:	((WORTH(I,J), J = 1, NRIN), I = 1, NZIN).
25	(6E12.5)	CP0(K) CP1(K) CP2(K)	= } Coefficients of specific heat of fuel below the melting point used in Kth region.
		CP3(K) CP4(K) CP5(K)	= } Coefficients of specific heat of fuel equal to or above the melting point used in Kth region.
26	(6E12.5)	PRA(K) PRB(K) PRC(K)	= } Coefficients of MARS-type equation of state used in Kth region.

Card No.	Format	Parameter and Description	
26 (Contd.)	(6E12.5) (Contd.)	TMELT =	Melting temperature in °K of fuel (TMELT = 3070°K).**
		HFUSE(K) =	Heat of fusion of fuel $\left(\text{HFUSE} = 280 \frac{\text{J}}{\text{g}} \right)$.*
		TOTWO(K) =	Total material reactivity worth of Kth region.
		NOTE:	If other than MARS-type equation of state is used, then $\text{PRA(K)} = \text{PRB(K)} = \text{PRC(K)} = 0$. If $\text{TOTWO(K)} \neq 0$, the material reactivity worth of Kth region is normalized to the value of TOTWO(K) .
27	(6E12.5)	DOPLA(K) = DOPLB(K) = DOPLC(K) = DOPLN(K) =	Coefficients associated with the reactivity-feedback calculations due to Doppler broadening.
		WT(K) =	
		NOTE:	
28	(6E12.5)	RRHOU(K) = RRHONA(K) = RRHOSS(K) = RVFU(K) = RVFNA(K) = RVFSS(K) =	Regionwise density of fuel, such as UO_2 in g/cc. Regionwise density of sodium in g/cc. Regionwise density of stainless steel or equivalent in g/cc. Regionwise volume fraction of fuel such as UO_2 . Regionwise volume fraction of sodium. Regionwise volume fraction of stainless steel (or equivalent).
		NOTE:	Delete this card if IFLVF = 2.
29	(6E12.5)	TEMPNA(K) = TEMPSS(K) = REGTEM(K) = RHOREG(K) = EPSI10(K) =	Regionwise temperature of sodium in °K. This in- formation provided only if ANL's energy-density- dependent equation of state is employed. Regionwise temperature of stainless steel (or equiv- alent) in °K providing ANL's energy-density- dependent equation of state is employed. Regionwise average temperature in °K of Kth region. Regionwise average density in g/cc of Kth region. Fraction of void space in Kth region, this infor- mation is needed only for blankets or reflections.
30**	(36I2)	KT(I,J) =	Pointwise equation of state index in Kth region.
		NOTE:	The input procedure is similar for Card No. 24, i.e., WORTH(I,J) . Delete this card if $\text{IFLKT} \neq 3$ and $\text{IREGKT(K)} \neq 0$, $((\text{KT(I,J)}, \text{I} = \text{I1(K)}, \text{I2(K)} - 1),$ $\text{J} = \text{J1(K)}, \text{J3(K)} - 1)$. See description for IREGKT.

Card No.	Format	Parameter and Description																																
31**	(6E12.5)	RHOU(I,J) = Pointwise densities of fuel such as UO_2 in g/cc in Kth region. NOTE: ((RHOU(I,J), I = I1(K), I2(K) - 1), J = J1(K), J3(K) - 1).																																
32**	(6E12.5)	RHONA(I,J) = Pointwise density of sodium in g/cc in Kth region. NOTE: ((RHONA(I,J), I = I1(K), I2(K) - 1), J = J(K), J3(K) - 1).																																
33**	(6E12.5)	RHOSS(I,J) = Pointwise density of stainless steel (or equivalent) in g/cc in Kth region. NOTE: ((RHOSS(I,J), I = I1(K), I2(K) - 1), J = J1(K), J3(K) - 1).																																
34**	(6E12.5)	VFU(I,J) = Pointwise volume fractions of fuel such as UO_2 in Kth region. NOTE: ((VFU(I,J), I = I1(K), I2(K) - 1), J = J1(K), J3(K) - 1).																																
35**	(6E12.5)	VFNA(I,J) = Pointwise volume fraction of sodium in Kth region. NOTE: ((VFNA(I,J), I = I1(K), I2(K) - 1), J = J1(K), J3(K) - 1).																																
36**	(6E12.5)	VFSS(I,J) = Pointwise volume fractions of stainless steel (or equivalent) in Kth region. NOTE: ((VFSS(I,J), I = I1(K), I2(K) - 1), J = J1(K), J3(K) - 1). NOTE: The input procedure of Card No. 31-36 is similar to Card No. 24, i.e., WORTH(I,J). Delete words 31-36 if IFLVF \neq 3 and RHPREC(K) \neq 0.																																
37**	(6E12.5)	<table><tr><td>EA(K)</td><td>= 42870*</td></tr><tr><td>EB(K)</td><td>= 5968*</td></tr><tr><td>EC(K)</td><td>= 4356*</td></tr><tr><td>ED(K)</td><td>= 99.2*</td></tr><tr><td>EE(K)</td><td>= 1271*</td></tr><tr><td>EF(K)</td><td>= 163.4*</td></tr><tr><td>EG(K)</td><td>= -466*</td></tr><tr><td>EH(K)</td><td>= -10730*</td></tr><tr><td>EI(K)</td><td>= 49740*</td></tr><tr><td>EJ(K)</td><td>= -49830*</td></tr><tr><td>EAA(K)</td><td>= 55.455*</td></tr><tr><td>EBB(K)</td><td>= -78847*</td></tr><tr><td>ECC(K)</td><td>= -4.2808*</td></tr><tr><td>EGG(K)</td><td>= 0.666*</td></tr><tr><td>EHH(K)</td><td>= -0.4811*</td></tr><tr><td>EII(K)</td><td>= 2.4877</td></tr></table> Coefficients associated with equations of state developed by BNWL. Delete these cards if other equations of state are used.	EA(K)	= 42870*	EB(K)	= 5968*	EC(K)	= 4356*	ED(K)	= 99.2*	EE(K)	= 1271*	EF(K)	= 163.4*	EG(K)	= -466*	EH(K)	= -10730*	EI(K)	= 49740*	EJ(K)	= -49830*	EAA(K)	= 55.455*	EBB(K)	= -78847*	ECC(K)	= -4.2808*	EGG(K)	= 0.666*	EHH(K)	= -0.4811*	EII(K)	= 2.4877
EA(K)	= 42870*																																	
EB(K)	= 5968*																																	
EC(K)	= 4356*																																	
ED(K)	= 99.2*																																	
EE(K)	= 1271*																																	
EF(K)	= 163.4*																																	
EG(K)	= -466*																																	
EH(K)	= -10730*																																	
EI(K)	= 49740*																																	
EJ(K)	= -49830*																																	
EAA(K)	= 55.455*																																	
EBB(K)	= -78847*																																	
ECC(K)	= -4.2808*																																	
EGG(K)	= 0.666*																																	
EHH(K)	= -0.4811*																																	
EII(K)	= 2.4877																																	
END OF REGIONWISE INPUT																																		
38**	(36I2)	KT(I,J) = Pointwise equation of state index. NOTE: Delete this card if IFLKT \neq 2, ((KT(I,J), I = 2, IMAX + 1), J = 2, JMAX + 1). See description for IREGKT.																																
39**	(6E12.5)	THETA(I,J) = Pointwise temperatures in $^{\circ}\text{K}$. NOTE: Delete this card if IFLTHT \neq 2 ((THETA(I,J), I = 2, IMAX + 1), J = 2, JMAX + 1).																																

Card No.	Format	Parameter and Description																										
40**	(6E12.5)	RHOU(I,J) = Pointwise densities of fuel such as UO ₂ in g/cc. NOTE: ((RHOU(I,J), I = 2, IMAX + 1), J = 2, JMAX + 1).																										
41**	(6E12.5)	RHONA(I,J) = Pointwise densities of sodium in g/cc. NOTE: ((RHONA(I,J), I = 2, IMAX + 1), J = 2, JMAX + 1).																										
42**	(6E12.5)	RHOSS(I,J) = Pointwise densities of stainless steel (or equivalent) in g/cm ³ . NOTE: ((RHOSS(I,J), I = 2, IMAX + 1), J = 2, JMAX + 1).																										
43**	(6E12.5)	VFU(I,J) = Pointwise volume fractions of fuel such as UO ₂ . NOTE: ((VFU(I,J), I = 2, IMAX + 2), J = 2, JMAX + 1).																										
44**	(6E12.5)	VFNA(I,J) = Pointwise volume fractions of sodium. NOTE: ((VFNA(I,J), I = 2, IMAX + 1), J = 2, JMAX + 1).																										
45**	(6E12.5)	VFSS(I,J) = Pointwise volume fractions of stainless steel or equivalent. NOTE: ((VFSS(I,J), I = 2, IMAX + 1), J = 2, JMAX + 1). NOTE: The input procedure of Cards No. 38-45 is the same as Card 10, i.e., H(I,J). Delete Cards 40-45 if IFLVF ≠ 2.																										
46	(6E12.5)	AVTEMP = Average temperature of reactor in °K. Delete this card if IFLTHT ≠ 3 or ≠ 5.																										
47**	(6E12.5)	THETA(I,J) = Pointwise temperatures is °K for Kth region; the input procedure is the same as for Card 10, i.e., H(I,J). Delete this card if IFLTHT ≠ 4 and REGTEM ≠ 0.																										
48**	(6E12.5)	<table><tr><td>EPMAX</td><td>= 600*</td></tr><tr><td>EVRMIN</td><td>= 0.315*</td></tr><tr><td>EVRMAX</td><td>= 0.50*</td></tr><tr><td>EM</td><td>= 270*</td></tr><tr><td>EVC</td><td>= 88.614*</td></tr><tr><td>ERHOST</td><td>= 8.74*</td></tr><tr><td>EALPH</td><td>= 1.05 × 10⁻⁴</td></tr><tr><td>ETSTAR</td><td>= 3070*</td></tr><tr><td>EPPRIM</td><td>= 2000*</td></tr><tr><td>EBETAS</td><td>= 3 × 10⁻⁵*</td></tr><tr><td>EPSTAR</td><td>= 1 × 10⁵*</td></tr><tr><td>EROMIN</td><td>= 2.99*</td></tr><tr><td>EROMAX</td><td>= 8.74*</td></tr></table> <div>Coefficients associated with equations of state developed by BNWL. Delete these cards if other equations of state are used.</div>	EPMAX	= 600*	EVRMIN	= 0.315*	EVRMAX	= 0.50*	EM	= 270*	EVC	= 88.614*	ERHOST	= 8.74*	EALPH	= 1.05 × 10 ⁻⁴	ETSTAR	= 3070*	EPPRIM	= 2000*	EBETAS	= 3 × 10 ⁻⁵ *	EPSTAR	= 1 × 10 ⁵ *	EROMIN	= 2.99*	EROMAX	= 8.74*
EPMAX	= 600*																											
EVRMIN	= 0.315*																											
EVRMAX	= 0.50*																											
EM	= 270*																											
EVC	= 88.614*																											
ERHOST	= 8.74*																											
EALPH	= 1.05 × 10 ⁻⁴																											
ETSTAR	= 3070*																											
EPPRIM	= 2000*																											
EBETAS	= 3 × 10 ⁻⁵ *																											
EPSTAR	= 1 × 10 ⁵ *																											
EROMIN	= 2.99*																											
EROMAX	= 8.74*																											

Coefficients associated with equations of state developed by BNWL. Delete these cards if other equations of state are used.

APPENDIX C

Sample Problems1. Typical Input

A typical input for the VENUS computer program is shown in the following pages.

CARD10.....20.....30.....40.....50.....60.....70.....80
0001	1FFTF VENUS , EQUATION OF STATE EQ. TO 7							
0002	16	28						
0003	1	0	0	0	1	20	1	10
0004	1	1	1	1	1	4	1	1
0005	2	16						
0006	2	16						
0007	3.0	+02	2.0	-36	5.0	-06	1.0	-06
0008		0.		5.455	10.909	16.364	21.818	27.273
0009	32.727		38.182		43.636	49.091	54.545	60.
0010	70.		80.		90.	100.	110.	
0011	0.		10.		20.	30.	40.	50.
0012	55.08		60.16		65.24	70.32	75.40	80.48
0013	85.56		90.64		95.72	100.80	105.88	110.96
0014	116.04		121.12		126.20	131.28	136.36	141.44
0015	151.44		161.44		171.44	181.44	191.44	
0016	1.365		1.348		1.310	1.260	1.198	1.126
0017	1.048		1.220		1.040	.842	.630	.020
0018	.315		.010		.005	.002		
0019	.002		.005		.010	.015	.020	.690
0020	.755		.850		.940	1.030	1.110	1.170
0021	1.215		1.240		1.240	1.215	1.170	1.110
0022	1.030		.940		.850	.755	.690	.020
0023	.015		.010		.005	.002		
0024	9	6						
0025	.00011		.0129					
0026	.00084		.0311					
0027	.00065		.1340					
0028	.00099		.3310					
0029	.00031		1.26					
0030	.00011		3.21					

CARD10.....20.....30.....40.....50.....60.....70.....80

0031	0.3571	-02 3.01	-01 0.0	+00 3.5	-07 9.97	-01	
0032	1.0	+20 1.524	+12 1.524	+11 3.0	+06		
0033			5.0	-02 5.0	-02		
0034	2	2	9	2	2	7	9 7 4
0035	8	6	7	5			
0036		50.	0.	0.	38.182		
0037		0.	5.455	10.909	16.364	21.818	27.273
0038		32.727	38.182				
0039		0.	10.	20.	30.	40.	50.
0040		.1082E-7	.1073E-7	.1041E-7	.0991E-7	.0922E-7	.0863E-7
0041		.0760E-7	.0644E-7				
0042		.1484E-7	.1475E-7	.1443E-7	.1393E-7	.1330E-7	.1264E-7
0043		.1162E-7	.1046E-7				
0044		.1670E-7	.1659E-7	.1624E-7	.1567E-7	.1496E-7	.1422E-7
0045		.1307E-7	.1176E-7				
0046		.2646E-7	.2630E-7	.2574E-7	.2483E-7	.2371E-7	.2254E-7
0047		.2071E-7	.1865E-7				
0048		.4918E-7	.4888E-7	.4783E-7	.4615E-7	.4407E-7	.4190E-7
0049		.3850E-7	.3465E-7				
0050		.9016E-7	.8962E-7	.8769E-7	.8461E-7	.8079E-7	.7682E-7
0051		.7058E-7	.6353E-7				
0052	3.884	-01 -1.619	-04 8.781	-08 .548	+00		
0053				3.04	+03 2.8	+02	
0054		-0.4	-02		1.0	-09	
0055			0.8	8.0		0.44	0.46
0056		600.	600.	600.	4.032	0.1	
0057	2	7	9	7	2 25	9 25	7
0058	8	19	7	18			
0059	141.44		50.	0.	38.182		
0060		0.	5.455	10.909	16.364	21.818	27.273
0061		32.727	38.182				
0062		50.	55.08	60.16	65.24	70.32	75.40
0063		80.48	85.56	90.64	95.72	100.80	105.88

CARD10.....20.....30.....40.....50.....60.....70.....80
0064	110.96	116.74	121.12	126.20	131.28	136.36		
0065	141.44							
0066	3.2093E-7	3.1907E-7	3.1214E-7	3.0118E-7	2.8758E-7	2.7343E-7		
0067	2.5124E-7	2.2614E-7						
0068	3.5465E-7	3.5252E-7	3.4493E-7	3.3283E-7	3.1780E-7	3.0215E-7		
0069	2.7764E-7	2.4997E-7						
0070	4.0250E-7	4.0009E-7	3.9148E-7	3.7774E-7	3.6068E-7	3.4293E-7		
0071	3.1510E-7	2.8363E-7						
0072	4.5400E-7	4.5128E-7	4.4157E-7	4.2607E-7	4.0683E-7	3.8680E-7		
0073	3.5542E-7	3.1992E-7						
0074	5.0549E-7	5.0246E-7	4.9164E-7	4.7439E-7	4.5797E-7	4.3067E-7		
0075	3.9573E-7	3.5620E-7						
0076	5.5250E-7	5.4919E-7	5.3737E-7	5.1851E-7	4.9510E-7	4.7073E-7		
0077	4.3253E-7	3.8933E-7						
0078	5.9745E-7	5.9387E-7	5.8109E-7	5.6069E-7	5.3538E-7	5.0902E-7		
0079	4.6772E-7	4.2100E-7						
0080	6.3250E-7	6.2871E-7	6.1518E-7	5.9359E-7	5.6679E-7	5.3889E-7		
0081	4.9516E-7	4.4570E-7						
0082	6.5510E-7	6.5117E-7	6.3716E-7	6.1478E-7	5.8704E-7	5.5814E-7		
0083	5.1285E-7	4.6162E-7						
0084	6.6000E-7	6.5604E-7	6.4193E-7	6.1940E-7	5.9143E-7	5.6232E-7		
0085	5.1669E-7	4.6508E-7						
0086	6.5510E-7	6.5117E-7	6.3716E-7	6.1478E-7	5.8704E-7	5.5814E-7		
0087	5.1285E-7	4.6162E-7						
0088	6.3250E-7	6.2871E-7	6.1518E-7	5.9359E-7	5.6679E-7	5.3889E-7		
0089	4.9516E-7	4.4570E-7						
0090	5.9745E-7	5.9387E-7	5.8109E-7	5.6069E-7	5.3538E-7	5.0902E-7		
0091	4.6772E-7	4.2100E-7						
0092	5.5250E-7	5.4919E-7	5.3737E-7	5.1851E-7	4.9510E-7	4.7073E-7		
0093	4.3253E-7	3.8933E-7						
0094	5.0549E-7	5.0246E-7	4.9164E-7	4.7439E-7	4.5797E-7	4.3067E-7		
0095	3.9573E-7	3.5620E-7						

CARD10.....20.....30.....40.....50.....60.....70.....80

0096	4.5400E-7	4.5128E-7	4.4157E-7	4.2607E-7	4.0683E-7	3.8680E-7
0097	3.5542E-7	3.1992E-7				
0098	4.0250E-7	4.0009E-7	3.9148E-7	3.7774E-7	3.6068E-7	3.4293E-7
0099	3.1510E-7	2.8363E-7				
0100	3.5465E-7	3.5252E-7	3.4493E-7	3.3283E-7	3.1780E-7	3.0215E-7
0101	2.7764E-7	2.4990E-7				
0102	3.2093E-7	3.1900E-7	3.1214E-7	3.0118E-7	2.8758E-7	2.7343E-7
0103	2.5124E-7	2.2614E-7				
0104	3.884 -01	-1.619 -04	8.781 -08	.548 +00		
0105				3.04 +03	2.8 +02	
0106		-0.4 -02			0.3 +00	
0107	8.74	0.8	8.0	.37	.33	.25
0108	1200.	1200.		5.498		
0109	42870.	5968.	4356.	99.2	1271.	163.4
0110	-466.	-10730.	49740.	-49830.	55.455	-78847.
0111	-4.2808	.666	.04811	2.4877		
0112	2 25	9 25	2 30	9 30	4	
0113	8 6	7 5				
0114	191.44	141.44	0.	38.182		
0115	0.	5.455	10.909	16.364	21.818	27.273
0116	32.727	38.182				
0117	141.44	151.44	161.44	171.44	181.44	191.44
0118	.9016E-7	.8962E-7	.8769E-7	.8461E-7	.8079E-7	.7682E-7
0119	.7058E-7	.6353E-7				
0120	.4918E-7	.4888E-7	.4783E-7	.4615E-7	.4407E-7	.4190E-7
0121	.3850E-7	.3465E-7				
0122	.2646E-7	.2630E-7	.2574E-7	.2483E-7	.2371E-7	.2254E-7
0123	.2071E-7	.1865E-7				
0124	.1670E-7	.1659E-7	.1624E-7	.1567E-7	.1496E-7	.1422E-7
0125	.1307E-7	.1176E-7				
0126	.1484E-7	.1475E-7	.1443E-7	.1393E-7	.1330E-7	.1264E-7

0127	.1162E-7	.1046E-7							
0128	.1082E-7	.1073E-7	.1041E-7	.0991E-7	.0922E-7	.0863E-7			
0129	.0760E-7	.0644E-7							
0130	3.884 -01	-1.619 -04	8.781 -08	.548 +00					
0131				3.04 +03	2.8 +02				
0132		-0.4 -02			1.0 -09				
0133		0.8	8.0		0.44	0.46			
0134	600.	600.	600.	4.032	0.1				
0135	9 2	13 2	9 7	13 7	4				
0136	5 6	4 5							
0137	50.	0.	38.182	60.					
0138	38.182	43.636	49.091	54.545	60.				
0139	0.	10.	20.	30.	40.	50.			
0140	.1405E-7	.1204E-7	.0979E-7	.0757E-7	.6299E-8				
0141	.1807E-7	.1606E-7	.1381E-7	.1158E-7	.9412E-8				
0142	.2033E-7	.1807E-7	.1553E-7	.1303E-7	.1059E-7				
0143	.3222E-7	.2864E-7	.2462E-7	.2066E-7	.1678E-7				
0144	.5989E-7	.5323E-7	.4575E-7	.3839E-7	.3119E-7				
0145	1.0980E-7	.9760E-7	.8388E-7	.7038E-7	.5718E-7				
0146	3.884 -01	-1.619 -04	8.781 -08	.548 +00					
0147				3.04 +03	2.8 +02				
0148		-0.4 -02			1.0 -09				
0149		0.8	8.0		0.44	0.46			
0150	600.	600	600.	4.032	0.1				
0151	9 7	13 7	9 25	13 25	7				
0152	5 19	4 18							
0153	141.44	50.	38.182	60.					
0154	38.182	43.636	49.091	54.545	60.				
0155	50.	55.08	60.16	65.24	70.32	75.40			
0156	80.48	85.56	90.64	95.72	100.80	105.88			
0157	110.96	116.04	121.12	126.20	131.28	136.36			
0158	141.44								

CARD10.....20.....30.....40.....50.....60.....70.....80

0159	3.9084E-7	3.4741E-7	2.9858E-7	2.5052E-7	2.0353E-7	
0160	4.3191E-7	3.8391E-7	3.2995E-7	2.7684E-7	2.2492E-7	
0161	4.9019E-7	4.3571E-7	3.7447E-7	3.1420E-7	2.5527E-7	
0162	5.5291E-7	4.9146E-7	4.2238E-7	3.5440E-7	2.8793E-7	
0163	6.1561E-7	5.4720E-7	4.7028E-7	3.9459E-7	3.2058E-7	
0164	6.7287E-7	5.9809E-7	5.1403E-7	4.3129E-7	3.5040E-7	
0165	7.2761E-7	6.4675E-7	5.5585E-7	4.6638E-7	3.7891E-7	
0166	7.7030E-7	6.8469E-7	5.8845E-7	4.9374E-7	4.0113E-7	
0167	7.9782E-7	7.0916E-7	6.0948E-7	5.1138E-7	4.1547E-7	
0168	8.0379E-7	7.1446E-7	6.1404E-7	5.1521E-7	4.1858E-7	
0169	7.9782E-7	7.0916E-7	6.0948E-7	5.1138E-7	4.1547E-7	
0170	7.7030E-7	6.8469E-7	5.8845E-7	4.9374E-7	4.0113E-7	
0171	7.2761E-7	6.4675E-7	5.5585E-7	4.6638E-7	3.7891E-7	
0172	6.7287E-7	5.9809E-7	5.1403E-7	4.3129E-7	3.5040E-7	
0173	6.1561E-7	5.4720E-7	4.7028E-7	3.9459E-7	3.2058E-7	
0174	5.5291E-7	4.9146E-7	4.2238E-7	3.5440E-7	2.8793E-7	
0175	4.9019E-7	4.3571E-7	3.7447E-7	3.1420E-7	2.5527E-7	
0176	4.3191E-7	3.8391E-7	3.2995E-7	2.7684E-7	2.2492E-7	
0177	3.9084E-7	3.4741E-7	2.9858E-7	2.5052E-7	2.0353E-7	
0178	3.884 -01	-1.619 -04	8.781 -08	.548 +00		
0179				3.04 +03	2.8 +02	
0180		-0.4 -02			0.2 +00	
0181	8.74	0.8	8.0	.37	.33	.25
0182	1200.	1200.		5.498		
0183	42870.	5968.	4356.	99.2	1271.	163.4
0184	-466.	-10730.	49740.	-49830.	55.455	-78847.
0185	-4.2808	.666	.04811	2.4877		
0186	9 25	13 25	9 30	13 30	4	
0187	5 6	4 5				
0188	191.44	141.44	38.182	60.		
0189	38.182	43.636	49.091	54.545	60.	

CARD10.....20.....30.....40.....50.....60.....70.....80

0190	141.44	151.44	161.44	171.44	181.44	191.44
0191	1.0980E-7	.9760E-7	.8388E-7	.7038E-7	.5718E-7	
0192	.5989E-7	.5323E-7	.4575E-7	.3839E-7	.3119E-7	
0193	.3222E-7	.2864E-7	.2462E-7	.2066E-7	.1678E-7	
0194	.2033E-7	.1807E-7	.1553E-7	.1303E-7	.1059E-7	
0195	.1807E-7	.1606E-7	.1381E-7	.1158E-7	.9412E-8	
0196	.1405E-7	.1204E-7	.0979E-7	.0757E-7	.6299E-8	
0197	3.884 -01	-1.619 -04	8.781 -08	.548 +00		
0198				3.04 +03	2.8 +02	
0199		-0.4 -02			1.0 -09	
0200		0.8	8.0		0.44	0.46
0201	600.	600.	600.	4.032	0.1	
0202	13 2	18 2	13 7	18 7	4	
0203	6 6	5 5				
0204	50.	0.	60.	110.		
0205	60.	70.	80.	90.	100.	110.
0206	0.	10.	20.	30.	40.	50.
0207	.2876E-8	.0275E-8	.5074E-9	.1893E-9	.1274E-9	.1270E-9
0208	.4.81E-8	.1477E-8	.6282E-9	.3097E-9	.2478E-9	.2473E-9
0209	.4591E-8	.1662E-8	.7068E-9	.3484E-9	.2788E-9	.2783E-9
0210	.7277E-8	.2634E-8	.1120E-8	.5523E-9	.4418E-9	.4410E-9
0211	.1352E-7	.4896E-8	.2082E-8	.1026E-8	.8211E-9	.8196E-9
0212	.2483E-7	.8976E-8	.3817E-8	.1882E-8	.1505E-8	.1503E-8
0213	3.884 -01	-1.619 -04	8.781 -08	.548 +00		
0214				3.04 +03	2.8 +02	
0215		-0.4 -02			1.0 -09	
0216		0.8	8.0		0.34	0.61
0217	600.	600.	600.	5.152	0.05	
0218	13 7	18 7	13 25	18 25	4	
0219	6 19	5 18				
0220	141.44	50.	60.	110.		
0221	60.	70.	80.	90.	100.	110.

CARD10.....20.....30.....40.....50.....60.....70.....80

0222	50.	55.08	60.16	65.24	70.32	75.40
0223	80.48	85.56	90.64	95.72	100.80	105.88
0224	110.96	116.04	121.12	126.20	131.28	136.36
0225	141.44					
0226	.8826E-7	.3195E-7	.1359E-7	.6698E-8	.5358E-8	.5349E-8
0227	.9753E-7	.3531E-7	.1501E-7	.7402E-8	.5921E-8	.5911E-8
0228	1.1069E-7	.4007E-7	.1704E-7	.8401E-8	.6721E-8	.6708E-8
0229	1.2486E-7	.4520E-7	.1922E-7	.9476E-8	.7580E-8	.7567E-8
0230	1.3902E-7	.5032E-7	.2140E-7	.1055E-7	.8440E-8	.8425E-8
0231	1.5195E-7	.5500E-7	.2339E-7	.1153E-7	.9225E-8	.9208E-8
0232	1.6431E-7	.5948E-7	.2529E-7	.1247E-7	.9976E-8	.9958E-8
0233	1.7395E-7	.6297E-7	.2678E-7	.1320E-7	.1056E-7	.1054E-7
0234	1.8016E-7	.6522E-7	.2773E-7	.1367E-7	.1094E-7	.1092E-7
0235	1.8151E-7	.6571E-7	.2794E-7	.1378E-7	.1102E-7	.1100E-7
0236	1.8016E-7	.6522E-7	.2773E-7	.1367E-7	.1094E-7	.1092E-7
0237	1.7395E-7	.6297E-7	.2678E-7	.1320E-7	.1056E-7	.1054E-7
0238	1.6431E-7	.5948E-7	.2529E-7	.1247E-7	.9976E-8	.9958E-8
0239	1.5195E-7	.5500E-7	.2339E-7	.1153E-7	.9225E-8	.9208E-8
0240	1.3902E-7	.5032E-7	.2140E-7	.1055E-7	.8440E-8	.8425E-8
0241	1.2486E-7	.4520E-7	.1922E-7	.9476E-8	.7580E-8	.7567E-8
0242	1.1069E-7	.4007E-7	.1704E-7	.8401E-8	.6721E-8	.6708E-8
0243	.9753E-7	.3531E-7	.1501E-7	.7402E-8	.5921E-8	.5911E-8
0244	.8826E-7	.3195E-7	.1359E-7	.6698E-8	.5358E-8	.5349E-8
0245	3.884 -01	-1.619 -04	8.781 -08	.548 +00		
0246				3.04 +03	2.8 +02	
0247		-0.4 -02			1.0 -09	
0248		0.8	8.0		0.34	0.61
0249	600.	600.	600.	5.152	0.05	
0250	13 25	18 25	13 30	18 30	4	
0251	6 6	5 5				
0252	191.44	141.44	60.	110.		

0253	60.	70.	80.	90.	100.	110.
0254	141.44	151.44	161.44	171.44	181.44	191.44
0255	.2480E-7	.8976E-8	.3817E-8	.1882E-8	.1505E-8	.1503E-8
0256	.1352E-7	.4896E-8	.2082E-8	.1026E-8	.8211E-9	.8196E-9
0257	.7277E-8	.2634E-8	.1120E-8	.5523E-9	.4418E-9	.4410E-9
0258	.4591E-8	.1662E-8	.7068E-9	.3484E-9	.2788E-9	.2783E-9
0259	.4081E-8	.1477E-8	.6282E-9	.3097E-9	.2478E-9	.2473E-9
0260	.2876E-8	.0275E-8	.5074E-9	.1893E-9	.1274E-9	.1270E-9
0261	3.884 -01	-1.619 -04	8.781 -08	.548 +00		
0262				3.04 +03	2.8 +02	
0263		-0.4 -02			1.0 -09	
0264		0.8	8.0		0.34	0.61
0265	600.	600.	600.	5.152	0.05	
0266	2.79830003	2.76480003	2.76480003	2.62460003	2.62460003	2.47114003
0267	2.47114003	2.92916003	2.90139003	2.90139003	2.76098003	2.76098003
0268	2.60284003	2.60284003	3.02523003	3.01579003	3.01579003	2.93283003
0269	2.93283003	2.78084003	2.78084003	3.08262003	3.06495003	3.06495003
0270	3.01895003	3.01895003	2.92758003	2.92758003	3.21095003	3.17446003
0271	3.17446003	3.06434003	3.06434003	3.01187003	3.01187003	3.39104003
0272	3.33663003	3.33663003	3.14637003	3.14637003	3.04911003	3.04911003
0273	3.57079003	3.49547003	3.49547003	3.24418003	3.24418003	3.08540003
0274	3.08540003	3.71016003	3.63205003	3.63205003	3.34056003	3.34056003
0275	3.13063003	3.13063003	3.79452003	3.71451003	3.71451003	3.39863003
0276	3.39863003	3.16866003	3.16866003	3.80803003	3.72743003	3.72743003
0277	3.40988003	3.40988003	3.17557003	3.17557003	3.74953003	3.67066003
0278	3.67066003	3.36920003	3.36920003	3.15086003	3.15086003	3.63397003
0279	3.55935003	3.55935003	3.29046003	3.29046003	3.10738003	3.10738003
0280	3.47682003	3.40655003	3.40655003	3.19362003	3.19362003	3.06524003
0281	3.06524003	3.29492003	3.24256003	3.24256003	3.09759003	3.09759003
0282	3.02862003	3.02862003	3.13703003	3.10858003	3.10858003	3.03818003
0283	3.03818003	2.97678003	2.97678003	3.05221003	3.03936003	3.03936003
0284	2.98545003	2.98545003	2.87252003	2.87252003	2.99087003	2.97412003

CARD10.....20.....30.....40.....50.....60.....70.....80

	5	5	5	5	5	5
0285	2.97412003	2.86515003	2.86515003	2.71222003	2.71222003	2.91081003
	5	5	5	5	5	5
0286	2.88233003	2.88233003	2.74397003	2.74397003	2.59532003	2.59532003
	5	5	5	5	5	5
0287	2.53931003	2.53931003	1.95472003	1.95472003	2.67262003	2.67262003
	5	5	5	5	5	5
0288	2.06572003	2.06572003	2.85359003	2.85359003	2.21791003	2.21791003
	5	5	5	5	5	5
0289	2.97687003	2.97687003	2.35416003	2.35416003	3.03349003	3.03349003
	5	5	5	5	5	5
0290	2.48344003	2.48344003	3.07673003	3.07673003	2.59319003	2.59319003
	5	5	5	5	5	5
0291	3.13955003	3.13955003	2.67423003	2.67423003	3.20533003	3.20533003
	5	5	5	5	5	5
0292	2.73511003	2.73511003	3.25468003	3.25468003	2.77115003	2.77115003
	5	5	5	5	5	5
0293	3.26357003	3.26357003	2.77752003	2.77752003	3.22701003	3.22701003
	5	5	5	5	5	5
0294	2.75442003	2.75442003	3.17114003	3.17114003	2.70681003	2.70681003
	5	5	5	5	5	5
0295	3.15857003	3.15857003	2.63922003	2.63922003	3.05150003	3.05150003
	5	5	5	5	5	5
0296	2.54276003	2.54276003	3.00981003	3.00981003	2.42754003	2.42754003
	5	5	5	5	5	5
0297	2.92757003	2.92757003	2.30555003	2.30555003	2.77444003	2.77444003
	5	5	5	5	5	5
0298	2.16809003	2.16809003	2.65469003	2.65469003	2.07016003	2.07016003
	5	5	5	5	5	5
0299	600.	.315	.500	270.	88.614	8.74
0300	1.05-04	3040.	2900.	3.-05	1.+05	2.99

0301 8.74
0033 BAD CARDS.

2. Typical Output

Because of the physical limitations of this report, it is not possible to present a complete set of VENUS output. Some of the results are displayed in the computer printout on the following pages, including Figs. C.1-C.5.

INPUT MATERIAL WORTH FOR REGION 1

0.108200-07 0.1C7300-07 0.104100-07 0.991000-08 0.922000-08 0.863000-08
 0.760000-08 0.644000-08
 0.148400-07 0.147500-07 0.144300-07 0.139300-07 0.133000-07 0.126400-07
 0.116200-07 0.1C4600-07
 0.167000-07 0.165900-07 0.162400-07 0.156700-07 0.149600-07 0.142200-07
 0.130700-07 0.117600-07
 0.264600-07 0.263000-07 0.257400-07 0.248300-07 0.237100-07 0.225400-07
 0.207100-07 0.186500-07
 0.491800-07 0.488800-07 0.478300-07 0.461500-07 0.440700-07 0.419000-07
 0.385000-07 0.346500-07
 0.901600-07 0.896200-07 0.876900-07 0.846100-07 0.807900-07 0.768200-07
 0.705800-07 0.635300-07

R LATTICE (CM)

C.0 0.54550 01 0.10910 02 0.16360 02 0.21820 02 0.27270 02 0.32730 02 0.38180 02

Z LATTICE (CM)

0.0 0.10000 02 0.20000 02 0.30000 02 0.40000 02 0.50000 02

INPUT MATERIAL WORTH FOR REGION 2

0.320930-06 0.319000-06 0.312140-06 0.301180-06 0.287580-06 0.273430-06
 0.251240-06 0.226140-06
 0.354650-06 0.352520-06 0.344930-06 0.332830-06 0.317800-06 0.302150-06
 0.277640-06 0.249900-06
 0.402500-06 0.400090-06 0.391480-06 0.377740-06 0.360680-06 0.342930-06
 0.315100-06 0.283630-06
 0.454000-06 0.451280-06 0.441570-06 0.426070-06 0.406830-06 0.386800-06
 0.355420-06 0.319920-06
 0.505490-06 0.502460-06 0.491640-06 0.474390-06 0.457970-06 0.430670-06
 0.395730-06 0.356200-06
 0.552500-06 0.549190-06 0.537370-06 0.518510-06 0.495100-06 0.470730-06
 0.432530-06 0.389330-06
 0.597450-06 0.593870-06 0.581090-06 0.560690-06 0.535380-06 0.509020-06
 0.467720-06 0.421000-06
 0.632500-06 0.628710-06 0.615180-06 0.593590-06 0.566790-06 0.538890-06
 0.495160-06 0.445700-06
 0.655100-06 0.651170-06 0.637160-06 0.614780-06 0.587040-06 0.558140-06
 0.512850-06 0.461620-06
 0.660000-06 0.656400-06 0.641930-06 0.619400-06 0.591430-06 0.562320-06
 0.516690-06 0.465080-06
 0.655100-06 0.651170-06 0.637160-06 0.614780-06 0.587040-06 0.558140-06

0.51285D-C6 C.46162D-06
 0.63250C-06 0.62871D-06 0.61518D-C6 C.59359D-C6 C.56679D-06 0.53889D-C6
 C.49516D-06 0.4457CD-06
 0.59745D-06 0.55387D-06 0.581C9D-C6 C.56069D-06 0.53538D-06 0.50902D-06
 0.46772D-06 0.42100D-06
 0.5525CD-C6 C.54515D-06 0.53737D-06 0.51851D-06 0.49510D-06 0.47073D-06
 0.43253D-C6 0.38933D-06
 C.5C549D-06 0.50246D-06 0.49164D-06 0.47435C-06 C.45797D-06 0.43067D-06
 0.39573D-C6 0.35620D-06
 0.454C0C-06 0.45128D-06 0.44157D-C6 C.42607D-C6 C.40683D-06 0.38680D-C6
 0.35542D-06 0.31992D-06
 0.40250D-C6 C.4C0C9D-06 0.39148D-C6 C.37774D-06 0.36068D-06 0.34293D-06
 0.31510D-06 0.28363D-06
 0.35465D-C6 C.35252D-C6 0.34493D-06 0.33283D-06 0.31780D-06 0.30215D-06
 0.27764D-06 0.24990D-06
 C.32C53D-06 0.31900D-06 0.31214D-06 C.30118C-06 0.28758D-06 0.27343D-06
 0.25124D-C6 C.22614D-06

R LATTICE (CM)

0.0 0.5455D 01 0.1091D 02 C.1636D 02 0.2182D 02 0.2727D 02 0.3273D 02 0.3818D 02

Z LATTICE (CM)

C.5C0CD 02 C.5508D 02 0.6016D 02 C.6524D 02 0.7032D 02 0.7540D 02 0.8048D 02 0.8556D 02 0.9064D 02 0.9572D 02
 0.1008D 03 0.1059D 03 0.1110D 03 C.1160D 03 0.1211D 03 0.1262D 03 0.1313D 03 0.1364D 03 0.1414D 03

INPUT MATERIAL WORTH FOR REGION 3

0.90160D-07 0.8962CD-07 0.87690D-07 0.84610D-07 0.80790D-07 0.76820D-07
 0.70580C-07 0.63530D-07
 0.49180C-07 0.48880D-07 0.4783CD-07 0.46150D-07 0.44070D-07 0.41900D-07
 0.385C0D-07 C.3465CD-07
 0.26460C-07 0.26300D-07 0.25740D-07 C.2483CD-07 0.23710D-07 0.22540D-07
 0.20710D-07 0.18650D-07
 0.167C0D-07 0.1655CD-07 0.16240D-07 C.1567CD-07 0.14960D-07 0.14220D-07
 0.13070C-07 0.11760D-07
 0.14840D-07 0.1475CD-07 0.14430D-07 0.13930C-07 0.13300D-07 0.12640D-07
 0.1162CD-07 0.10460D-07
 0.10820C-07 0.10730D-07 0.10410D-07 0.99100D-C8 0.92200D-08 0.86300D-08
 0.760C0D-08 0.644C0D-08

R LATTICE (CM)

0.0 0.5455D 01 0.1091D 02 0.1636D 02 0.2182D 02 0.2727D 02 0.3273D 02 0.3818D 02

Z LATTICE (CM)

C.1414D C2 C.1514D C3 C.1614D 03 C.1714D 03 C.1814D 03 C.1914D 03

INPUT MATERIAL WCRTH FCR REGION 4

0.14050C-C7 0.12040D-07 0.9790CD-08 C.7570CD-C8 C.62990D-08
 0.18C70D-07 0.16060D-07 0.13810D-07 0.11580D-07 0.94120D-08
 0.20330D-C7 C.18C7CD-C7 0.15530D-C7 C.13030D-07 0.10590D-07
 0.32220D-07 0.28640D-07 0.24620D-C7 C.20660D-07 0.16780D-07
 0.5985CD-C7 C.5323CD-C7 0.45750D-07 0.38390D-07 0.31190D-07
 0.10980D-06 C.576CCD-07 0.8388CD-C7 C.7038CD-07 0.57180D-C7

R LATTICE (CM)

0.3818C 02 0.4364D 02 0.4909D 02 C.5455D C2 C.6000D 02

Z LATTICE (CM)

0.0 C.1000D 02 0.20C0D 02 C.30C0D 02 C.4000D C2 0.5000D 02

INPUT MATERIAL WCRTH FCR REGION 5

C.39C84D-06 0.34741D-06 0.29858D-06 0.25052C-06 0.20353D-06
 0.43191D-06 0.38391D-06 0.32995D-06 C.27684D-06 0.22492D-06
 0.49019D-06 0.43571C-06 0.37447D-06 C.31420D-06 0.25527D-06
 C.55251D-06 0.49146D-06 0.42238D-06 0.35440C-06 0.28793D-06
 0.61561C-06 0.5472CD-C6 0.47028D-C6 C.39459D-06 0.32058D-06
 0.67287C-06 0.59809D-06 0.51403D-06 0.43129D-06 0.35040D-06
 0.72761D-C6 0.64675D-C6 0.55585D-06 0.46638D-06 0.37891D-06
 0.77030C-06 0.68469D-06 0.58845D-06 C.49374D-06 0.40113D-06
 C.75782D-06 0.70916D-06 0.60948D-06 0.51138C-06 0.41547D-06
 0.80379D-06 0.71446D-06 0.61404D-06 C.51521D-06 0.41858D-06
 0.79782D-06 0.70916D-06 0.60948D-06 C.51138D-06 0.41547D-06
 0.77020D-06 0.68465D-06 0.58845D-06 0.49374C-06 0.40113D-06
 0.72761C-06 0.64675D-C6 0.55585D-C6 C.46638D-06 0.37891D-06
 0.67287D-C6 0.59809D-06 0.51403D-06 0.43129D-06 0.35040D-06
 0.61561D-C6 0.5472CD-C6 0.47028D-06 C.39459D-06 0.32058D-06
 0.55251C-06 0.49146D-06 0.42238D-06 C.35440D-06 0.28793D-06
 C.49C19D-06 0.43571D-06 0.37447D-06 0.31420C-06 0.25527D-06
 0.43191D-C6 C.38391D-06 0.32995D-C6 C.27684D-06 0.22492D-06
 0.39084D-06 0.34741D-06 0.29858D-C6 C.25052D-C6 C.20353D-06

R LATTICE (CM)

C.3818D 02 0.4364D 02 0.4909D 02 C.5455D 02 0.6000D 02

Z LATTICE (CM)

C.5000D 02 0.5508D 02 0.6016D 02 0.6524D 02 0.7032D 02 0.7540D 02 0.8048D 02 0.8556D 02 0.9064D 02 0.9572D 02
C.10C8D C3 0.1059D C3 0.1110D C3 0.1160D C3 0.1211D C3 0.1262D C3 0.1313D C3 0.1364D C3 0.1414D C3

INPLT MATERIAL WORTH FOR REGION 6

0.1099CD-06 0.57600D-07 0.8388CD-C7 C.70380D-C7 0.57180D-07
C.5989CD-07 0.53230D-07 0.45750D-07 0.38390D-07 0.31190D-07
0.32220D-07 0.2864CD-07 0.24620D-C7 C.2066CD-07 0.16780D-07
0.20330D-07 0.18070D-07 0.15530D-07 C.1303CD-C7 0.10590D-07
C.1807CD-C7 C.16C6CD-07 0.13810D-07 0.11580D-07 0.94120D-08
0.14C50D-C7 0.12040D-07 0.97900D-08 C.757C0D-08 0.62990D-08

R LATTICE (CM)

C.3818D 02 0.4364D 02 C.49C9D 02 C.5455D 02 C.6000D 02

Z LATTICE (CM)

0.1414D C3 C.1514D C3 0.1614D C3 C.1714D C3 0.1814D C3 C.1914D C3

INPLT MATERIAL WORTH FOR REGION 7

C.2876CD-08 0.27500D-09 0.50740D-09 0.18930D-09 0.12740D-09 0.12700D-09
0.40810D-08 0.14770D-08 0.62820D-09 C.30970D-09 0.24780D-09 0.24730D-09
0.45910C-08 0.16620D-08 0.7068CD-C9 C.34840D-09 0.27880D-09 0.27830D-C9
0.72770D-C8 0.2634CD-08 0.11200D-08 0.55230D-09 0.44180D-09 0.44100D-09
0.13520D-07 0.4896CD-08 0.2082CD-C8 C.1026CD-C8 0.82110D-C9 0.81960D-09
C.248CCD-07 0.89760D-08 0.38170D-08 0.18820D-C8 0.15050D-08 0.15030D-08

R LATTICE (CM)

C.60C0D 02 0.7000D 02 0.8000D 02 0.9000D 02 C.1000D C3 C.1100D C3

Z LATTICE (CM)

0.0 0.1000D 02 0.2000D 02 0.3000D 02 0.4000D 02 0.5000D 02

INPUT MATERIAL WCRTH FOR REGION 8

0.8826CD-07 C.31950D-07 0.13590D-07 C.66980D-08 0.53580D-08 0.53490D-08
 0.97530D-07 0.35310D-07 0.15010D-07 0.7402CD-08 0.59210D-08 0.59110D-08
 C.11C69D-06 0.40070D-07 0.17040D-07 0.84010D-08 0.67210D-08 0.67080D-08
 0.12486D-06 0.45200D-07 0.19220D-07 C.9476CD-08 0.75800D-08 0.75670D-08
 0.13902D-06 0.50320D-07 0.21400D-07 0.10550D-07 0.84400D-08 0.84250D-08
 0.1515D-06 0.5500D-07 0.23390D-07 0.11530D-07 0.92250D-08 0.92080D-08
 0.16431D-06 0.59480D-07 0.25290D-07 C.1247CD-07 0.99760D-08 0.99580D-08
 0.17355D-06 0.62970D-07 0.26780D-07 0.13200D-07 0.10560D-07 0.10540D-07
 0.18016D-06 C.6522CD-07 0.2773CD-07 C.1367CD-07 0.10940D-07 0.10920D-07
 0.18151D-06 0.65710D-07 0.2794CD-07 C.1378CD-07 C.11020D-07 0.11000D-07
 C.18016D-06 0.6522CD-07 0.2773CD-07 0.13670D-07 0.10940D-07 0.10920D-07
 0.17395D-06 0.62970D-07 0.2678CD-07 0.13200D-07 0.10560D-07 0.10540D-07
 0.16431D-06 0.59480D-07 0.25290D-07 0.12470D-07 0.99760D-08 0.99580D-08
 0.15155D-06 0.5500CD-07 0.23390D-07 0.11530D-07 0.92250D-08 0.92080D-08
 0.13902D-06 0.50320D-07 0.21400D-07 0.10550D-07 0.84400D-08 0.84250D-08
 0.12486D-06 0.45200D-07 0.19220D-07 C.94760D-08 0.75800D-08 0.75670D-08
 0.11069D-06 0.40070D-07 C.17040D-07 C.84010D-08 0.67210D-08 0.67080D-08
 0.97530D-07 0.35310D-07 0.15010D-07 C.7402CD-08 0.59210D-08 0.59110D-08
 0.88260D-07 0.31950D-07 0.13590D-07 0.66980D-08 0.53580D-08 0.53490D-08

R LATTICE (CM)

C.60CCD 02 0.70CCD 02 0.8000D 02 0.9000D 02 0.1000D 03 0.1100D 03

Z LATTICE (CM)

C.50CCD 02 0.5508D 02 0.6016D 02 0.6524D 02 0.7032D 02 0.7540D 02 0.8048D 02 0.8556D 02 0.9064D 02 0.9572D 02
 C.1008D 03 0.1059D 03 0.1110D 03 0.1160D 03 0.1211D 03 0.1262D 03 0.1313D 03 0.1364D 03 0.1414D 03

INPUT MATERIAL WORTH FOR REGION 9

0.2480CD-07 0.89760D-08 0.38170D-08 0.18820D-08 0.15050D-08 0.15030D-08
 0.13520D-07 0.4856CD-08 0.20820D-08 0.10260D-08 0.82110D-09 0.81960D-09
 0.72770D-08 0.26340D-08 0.11200D-08 C.5523CD-09 0.44180D-09 0.44100D-09
 C.45910D-08 0.16620D-08 0.70680D-09 0.34840D-09 0.27880D-09 0.27830D-09
 0.40810D-08 0.14770D-08 0.62820D-09 C.30970D-09 0.24780D-09 0.24730D-09
 0.28760D-08 0.27500D-09 0.5074CD-09 0.18930D-09 0.12740D-09 0.12700D-09

R LATTICE (CM)

C.6000D 02 0.7000D 02 0.8000D 02 0.9000D 02 0.1000D 03 0.1100D 03

Z LATTICE (CM)

0.1414D 03 0.1514D 03 0.1614D 03 0.1714D 03 0.1814D 03 0.1914D 03

THESE ARE THE REACTOR REGIONS YOU ARE USING IN THE WEAK EXPLOSION CODE

191.4 *****

141.4 *****

50.0 *****

C.C *****

0

3
8

6
0

1
1
0

FFTF VENUS , EQUATION OF STATE EQ. TO 7

RADIAL DISTANCE

C.O	5.455	10.909	16.364	21.818	27.273	32.727	38.182
43.636	49.091	54.545	60.000	70.000	80.000	90.000	100.000
110.000							

AXIAL DISTANCE

0.0	10.000	20.000	30.000	40.000	50.000	55.080	60.160
65.240	70.320	75.400	80.480	85.560	90.640	95.720	100.800
105.880	110.960	116.040	121.120	126.200	131.280	136.360	141.440
151.440	161.440	171.440	181.440	191.440			

RADIAL POWER DENSITY DISTRIBUTION

1.365	1.348	1.310	1.260	1.198	1.126	1.048	1.220
1.040	0.842	0.630	0.020	0.015	0.010	0.005	0.002
0.0							

AXIAL POWER DENSITY DISTRIBUTION

0.002	0.005	0.010	0.015	0.020	0.690	0.755	0.850
0.940	1.030	1.110	1.170	1.215	1.240	1.240	1.215
1.170	1.110	1.030	0.940	0.850	0.755	0.690	0.620
0.015	0.010	0.005	0.002	0.0			

NUMBER OF RADIAL ZONES = 16 NUMBER OF AXIAL ZONES = 28

STCP CONDITIONS ARE:

```

STEP CONDITIONS ARE:
MAX. TIME = C.10000D 01      MAX. CYCLE = 300      MAX. DISTORTION = 0.10000D 04
MAX. POWER = 0.10000D 21      MIN. POWER = 0.15240D 12      K-EFF-LIMIT = 0.99700D 00

```

EPS1	=	0.0	EPS2	=	0.0	EPS3	=	0.500000-01	EPS4	=	0.500000-01
CELT	=	0.200000-05	DELTMX	=	0.500000-05	DELTMN	=	0.100000-05	RHOCRT	=	0.300000 01

OUTPUT PARAMETERS	0	0	0	1	20	1	10
-------------------	---	---	---	---	----	---	----

INDEX OF EQUATION OF STATE

[illegible]

NUMBER OF REGIONS 9

EFFECTIVE NEUTRON LIFETIME 0.35000D-06SEC

SCURCE TERM 0.15240D 13 BETA = 0.30100D-02

REACTIVITY INSERTION FORM

$K(T)-1 = 0.35710D-02 + (0.30100D 00 * T) + (0.0 * T ** 2)$ T IS NOT LARGER THAN 0.10000D 01

NUMBER OF DELAYED NEUTRON EMITTER 6

I	BETA	LAMDA	C
1	0.11000D-03	0.12900D-01	0.37130D 17
2	0.04000D-03	0.31100D-01	0.11761D 18
3	0.65000D-03	0.13400D 00	0.21122D 17
4	0.99000D-03	0.33100D 00	0.13023D 17
5	0.31000D-03	0.12600D 01	0.10713D 16
6	0.11000D-03	0.32100D 01	0.14921D 15

OPTIONS SELECTED FOR THIS JOB

INPUT POWER DENSITIES AT CENTER LINES

POINTWISE TEMPERATURE INPUT FOR CORE REGION AND REGIONWISE INPUT FOR BLANKET

REGIONWISE EQUATION OF STATE INDEX INPUT

REGIONWISE VOLUME FRACTION INPUT

DELAYED PREC. CONC.S CALC.ED FROM STEADY STATE

REACTIVITY FEEDBACK COEFF.S ARE EVALUATED FROM VENUS

ENERGY, K-EFF, K-DOPPLER AND K-DISPLACEMENT VS. TIME PLOTS SELECTED

POINTWISE TEMPERATURE PLOT OPTION SELECTED

PCNIT(S) SELECTED ARE:

1 J
2 16

POINTWISE PRESSURE PLOT OPTION SELECTED

PONIT(S) SELECTED ARE:

1 J
2 16

 REACTOR VOLUME (CM**3) AND POWER (WATTS) SPECIFICATIONS

TOTAL REACTOR VOLUME = 0.72773D 07

 TOTAL REACTOR POWER = 0.15240D 13

REGIONWISE SPECIFICATIONS ARE AS FOLLOWS:

REGION 1	VOLUME = 0.22900D 06	POWER = 0.39329D 10
REGION 2	VOLUME = 0.41880D 06	POWER = 0.69158D 12
REGION 3	VOLUME = 0.22900D 06	POWER = 0.39329D 10
REGION 4	VOLUME = 0.33649D 06	POWER = 0.44545D 10
REGION 5	VOLUME = 0.61537D 06	POWER = 0.78330D 12
REGION 6	VOLUME = 0.33649D 06	POWER = 0.44545D 10
REGION 7	VOLUME = 0.13352D 07	POWER = 0.18185D 09
REGION 8	VOLUME = 0.24418D 07	POWER = 0.31977D 11
REGION 9	VOLUME = 0.13352D 07	POWER = 0.18185D 09

 TOTAL MATERIAL REACTIVITY WORTH = 0.57030D 00

DATA FOR THE REGION 1

REGIONWISE MESH OVERLAY

LOWER LEFT CORNER (2, 2)
 LOWER RIGHT CORNER (9, 2)
 UPPER LEFT CORNER (2, 7)
 UPPER RIGHT CORNER (9, 7)

PRESSURE (DYNES/CM**2) FUNCTION PARAMETERS

A = C.0 B = 0.0 C = 0.0

SPECIFIC HEAT FUNCTION

CP(JOULES/GM-K) = 0.388400 00 + (-0.161900-03 * TH) + (0.878100-07 * TH ** 2)

CP(JOULES/GM-K) = 0.548000 00 + (0.0 * TH) + (0.0 * TH ** 2)

TMELT = 0.304000 C4 HFUSE = C.280000 03 NA TEMP = 0.600000 03 SS TEMP = 0.600000 03

DOPPLER COEFFICIENT TERM

DK/DT = 0.0 * (TH** - 3/2) + -0.400000-02 * (TH** - 1) + 0.0 / TH** (1.0 - 0.0

CCPLER WEIGHTING = 0.100000-08

LATTICE SIZE NZ = 5 NR = 7

R LATTICE (CM)

C.27280 C1 C.61820 C1 0.13640 02 C.19090 02 0.24550 02 0.30000 02 0.35450 02

Z LATTICE (CM)

C.50000 C1 C.15000 02 0.25000 02 C.35000 02 0.45000 02

DW/DZ (R,Z)

0.21310-09 0.21460-09 0.21810-09 C.22420-09 C.23060-09 0.23220-09 0.24200-09

0.37400-09 0.37000-09 0.36190-09 0.35020-09 0.33750-09 0.32040-09 0.29790-09

C.10070-C6 C.95300-C5 C.96390-09 0.92330-09 0.87790-09 0.82280-09 0.74440-09

0.23370-08 0.23050-08 0.22390-08 C.21490-08 0.20460-08 0.19200-08 0.17430-08

0.38930-08 0.38390-08 0.37300-08 0.35790-08 0.34080-08 0.31990-08 0.29030-08

CW/CR (R,Z)

-0.16040-10-C.57980-10-0.90050-10-0.11780-C9-C.11430-C9-0.18470-09-0.20920-09

-C.17870-10-0.60740-10-0.96470-10-0.11960-09-0.12810-09-0.19570-09-0.22300-09

-C.24060-10-C.75300-10-0.12950-09-C.16020-09-0.16700-09-0.26060-09-0.29510-09

-0.40100-10-0.14120-09-0.22750-09-C.28080-C9-0.29310-09-0.45910-09-0.51790-09

-C.74700-10-0.26430-C9-0.42190-09-0.52300-09-0.54450-09-0.85460-09-0.96680-09

MATERIAL REACTIVITY WORTH OF THIS REGION = 0.597530-02

EPSIIC = C.100000 00

DATA FOR THE REGION 2

REGIONWISE MESH OVERLAY

LCWER LEFT CORNER (2, 7)
 LOWER RIGHT CORNER (9, 7)
 UPPER LEFT CORNER (2,25)
 UPPER RIGHT CORNER (9,25)

PRESSURE (DYNES/CM**2) FUNCTION PARAMETERS

A = 0.0 B = 0.0 C = 0.0

SPECIFIC HEAT FUNCTION

CP(JOULES/GM-K)= 0.388400 00 + (-0.161900-03 * TH) + (0.878100-07 * TH ** 2)

CP(JOULES/GM-K)= 0.542000 00 + (0.0 * TH) + (0.0 * TH ** 2)

TFELT= 0.304000 04 HFUSE= 0.280000 03 NA_TEMP= 0.120000 04 SS_TEMP= 0.120000 04

DOPPLER COEFFICIENT TERM

CK/CT = 0.0 * (TH** -3/2) + -0.400000-02 * (TH** -1) + 0.0 / TH** (1.0 - 0.0)

DOPPLER WEIGHTING= 0.300000 00

LATTICE SIZE NZ = 18 NR = 7

R LATTICE (CM)

0.27280 01 0.81820 01 0.13640 02 0.19090 02 0.24550 02 0.30000 02 0.35450 02

Z LATTICE (CM)

0.52540 02 0.57620 02 0.62700 02 0.67780 02 0.72860 02 0.77940 02 0.83020 02 0.88100 02 0.93180 02 0.98260 02
 0.10330 03 0.10840 03 0.11350 03 0.11860 03 0.12370 03 0.12870 03 0.13380 03 0.13890 03

CM/CZ (R,Z)

C.70180-08 0.65210-08 0.67240-08 0.64520-08 0.61420-08 0.57640-08 0.52330-08
 C.90230-08 0.89000-08 0.86460-08 0.82550-08 0.78970-08 0.74120-08 0.67290-08
 C.10120-07 0.59820-08 0.96980-08 0.93730-08 0.89960-08 0.82910-08 0.75470-08
 C.10010-07 0.56670-08 0.55860-08 0.53360-08 0.90330-08 0.81720-08 0.74610-08
 C.93880-08 0.92600-08 0.89960-08 0.85380-08 0.80330-08 0.77430-08 0.70000-08
 C.85200-08 0.84040-08 0.81640-08 0.76940-08 0.71800-08 0.70450-08 0.63530-08
 C.68940-08 0.68000-08 0.66060-08 0.63610-08 0.60800-08 0.56560-08 0.51410-08
 C.42810-08 0.42230-08 0.41020-08 0.39360-08 0.37480-08 0.35170-08 0.31930-08
 C.13190-08 0.13010-08 0.12640-08 0.12130-08 0.11540-08 0.10840-08 0.98400-09
 -0.13520-08 -0.13330-08 -0.12560-08 -0.12430-08 -0.11830-08 -0.11110-08 -0.10080-08
 -C.41530-08 -0.40960-08 -0.39800-08 -0.38180-08 -0.36350-08 -0.34120-08 -0.30970-08
 -C.68630-08 -0.67680-08 -0.65750-08 -0.63380-08 -0.60070-08 -0.56370-08 -0.51170-08
 -0.85810-08 -0.84640-08 -0.82230-08 -0.78200-08 -0.73720-08 -0.70720-08 -0.63990-08
 -C.94300-08 -0.93010-08 -0.90350-08 -0.85300-08 -0.79760-08 -0.77920-08 -0.70310-08
 -C.99300-08 -0.97940-08 -0.95140-08 -0.92210-08 -0.88760-08 -0.81270-08 -0.74050-08
 -C.10050-07 -0.59050-08 -0.96260-08 -0.93750-08 -0.90700-08 -0.82070-08 -0.74920-08
 -0.90680-08 -0.89440-08 -0.86890-08 -0.83130-08 -0.78900-08 -0.74570-08 -0.67620-08
 -C.74880-08 -0.73860-08 -0.71750-08 -0.69070-08 -0.66000-08 -0.61440-08 -0.55840-08

DW/DR (R,Z)

-C.37C3D-09-0.1318D-08-0.21C2D-08-C.2611D-08-0.2718D-08-0.4258D-08-0.4818D-08
 -0.4143D-09-0.1479D-08-0.2357D-08-0.2928D-08-0.3048D-08-0.4775D-08-0.5402D-08
 -C.4655D-C9-0.1678D-C8-0.2677D-08-0.3324D-08-0.3459D-08-0.5423D-08-0.6132D-08
 -0.5270D-09-0.1882D-08-0.3002D-08-C.3384D-C8-C.4224D-08-0.6080D-08-0.6877D-08
 -C.5818D-09-0.2078D-08-0.3313D-08-0.3427D-08-0.4970D-08-0.6712D-08-0.7591D-08
 -C.6318D-09-0.2256D-08-0.3600D-08-0.4583D-08-0.4537D-08-0.7292D-08-0.8245D-08
 -C.6769D-09-0.2417D-08-C.3857D-C8-0.4787D-C8-0.4984D-08-0.7811D-08-0.8834D-08
 -0.7092C-09-0.2531D-08-0.4039D-08-C.5C13D-C8-C.5219D-08-0.8181D-08-0.9251D-08
 -C.7257D-09-0.2587D-08-0.4131C-08-0.5124D-08-0.5335D-08-0.8363D-08-0.9458D-08
 -0.7246D-09-0.2583D-08-0.4123D-08-C.5118D-08-0.5327D-08-0.8351D-08-0.9444D-08
 -0.71C1D-09-0.2533D-08-0.4045D-08-0.5016D-08-0.5224D-08-0.8189D-08-0.9261D-08
 -C.6771D-C9-0.2418D-08-0.3858D-08-0.4790D-08-0.4986D-08-0.7815D-08-0.8838D-08
 -0.6329D-09-0.2260D-08-0.3607D-08-C.4476D-C8-C.4660D-08-0.7304D-08-0.8260D-08
 -C.5813D-09-0.2076D-08-0.3311D-08-C.3768D-08-0.4623D-08-0.6709D-08-0.7586D-08
 -0.5277D-C9-0.1885D-C8-0.3005D-08-C.3C44D-08-0.4572D-08-0.6087D-08-0.6885D-08
 -C.4762C-09-0.1679D-08-0.2680D-08-C.3442D-C8-C.3349D-08-0.5428D-08-0.6138D-08
 -C.4154D-05-0.1483D-08-0.2366D-08-0.2938D-08-0.3057D-08-0.4793D-08-0.5420D-08
 -C.37C3D-09-0.1318D-08-C.2102D-08-C.2611D-08-0.2718D-08-0.4258D-08-0.4818D-08

MATERIAL REACTIVITY WORTH OF THIS REGION = 0.18431D 00

EPS10 = 0.0

EA= C.42870D C5	EB= 0.5968CD C4	EC= 0.43560D 04	ED= 0.99200D 02
EE= 0.12710D 04	EF= 0.16340D C3	EG= -0.46600D 03	EH= -0.10730D 05
EI= C.4574CD C5	EJ= -0.49830D C5	EAA= 0.55455D C2	EBB= -0.78847D 05
ECC= -0.428C8D C1	EGG= 0.6660CD CC	EHH= 0.48110D-01	EII= 0.24877D 01

DATA FOR THE REGION 9

REGIONWISE MESH OVERLAY

LOWER LEFT CORNER (13,25)
 LOWER RIGHT CORNER (18,25)
 UPPER LEFT CORNER (13,30)
 UPPER RIGHT CORNER (18,30)

PRESSURE (DYNES/CM**2) FUNCTION PARAMETERS

A = 0.0 B = 0.0 C = 0.0

SPECIFIC HEAT FUNCTION

CP(JOULES/GM-K) = 0.38840D 00 + (-0.16190D-03 * TH) + (0.87810D-07 * TH ** 2)

CP(JOULES/GM-K) = 0.54200D 00 + (0.0 * TH) + (0.0 * TH ** 2)

TMELT = 0.30400D 04 HFUSE = 0.28000D 03 NA TEMP = 0.60000D 03 SS TEMP = 0.60000D 03

DOPPLER COEFFICIENT TERM

DK/DT = 0.0 * (TH**3/2) + -0.40000D-02 * (TH**1) + 0.0 / TH** (1.0 - 0.0

DCPPLER WEIGHTING = 0.10000D-08

LATTICE SIZE NZ = 5 NR = 5

R LATTICE (CM)

C.6500D 02 0.7500D 02 0.8500D 02 C.9500D 02 0.1050D 03

Z LATTICE (CM)

0.1464D 03 0.1564D 03 0.1664D 03 C.1764D 03 0.1864D 03

DW/DZ (R,Z)

-C.6900D-09-0.2245D-09-0.1085D-09-C.6648D-10-0.6462D-10
 -0.4090D-09-0.1332D-09-0.6435D-10-0.3940D-10-0.3833D-10
 -0.1750D-09-0.5832D-10-0.2815D-10-0.1724D-10-0.1678D-10
 -0.7126D-10-0.2996D-10-0.6984D-11-C.67C8D-11-0.6582D-11
 -C.3502D-10-0.3172D-10 0.7143D-11-C.2882D-11-0.3007D-11

DW/DR (R,Z)

-C.1182D-08-C.3856D-09-0.1447D-09-C.2812D-10-0.1775D-12
 -0.6231D-09-0.2033D-09-0.7630D-10-C.1480D-10-0.1175D-12
 -C.35C3D-09-0.1142D-09-0.4282D-10-0.8336D-11-0.6000D-13
 -0.2553D-09-0.8454D-10-0.3173D-11-C.6160D-11-0.4625D-13
 -0.2562D-09-0.4301D-10-0.3134D-10-C.6094D-11-0.4625D-13

MATERIAL REACTIVITY WORTH OF THIS REGION = 0.19658D-02

EPSIIC = C.50000D-01

EPMAX = 0.60000D 03	EVRMIN = 0.31500D 00	EVRMAX = 0.50000D 00	EM = 0.27000D 03
EVC = 0.88614D 02	ERHOST = 0.87400D 01	EALPH = 0.10500D-03	ETSTAR = 0.30400D 04
EPPRIM = 0.20000D 04	EBETAS = 0.30000D-04	EPSTAR = 0.10000D 06	EROMIN = 0.29900D 01
EROMAX = 0.87400D 01			

FFTF VENUS , EQUATION OF STATE EQ. TC 7																		
RACIAL POSITION OF MESH POINTS AT TIME = C.O																		
	2	3	4	5	6	7	8	9	10	11	12	13	14	15	16	17	18	
	**	**	**	**	**	**	**	**	**	**	**	**	**	**	**	**	**	**
30*	0	5	10	16	21	27	32	38	43	49	54	60	70	80	90	100	110	
29*	0	5	10	16	21	27	32	38	43	49	54	60	70	80	90	100	110	
28*	0	5	10	16	21	27	32	38	43	49	54	60	70	80	90	100	110	
27*	0	5	10	16	21	27	32	38	43	49	54	60	70	80	90	100	110	
26*	0	5	10	16	21	27	32	38	43	49	54	60	70	80	90	100	110	
25*	0	5	10	16	21	27	32	38	43	49	54	60	70	80	90	100	110	
24*	0	5	10	16	21	27	32	38	43	49	54	60	70	80	90	100	110	
23*	0	5	10	16	21	27	32	38	43	49	54	60	70	80	90	100	110	
22*	0	5	10	16	21	27	32	38	43	49	54	60	70	80	90	100	110	
21*	0	5	10	16	21	27	32	38	43	49	54	60	70	80	90	100	110	
20*	0	5	10	16	21	27	32	38	43	49	54	60	70	80	90	100	110	
19*	0	5	10	16	21	27	32	38	43	49	54	60	70	80	90	100	110	
18*	0	5	10	16	21	27	32	38	43	49	54	60	70	80	90	100	110	
17*	0	5	10	16	21	27	32	38	43	49	54	60	70	80	90	100	110	
16*	0	5	10	16	21	27	32	38	43	49	54	60	70	80	90	100	110	
15*	0	5	10	16	21	27	32	38	43	49	54	60	70	80	90	100	110	
14*	0	5	10	16	21	27	32	38	43	49	54	60	70	80	90	100	110	
13*	0	5	10	16	21	27	32	38	43	49	54	60	70	80	90	100	110	
12*	0	5	10	16	21	27	32	38	43	49	54	60	70	80	90	100	110	
11*	0	5	10	16	21	27	32	38	43	49	54	60	70	80	90	100	110	
10*	0	5	10	16	21	27	32	38	43	49	54	60	70	80	90	100	110	
9*	0	5	10	16	21	27	32	38	43	49	54	60	70	80	90	100	110	
8*	0	5	10	16	21	27	32	38	43	49	54	60	70	80	90	100	110	
7*	0	5	10	16	21	27	32	38	43	49	54	60	70	80	90	100	110	
6*	0	5	10	16	21	27	32	38	43	49	54	60	70	80	90	100	110	
5*	0	5	10	16	21	27	32	38	43	49	54	60	70	80	90	100	110	
4*	0	5	10	16	21	27	32	38	43	49	54	60	70	80	90	100	110	
3*	0	5	10	16	21	27	32	38	43	49	54	60	70	80	90	100	110	
2*	0	5	10	16	21	27	32	38	43	49	54	60	70	80	90	100	110	

0.110000000 03

FFTF VENUS , EQUATION OF STATE EQ. TO 7

AXIAL POSITION OF MESH POINTS AT TIME = 0.0

MAXIMUM VALUE OF $Z =$

0.19144000D 03

[illegible]

30* 151 191 151 151 191 191 191 191 191 191 191 191 191 191 191 191 191

29* 181 181 181 181 181 181 181 181 181 181 181 181 181 181 181 181 181 181

28* 171 171 171 171 171 171 171 171 171 171 171 171 171 171 171 171 171 171

27* 161 161 161 161 161 161 161 161 161 161 161 161 161 161 161 161 161

26* 151 151 151 151 151 151 151 151 151 151 151 151 151 151 151 151 151 151

25* 141 141 141 141 141 141 141 141 141 141 141 141 141 141 141 141 141

24* 136 136 136 136 136 136 136 136 136 136 136 136 136 136 136 136 136

23* 131 131 131 131 131 131 131 131 131 131 131 131 131 131 131 131 131

22* 126 126 126 126 126 126 126 126 126 126 126 126 126 126 126 126 126 126

21* 121 121 121 121 121 121 121 121 121 121 121 121 121 121 121 121 121 121

20* 116 116 116 116 116 116 116 116 116 116 116 116 116 116 116 116 116

19* 110 110 110 110 110 110 110 110 110 110 110 110 110 110 110 110 110

18* 105 105 105 105 105 105 105 105 105 105 105 105 105 105 105 105 105 105

17* 100 100 100 100 100 100 100 100 100 100 100 100 100 100 100 100 100 100

16* 95 95 95 95 95 95 95 95 95 95 95 95 95 95 95 95 95

15* 9C 5C 90 90 90 90 9C 9C 90 90 90 90 90 90 90. 90 90 90

14* 85 85 85 85 85 85 85 85 85 85 85 85 85 85 85 85 85

[illegible]

12* 75 75 75 75 75 75 75 75 75 75 75 75 75 75 75 75 75

11* 70 70 70 70 70 70 70 70 70 70 70 70 70 70 70 70 70 70

10* 65 65 65 65 65 65 65 65 65 65 65 65 65 65 65 65 65

9* 60 60 60 60 60 60 60 60 60 60 60 60 60 60 60 60

8* 55 55 55 55 55 55 55 55 55 55 55 55 55 55 55 55 55

7* 50 50 50 50 50 50 50 50 50 50 50 50 50 50 50 50 50 50

6* 40 40 40 40 40 40 40 40 40 40 40 40 40 40 40 40 40

5* 30 30 30 30 30 30 30 30 30 30 30 30 30 30 30 30 30 30

4* 20 20 20 20 20 20 20 20 20 20 20 20 20 20 20 20 20

3* 10 10 10 10 10 10 10 10 10 10 10 10 10 10 10 10 10

2* 0 0 0 0 0 0 0 0 0 0 0 0 0 0 0 0

FFTF VENUS , EQUATION OF STATE EQ. TO 7																	
RACIAL VELOCITY OF MESH POINTS AT TIME =0.0																	
	2	3	4	5	6	7	8	9	10	11	12	13	14	15	16	17	18
	**	**	**	**	**	**	**	**	**	**	**	**	**	**	**	**	**
30*	0	0	0	0	0	0	0	0	0	0	0	0	0	0	0	0	0
29*	0	0	0	0	0	0	0	0	0	0	0	0	0	0	0	0	0
28*	0	0	0	0	0	0	0	0	0	0	0	0	0	0	0	0	0
27*	0	0	0	0	0	0	0	0	0	0	0	0	0	0	0	0	0
26*	0	0	0	0	0	0	0	0	0	0	0	0	0	0	0	0	0
25*	0	0	0	0	0	0	0	0	0	0	0	0	0	0	0	0	0
24*	0	0	0	0	0	0	0	0	0	0	0	0	0	0	0	0	0
23*	0	0	0	0	0	0	0	0	0	0	0	0	0	0	0	0	0
22*	0	0	0	0	0	0	0	0	0	0	0	0	0	0	0	0	0
21*	0	0	0	0	0	0	0	0	0	0	0	0	0	0	0	0	0
20*	0	0	0	0	0	0	0	0	0	0	0	0	0	0	0	0	0
19*	0	0	0	0	0	0	0	0	0	0	0	0	0	0	0	0	0
18*	0	0	0	0	0	0	0	0	0	0	0	0	0	0	0	0	0
17*	0	0	0	0	0	0	0	0	0	0	0	0	0	0	0	0	0
16*	0	0	0	0	0	0	0	0	0	0	0	0	0	0	0	0	0
15*	0	0	0	0	0	0	0	0	0	0	0	0	0	0	0	0	0
14*	0	0	0	0	0	0	0	0	0	0	0	0	0	0	0	0	0
13*	0	0	0	0	0	0	0	0	0	0	0	0	0	0	0	0	0
12*	0	0	0	0	0	0	0	0	0	0	0	0	0	0	0	0	0
11*	0	0	0	0	0	0	0	0	0	0	0	0	0	0	0	0	0
10*	0	0	0	0	0	0	0	0	0	0	0	0	0	0	0	0	0
9*	0	0	0	0	0	0	0	0	0	0	0	0	0	0	0	0	0
8*	0	0	0	0	0	0	0	0	0	0	0	0	0	0	0	0	0
7*	0	0	0	0	0	0	0	0	0	0	0	0	0	0	0	0	0
6*	0	0	0	0	0	0	0	0	0	0	0	0	0	0	0	0	0
5*	0	0	0	0	0	0	0	0	0	0	0	0	0	0	0	0	0
4*	0	0	0	0	0	0	0	0	0	0	0	0	0	0	0	0	0
3*	0	0	0	0	0	0	0	0	0	0	0	0	0	0	0	0	0
2*	0	0	0	0	0	0	0	0	0	0	0	0	0	0	0	0	0

0.0

[illegible]

FFTF VENUS . EQUATION OF STATE EQ. TO 7																
TOTAL PRESSURE OF ZONES AT TIME =0.0																
	2	3	4	5	6	7	8	9	10	11	12	13	14	15	16	17
	**	**	**	**	**	**	**	**	**	**	**	**	**	**	**	**
30*																
29*	C	0	0	0	0	0	C	C	C	0	0	0	0	0	0	0
28*	C	C	C	0	0	0	C	C	C	0	0	0	0	0	0	0
27*	C	C	C	0	0	0	0	0	0	0	0	0	0	0	0	0
26*	0	0	0	0	0	0	0	0	0	0	0	0	0	0	0	0
25*	C	C	0	C	0	C	C	C	0	0	0	0	0	0	0	0
24*	C	C	C	0	0	0	C	0	0	0	0	0	0	0	0	0
23*	0	0	0	0	0	0	0	0	0	0	0	0	0	0	0	0
22*	8	C	0	0	0	C	C	C	C	0	0	0	0	0	0	0
21*	15	13	13	C	C	C	C	C	0	0	0	0	0	0	0	0
20*	42	31	31	12	12	0	0	8	8	0	0	0	0	0	0	0
19*	119	81	81	22	22	9	9	18	18	0	0	0	0	0	0	0
18*	262	182	182	41	41	12	12	19	19	0	0	0	0	0	0	0
17*	448	312	312	66	66	17	17	28	28	0	0	0	0	0	0	0
16*	579	406	406	82	82	20	20	35	35	0	0	0	0	0	0	0
15*	546	382	382	77	77	15	15	33	33	0	0	0	0	0	0	0
14*	375	260	260	56	56	15	15	24	24	0	0	0	0	0	0	0
13*	152	131	131	31	31	11	11	16	16	0	0	0	0	0	0	0
12*	74	54	54	16	16	8	8	10	10	0	0	0	0	0	0	0
11*	25	20	20	9	9	C	C	0	0	0	0	0	0	0	0	0
10*	10	5	5	0	0	0	0	0	0	0	0	0	0	0	0	0
9*	0	0	0	0	0	0	0	0	0	0	0	0	0	0	0	0
8*	C	C	C	C	0	C	C	C	0	0	0	0	0	0	0	0
7*	C	C	C	C	0	0	0	0	0	0	0	0	0	0	0	0
6*	C	C	C	C	C	C	C	C	0	0	0	0	0	0	0	0
5*	0	0	0	0	0	0	0	0	0	0	0	0	0	0	0	0
4*	0	C	0	0	0	C	C	C	C	0	C	0	0	0	0	0
3*	C	C	C	0	0	0	0	0	0	0	0	0	0	0	0	0
2*	C	C	C	0	0	0	C	0	C	0	C	0	0	0	0	0

0.57979282D 06

FFTF VENUS , EQUATION OF STATE EQ. TO 7																
VISCOUS PRESSURE OF ZONES AT TIME =0.0																
	2	3	4	5	6	7	8	9	10	11	12	13	14	15	16	17
	**	**	**	**	**	**	**	**	**	**	**	**	**	**	**	**
30*		C	C	0	0	0	C	C	C	C	0	0	0	0	0	0
29*		C	C	C	0	0	C	C	0	0	0	0	0	0	0	0
28*		C	C	0	0	0	0	0	0	0	0	0	0	0	0	0
27*		C	C	0	0	0	C	C	C	C	0	0	0	0	0	0
26*		C	C	C	0	0	C	C	C	0	0	0	0	0	0	0
25*		C	C	0	0	0	0	0	0	0	0	0	0	0	0	0
24*		C	0	0	0	0	0	C	0	0	0	0	0	0	0	0
23*		0	C	0	0	0	0	C	C	0	0	0	0	0	0	0
22*		C	C	C	0	0	0	0	0	0	0	0	0	0	0	0
21*		0	0	0	0	0	0	0	0	0	0	0	0	0	0	0
20*		0	C	0	0	0	C	C	C	0	0	0	0	0	0	0
19*		C	C	C	0	0	0	C	0	0	0	0	0	0	0	0
18*		0	0	C	0	0	0	0	0	0	0	0	0	0	0	0
17*		0	C	0	0	C	C	C	C	C	C	0	0	0	0	0
16*		C	C	0	0	0	C	C	C	0	0	0	0	0	0	0
15*		C	C	C	0	0	0	0	0	0	0	0	0	0	0	0
14*		0	C	C	0	0	0	0	0	0	0	0	0	0	0	0
13*		C	C	0	0	0	C	C	0	C	0	C	0	0	0	0
12*		C	C	0	0	0	C	C	C	0	0	0	0	0	0	0
11*		C	C	C	0	0	C	0	0	0	0	0	0	0	0	0
10*		0	C	0	0	0	C	C	0	C	0	0	0	0	0	0
9*		C	C	C	0	0	C	C	C	0	0	0	0	0	0	0
8*		0	0	0	0	0	0	0	0	0	0	0	0	0	0	0
7*		0	0	0	0	0	C	C	C	C	0	0	0	0	0	0
6*		C	C	C	0	0	C	C	C	0	0	0	0	0	0	0
5*		C	C	C	0	0	0	0	0	0	0	0	0	0	0	0
4*		0	0	0	0	0	0	0	0	C	0	0	0	0	0	0
3*		C	0	0	0	0	C	C	C	C	0	0	0	0	0	0
2*																

0.0

FFTF VENUS , EQUATION OF STATE EQ. TO 7																	
DENSITY OF ZONES AT TIME =0.0										MAXIMUM VALUE OF RHO =							
2	3	4	5	6	7	8	9	10		11	12	13	14	15	16	17	0.54978000D 01
**	**	**	**	**	**	**	**	**	**	**	**	**	**	**	**	**	**
30*	403	403	403	403	403	403	403	403	403	403	403	515	515	515	515	515	
29*	403	403	403	403	403	403	403	403	403	403	403	515	515	515	515	515	
28*	403	403	403	403	403	403	403	403	403	403	403	515	515	515	515	515	
27*	403	403	403	403	403	403	403	403	403	403	403	515	515	515	515	515	
26*	403	403	403	403	403	403	403	403	403	403	403	515	515	515	515	515	
25*	549	549	549	549	549	549	549	549	549	549	549	515	515	515	515	515	
24*	549	549	549	549	549	549	549	549	549	549	549	515	515	515	515	515	
23*	549	549	549	549	549	549	549	549	549	549	549	515	515	515	515	515	
22*	549	549	549	549	549	549	549	549	549	549	549	515	515	515	515	515	
21*	549	549	549	549	549	549	549	549	549	549	549	515	515	515	515	515	
20*	549	549	549	549	549	549	549	549	549	549	549	515	515	515	515	515	
19*	549	549	549	549	549	549	549	549	549	549	549	515	515	515	515	515	
18*	549	549	549	549	549	549	549	549	549	549	549	515	515	515	515	515	
17*	549	549	549	549	549	549	549	549	549	549	549	515	515	515	515	515	
16*	549	549	549	549	549	549	549	549	549	549	549	515	515	515	515	515	
15*	549	549	549	549	549	549	549	549	549	549	549	515	515	515	515	515	
14*	549	549	549	549	549	549	549	549	549	549	549	515	515	515	515	515	
13*	549	549	549	549	549	549	549	549	549	549	549	515	515	515	515	515	
12*	549	549	549	549	549	549	549	549	549	549	549	515	515	515	515	515	
11*	549	549	549	549	549	549	549	549	549	549	549	515	515	515	515	515	
10*	549	549	549	549	549	549	549	549	549	549	549	515	515	515	515	515	
9*	549	549	549	549	549	549	549	549	549	549	549	515	515	515	515	515	
8*	549	549	549	549	549	549	549	549	549	549	549	515	515	515	515	515	
7*	403	403	403	403	403	403	403	403	403	403	403	515	515	515	515	515	
6*	403	403	403	403	403	403	403	403	403	403	403	515	515	515	515	515	
5*	403	403	403	403	403	403	403	403	403	403	403	515	515	515	515	515	
4*	403	403	403	403	403	403	403	403	403	403	403	515	515	515	515	515	
3*	403	403	403	403	403	403	403	403	403	403	403	515	515	515	515	515	
2*	403	403	403	403	403	403	403	403	403	403	403	515	515	515	515	515	

AT CYCLE 1 TIME =0.000002 DELT =C.000002 DISTRT = 1.97 WMAX =0.00000 AT ZONE 2 16
 POWER = 0.154D 13 ENERGY = 0.306C 07 XK = 1.0035705 XKDOPL = -0.0000011 XKDISP = -0.0000000

ECUBLE DELTA T WMAX =C.000000 DELT NOW =C.000004
 AT CYCLE 2 TIME =C.000006 DELT =0.000004 DISTRT = 1.97 WMAX =0.00000 AT ZONE 2 16
 POWER = 0.162D 13 ENERGY = 0.937D 07 XK = 1.0035695 XKDOPL = -0.0000033 XKDISP = -0.0000000

AT CYCLE 3 TIME =0.000010 DELT =0.000004 DISTRT = 1.97 WMAX =0.00000 AT ZONE 2 16
 POWER = 0.168D 13 ENERGY = 0.160D 08 XK = 1.0035684 XKDOPL = -0.0000056 XKDISP = -0.0000000

AT CYCLE 4 TIME =0.000014 DELT =0.000004 DISTRT = 1.97 WMAX =0.00000 AT ZONE 2 16
 POWER = 0.174D 13 ENERGY = 0.228D 08 XK = 1.0035672 XKDOPL = -0.0000080 XKDISP = -0.0000000

AT CYCLE 5 TIME =C.000018 DELT =0.000004 DISTRT = 1.97 WMAX =0.00000 AT ZONE 2 16
 POWER = 0.181D 13 ENERGY = 0.299D 08 XK = 1.0035660 XKDOPL = -0.0000105 XKDISP = -0.0000000

AT CYCLE 6 TIME =0.000022 DELT =0.000004 DISTRT = 1.97 WMAX =0.00000 AT ZONE 2 16
 POWER = 0.187D 13 ENERGY = 0.372D 08 XK = 1.0035647 XKDOPL = -0.0000130 XKDISP = -0.0000000

DCUBLE DELTA T WMAX =0.000000 DELT NOW =0.000005
 AT CYCLE 7 TIME =C.000027 DELT =C.000005 DISTRT = 1.97 WMAX =0.00000 AT ZONE 2 16
 POWER = 0.195D 13 ENERGY = 0.468D 08 XK = 1.0035629 XKDOPL = -0.0000162 XKDISP = -0.0000000

AT CYCLE 8 TIME =C.000032 DELT =C.C00005 DISTRT = 1.97 WMAX =0.00000 AT ZONE 2 16
 POWER = 0.203D 13 ENERGY = 0.567D 08 XK = 1.0035610 XKDOPL = -0.0000196 XKDISP = -0.0000000

AT CYCLE 9 TIME =C.000037 DELT =C.C00005 DISTRT = 1.97 WMAX =0.00000 AT ZONE 2 16
 POWER = 0.211D 13 ENERGY = 0.671D 08 XK = 1.0035591 XKDOPL = -0.0000230 XKDISP = -0.0000000

AT CYCLE 10 TIME =0.000042 DELT =C.C00005 DISTRT = 1.97 WMAX =0.00000 AT ZONE 2 16
 POWER = 0.219D 13 ENERGY = 0.779D 08 XK = 1.0035571 XKDOPL = -0.0000265 XKDISP = -0.0000000

AT CYCLE 11 TIME =C.000047 DELT =C.C00005 DISTRT = 1.97 WMAX =0.00000 AT ZONE 2 16
 POWER = 0.228D 13 ENERGY = 0.890D 08 XK = 1.0035549 XKDOPL = -0.0000302 XKDISP = -0.0000000

DCUBLE DELTA T WMAX =C.000000 DELT NOW =0.000005
 AT CYCLE 12 TIME =0.000052 DELT =0.000005 DISTRT = 1.97 WMAX =0.00000 AT ZONE 2 16
 POWER = 0.236D 13 ENERGY = 0.101C 09 XK = 1.0035525 XKDOPL = -0.0000341 XKDISP = -0.0000000

AT CYCLE 13 TIME =0.000057 DELT =0.000005 DISTRT = 1.97 WMAX =0.00000 AT ZONE 2 16
 POWER = 0.244D 13 ENERGY = 0.113C 09 XK = 1.0035501 XKDOPL = -0.0000380 XKDISP = -0.0000000

AT CYCLE 14 TIME =0.000062 DELT =C.C00005 DISTRT = 1.97 WMAX =0.00000 AT ZONE 2 16
 POWER = 0.253D 13 ENERGY = 0.125C 09 XK = 1.0035475 XKDOPL = -0.0000421 XKDISP = -0.0000000

AT CYCLE 15 TIME =0.000067 DELT =C.C00005 DISTRT = 1.97 WMAX =0.00000 AT ZONE 2 16
 POWER = 0.261D 13 ENERGY = 0.138C 09 XK = 1.0035448 XKDOPL = -0.0000463 XKDISP = -0.0000000

AT CYCLE 16 TIME =0.000072 DELT =C.C00005 DISTRT = 1.97 WMAX =0.00001 AT ZONE 2 16
 POWER = 0.270D 13 ENERGY = 0.151C 09 XK = 1.0035421 XKDOPL = -0.0000506 XKDISP = -0.0000000

ECUBLE DELTA T WMAX =C.000001 DELT NOW =0.000005
 AT CYCLE 17 TIME =0.000077 DELT =0.000005 DISTRT = 1.97 WMAX =0.00001 AT ZONE 2 16
 POWER = 0.278D 13 ENERGY = 0.165D 09 XK = 1.0035393 XKDOPL = -0.0000549 XKDISP = -0.0000000

AT CYCLE 18 TIME =0.000082 DELT =0.000005 DISTRT = 1.97 WMAX =0.00001 AT ZONE 2 16
 POWER = 0.287D 13 ENERGY = 0.179D 09 XK = 1.0035364 XKDOPL = -0.0000593 XKDISP = -0.0000000

FFTF VENUS , EQUATION OF STATE EC. TC 7		RACIAL DISPLACEMENT OF MESH POINTS AT TIME =0.000587																	MAXIMUM VALUE OF DELR =			0.698385470
	2	3	4	5	6	7	8	9	10	11	12	13	14	15	16	17	18					
	**	**	**	**	**	**	**	**	**	**	**	**	**	**	**	**	**					
30*	0	0	0	0	0	0	0	0	0	0	0	0	0	0	0	0	0					
29*	0	0	0	0	0	0	0	0	0	0	0	0	0	0	0	0	0					
28*	C	0	C	C	0	0	0	0	0	0	0	0	0	0	0	0	0					
27*	C	C	0	0	0	0	C	C	C	0	C	C	C	0	0	0	0					
26*	0	0	0	0	0	0	0	0	0	0	0	0	0	0	0	0	0					
25*	0	41	47	30	5	0	0	0	0	0	0	0	0	0	0	0	0					
24*	0	78	114	124	81	42	5	1	0	0	0	0	0	C	0	0	0					
23*	0	91	142	205	199	134	80	25	43	14	0	0	0	0	0	0	0					
22*	0	116	170	253	255	225	161	77	149	133	3	0	0	0	0	0	0					
21*	0	136	224	319	286	281	220	157	271	323	45	0	0	0	0	0	0					
20*	0	137	252	368	332	304	277	277	403	455	179	2	0	0	0	0	0					
19*	0	153	282	386	352	365	325	351	542	512	349	10	0	0	0	0	0					
18*	0	196	303	381	369	417	394	398	629	581	439	35	0	0	0	0	0					
17*	0	256	304	370	389	448	420	447	643	672	454	66	0	0	0	0	0					
16*	0	274	304	370	391	462	426	460	647	698	456	77	C	0	0	0	0					
15*	0	239	303	372	388	441	427	435	651	647	456	56	0	0	0	0	0					
14*	0	175	296	381	367	421	390	406	615	557	414	23	0	0	0	0	0					
13*	0	143	269	382	355	366	344	367	503	500	277	5	0	0	0	0	0					
12*	C	125	246	347	340	321	296	278	366	417	105	1	0	0	0	0	0					
11*	0	126	214	300	290	304	226	173	248	241	15	0	0	0	0	0	0					
10*	0	105	166	240	259	225	174	80	114	70	1	0	0	0	0	0	0					
9*	0	86	145	196	188	114	75	18	18	2	0	C	0	0	0	0	0					
8*	C	105	59	112	63	23	1	0	0	0	0	0	0	0	0	0	0					
7*	C	56	37	11	1	C	C	C	0	0	0	0	C	C	0	0	0					
6*	0	0	0	0	0	0	0	0	0	0	0	0	0	0	0	0	0					
5*	0	0	0	0	0	C	C	0	0	0	0	0	0	0	0	0	0					
4*	0	0	C	0	0	0	0	0	0	0	0	0	0	0	0	0	0					
3*	C	0	C	0	0	0	C	0	0	0	0	0	0	0	0	0	0					
2*	0	0	0	0	0	0	0	0	0	0	C	0	0	0	0	0	0					

[illegible]

FFTF VENUS , EQUATION OF STATE EC. TC 7																	
AXIAL VELOCITY OF MESH POINTS AT TIME =0.000587																	
	2	3	4	5	6	7	8	9	10	11	12	13	14	15	16	17	18
	**	**	**	**	**	**	**	**	**	**	**	**	**	**	**	**	**
30*	0	0	C	C	0	0	C	C	0	0	0	0	0	0	0	0	0
29*	0	0	0	0	0	0	C	C	0	C	0	0	0	0	0	0	0
28*	0	0	C	0	0	0	0	0	0	0	0	0	0	0	0	0	0
27*	0	C	C	0	0	0	C	C	0	0	0	0	0	0	0	0	0
26*	0	0	0	0	0	0	0	C	0	C	0	C	0	0	0	0	0
25*	76	69	46	19	4	0	0	0	0	0	0	0	0	0	0	0	0
24*	1	9	41	73	69	34	8	2	0	0	0	0	C	0	0	0	0
23*	32	25	15	17	41	81	93	67	34	9	0	0	0	0	0	0	0
22*	48	54	56	41	28	24	27	31	30	15	0	0	0	0	0	0	0
21*	29	29	35	45	45	39	35	26	17	28	20	0	C	0	0	0	0
20*	49	48	36	31	40	33	22	28	28	20	11	0	0	0	0	0	0
19*	43	37	33	36	30	22	18	16	27	21	11	7	0	0	0	0	0
18*	25	20	22	27	25	23	21	15	18	13	13	15	0	0	0	0	0
17*	10	7	11	13	11	13	12	10	10	7	5	5	C	0	0	0	0
16*	0	0	0	0	0	-1	-1	0	-1	-1	-1	-1	0	0	0	0	0
15*	-11	-7	-11	-14	-12	-14	-15	-12	-14	-10	-10	-11	0	0	0	0	0
14*	-27	-21	-21	-28	-27	-25	-24	-15	-25	-16	-12	-13	0	0	0	0	0
13*	-46	-42	-36	-37	-35	-26	-14	-8	-16	-14	-9	-3	0	0	0	0	0
12*	-41	-40	-34	-33	-39	-34	-33	-41	-32	-31	-21	0	0	0	0	0	0
11*	-30	-31	-39	-47	-45	-38	-26	-12	-12	-18	-8	0	0	0	0	0	0
10*	-66	-66	-55	-34	-26	-15	-31	-58	-48	-20	0	0	0	0	0	0	0
9*	-4	-3	-7	-21	-51	-97	-91	-44	-16	-2	0	C	0	0	0	0	0
8*	89	34	-50	-80	-58	-20	-2	C	0	0	0	0	0	0	0	0	0
7*-152-109	-41	-9	-1	0	0	0	0	0	0	0	0	0	0	0	0	0	0
6*	C	0	C	0	0	C	C	C	0	0	0	C	0	0	0	0	0
5*	0	0	0	0	0	0	0	0	0	0	0	0	0	0	0	0	0
4*	C	C	C	0	0	0	0	0	0	0	0	0	0	0	0	0	0
3*	0	0	0	0	0	0	0	C	0	0	0	0	C	0	0	0	0
2*	0	0	0	0	0	0	C	C	C	0	0	0	0	0	0	0	0

FFTF VENUS , EQUATION OF STATE EC. TO 7																	
TOTAL PRESSURE OF ZONES AT TIME = 0.000587																	
	2	3	4	5	6	7	8	9	10	11	12	13	14	15	16	17	0.169621550 11
	**	**	**	**	**	**	**	**	**	**	**	**	**	**	**	**	**
30*																	
29*	0	0	0	0	0	0	0	0	0	0	0	0	0	0	0	0	0
28*	C	C	0	0	C	C	C	C	C	C	0	0	0	0	0	0	0
27*	C	C	C	C	C	C	C	C	C	0	0	0	C	0	0	0	0
26*	0	C	0	0	0	0	C	C	C	0	C	C	0	0	0	0	0
25*	1	C	C	C	0	0	0	0	0	0	0	0	0	0	0	0	0
24*	34	60	64	27	2	0	C	0	0	0	C	0	0	0	0	0	0
23*	0	0	13	33	91	38	14	4	0	0	0	0	0	0	0	0	0
22*	47	27	11	14	26	30	45	35	21	0	C	0	0	0	0	0	0
21*	18	32	35	24	24	29	24	5	4	4	0	0	0	0	0	0	0
20*	23	24	23	39	37	15	15	30	27	34	0	0	0	0	0	0	0
19*	29	28	27	38	36	27	14	15	22	7	6	0	0	0	0	0	0
18*	28	28	31	36	27	26	15	14	35	0	36	0	0	0	0	0	0
17*	21	36	35	34	26	24	17	14	32	4	72	0	0	0	0	0	0
16*	15	41	43	34	28	28	18	18	27	12	44	C	0	0	0	0	0
15*	17	40	43	35	28	27	15	17	28	9	48	C	0	0	0	0	0
14*	24	35	38	35	26	23	16	12	32	0	70	0	0	0	0	0	0
13*	31	28	29	35	27	26	17	18	34	4	21	0	0	0	0	0	0
12*	28	27	26	37	35	24	18	24	23	21	1	0	0	0	0	0	0
11*	26	24	26	35	35	22	15	16	15	33	0	0	0	0	0	0	0
10*	20	33	34	20	21	24	22	17	16	0	0	0	0	0	0	0	0
9*	30	24	12	12	29	36	159	37	15	0	0	0	0	0	0	0	0
8*	0	0	14	45	106	18	4	0	0	0	0	0	0	0	0	0	0
7*	30	165	46	14	1	C	C	C	C	0	C	0	0	0	0	0	0
6*	C	1	C	0	0	0	C	0	0	0	0	0	0	0	0	0	0
5*	0	0	0	0	0	0	0	0	0	0	0	0	0	0	0	0	0
4*	0	C	C	0	0	C	C	C	C	0	0	0	0	0	0	0	0
3*	C	C	C	C	C	C	C	C	C	0	0	0	0	0	0	0	0
2*	0	0	0	0	0	0	C	C	C	0	0	0	0	0	0	0	0

FFTF VENUS , EQUATION OF STATE EQ. TO 7

DENSITY OF ZONES AT TIME = 0.000587

MAXIMUM VALUE OF RHO =

0.58961795D 01

	2	3	4	5	6	7	8	9	10	11	12	13	14	15	16	17
	**	**	**	**	**	**	**	**	**	**	**	**	**	**	**	**
30*	403	403	403	403	403	403	403	403	403	403	403	403	515	515	515	515
29*	403	403	403	403	403	403	403	403	403	403	403	403	515	515	515	515
28*	403	403	403	403	403	403	403	403	403	403	403	403	515	515	515	515
27*	403	403	403	403	403	403	403	403	403	403	403	403	515	515	515	515
26*	406	406	406	406	403	403	403	403	403	403	403	403	515	515	515	515
25*	574	582	585	579	564	555	550	549	549	549	549	515	515	515	515	515
24*	527	545	556	575	587	585	574	561	556	551	549	515	515	515	515	515
23*	556	557	548	554	563	572	581	571	569	562	550	515	515	515	515	515
22*	525	537	541	553	556	564	564	542	551	576	554	515	515	515	515	515
21*	519	521	523	542	543	548	552	539	546	584	564	515	515	515	515	515
20*	510	513	515	533	535	536	531	519	536	565	576	515	515	515	515	515
19*	499	503	508	524	521	531	530	514	541	556	587	517	515	515	515	515
18*	484	503	508	517	515	525	525	509	533	556	587	517	515	515	515	515
17*	474	503	507	514	513	526	523	510	526	560	584	517	515	515	515	515
16*	477	504	508	515	514	525	524	509	528	558	585	517	515	515	515	515
15*	489	504	508	518	516	525	525	508	534	555	588	517	515	515	515	515
14*	504	505	509	524	522	532	530	518	541	560	583	516	515	515	515	515
13*	512	515	517	533	535	536	535	527	538	575	570	515	515	515	515	515
12*	523	523	527	540	543	554	556	544	552	586	559	515	515	515	515	515
11*	528	539	542	551	555	563	564	551	559	569	551	515	515	515	515	515
10*	555	556	549	554	567	577	589	575	567	557	549	515	515	515	515	515
9*	534	546	555	581	589	577	565	554	552	550	549	515	515	515	515	515
8*	569	587	584	573	559	552	550	549	545	545	549	515	515	515	515	515
7*	404	406	405	403	403	403	403	403	403	403	403	515	515	515	515	515
6*	403	403	403	403	403	403	403	403	403	403	403	515	515	515	515	515
5*	403	403	403	403	403	403	403	403	403	403	403	515	515	515	515	515
4*	403	403	403	403	403	403	403	403	403	403	403	515	515	515	515	515
3*	403	403	403	403	403	403	403	403	403	403	403	515	515	515	515	515
2*	403	403	403	403	403	403	403	403	403	403	403	515	515	515	515	515

AT CYCLE 121	TIME = 0.000589	DELT = 0.000003	DISTR = 1.98	WMAX = 0.05916	AT ZONE 2	7	
PCWER =	0.4340 13	ENERGY = 0.3450	10 XK = 0.9981420	XKDOPL = -0.0008911			XKDISP = -0.0047153
AT CYCLE 122	TIME = 0.000592	DELT = 0.000003	DISTR = 1.98	WMAX = 0.05874	AT ZONE 2	7	
PCWER =	0.4220 13	ENERGY = 0.3460	10 XK = 0.9980275	XKDOPL = -0.0008938			XKDISP = -0.0048279
AT CYCLE 123	TIME = 0.000594	DELT = 0.000003	DISTR = 1.98	WMAX = 0.05805	AT ZONE 2	7	
PCWER =	0.4100 13	ENERGY = 0.3470	10 XK = 0.9979116	XKDOPL = -0.0008965			XKDISP = -0.0049419
AT CYCLE 124	TIME = 0.000597	DELT = 0.000003	DISTR = 1.98	WMAX = 0.05726	AT ZONE 2	7	
PCWER =	0.3990 13	ENERGY = 0.3480	10 XK = 0.9977945	XKDOPL = -0.0008990			XKDISP = -0.0050572
AT CYCLE 125	TIME = 0.000599	DELT = 0.000003	DISTR = 1.98	WMAX = 0.05653	AT ZONE 2	7	
PCWER =	0.3870 13	ENERGY = 0.3490	10 XK = 0.9976761	XKDOPL = -0.0009015			XKDISP = -0.0051739
AT CYCLE 126	TIME = 0.000602	DELT = 0.000003	DISTR = 1.98	WMAX = 0.07138	AT ZONE 7	23	
PCWER =	0.3760 13	ENERGY = 0.3500	10 XK = 0.9975564	XKDOPL = -0.0009039			XKDISP = -0.0052919
AT CYCLE 127	TIME = 0.000604	DELT = 0.000003	DISTR = 1.98	WMAX = 0.11237	AT ZONE 7	23	
PCWER =	0.3640 13	ENERGY = 0.3510	10 XK = 0.9974365	XKDOPL = -0.0009047			XKDISP = -0.0054118
HALVE DELTA T WMAX = 0.11237 DELT NGW = 0.000001							
AT CYCLE 128	TIME = 0.000606	DELT = 0.000001	DISTR = 1.98	WMAX = 0.05571	AT ZONE 7	23	
PCWER =	0.3590 13	ENERGY = 0.3510	10 XK = 0.9973753	XKDOPL = -0.0009060			XKDISP = -0.0054721
AT CYCLE 129	TIME = 0.000607	DELT = 0.000001	DISTR = 1.98	WMAX = 0.05499	AT ZONE 7	23	
PCWER =	0.3530 13	ENERGY = 0.3520	10 XK = 0.9973135	XKDOPL = -0.0009076			XKDISP = -0.0055326
AT CYCLE 130	TIME = 0.000608	DELT = 0.000001	DISTR = 1.98	WMAX = 0.05423	AT ZONE 7	23	
PCWER =	0.3480 13	ENERGY = 0.3520	10 XK = 0.9972520	XKDOPL = -0.0009085			XKDISP = -0.0055936
AT CYCLE 131	TIME = 0.000609	DELT = 0.000001	DISTR = 1.98	WMAX = 0.05322	AT ZONE 7	23	
PCWER =	0.3420 13	ENERGY = 0.3520	10 XK = 0.9971900	XKDOPL = -0.0009096			XKDISP = -0.0056548
AT CYCLE 132	TIME = 0.000611	DELT = 0.000001	DISTR = 1.98	WMAX = 0.05261	AT ZONE 7	23	
PCWER =	0.3370 13	ENERGY = 0.3530	10 XK = 0.9971277	XKDOPL = -0.0009107			XKDISP = -0.0057164
AT CYCLE 133	TIME = 0.000612	DELT = 0.000001	DISTR = 1.98	WMAX = 0.05201	AT ZONE 7	23	
PCWER =	0.3310 13	ENERGY = 0.3530	10 XK = 0.9970651	XKDOPL = -0.0009117			XKDISP = -0.0057784
AT CYCLE 134	TIME = 0.000613	DELT = 0.000001	DISTR = 1.98	WMAX = 0.05140	AT ZONE 7	23	
PCWER =	0.3260 13	ENERGY = 0.3540	10 XK = 0.9970022	XKDOPL = -0.0009128			XKDISP = -0.0058406
AT CYCLE 135	TIME = 0.000614	DELT = 0.000001	DISTR = 1.98	WMAX = 0.05079	AT ZONE 7	23	
PCWER =	0.3210 13	ENERGY = 0.3540	10 XK = 0.9969390	XKDOPL = -0.0009138			XKDISP = -0.0059032

STOP KEFF LESS THAN KEFF LIMIT

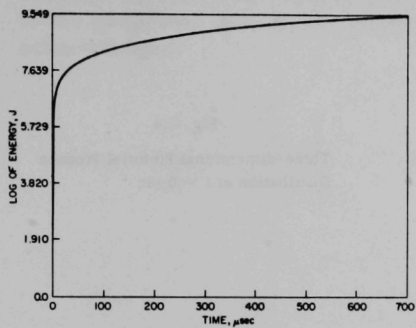


Fig. C.1. Energy Release vs Time

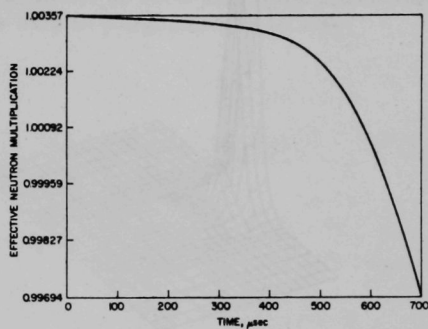


Fig. C.2. Effective Neutron Multiplication vs Time

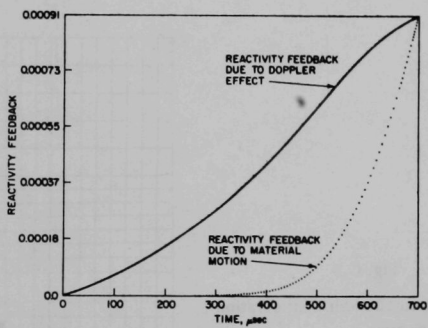


Fig. C.3. Reactivity Feedbacks due to Doppler and Material Motion vs Time

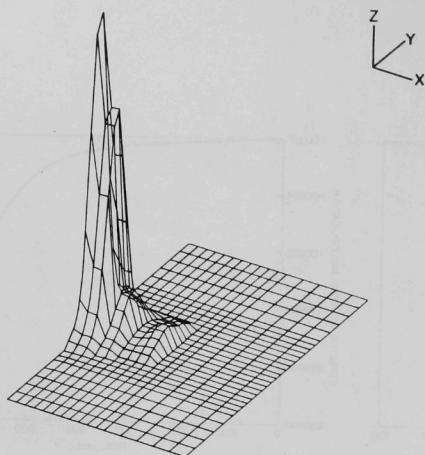


Fig. C.4

Three-dimensional Pictorial Pressure
Distribution at $t = 0$ sec

ALPHA = 0° , $X_{\min} = 0$, $X_{\max} = 110$,
BETA = 30° , $Y_{\min} = 0$, $Y_{\max} = 190$,
GAMMA = 60° , $Z_{\min} = 0$, $Z_{\max} = 6 \times 10^5$.

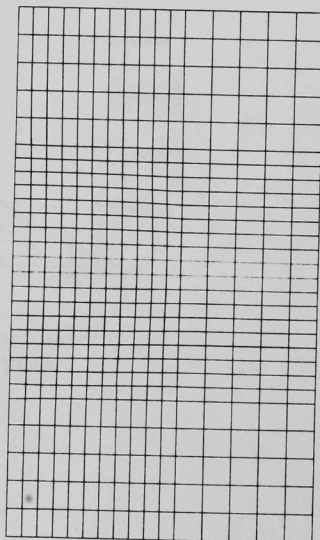


Fig. C.5

Distant-deformed Mesh Configuration
at $t = 0.608$ msec

ACKNOWLEDGMENTS

We are grateful to Drs. R. B. Nicholson and J. F. Jackson for many valuable discussions regarding the equations of state and some refinements to the program. Mr. P. M. Margel's help in programming is also acknowledged.

REFERENCES

1. H. A. Bethe and J. H. Tait, *An Estimate of the Order of Magnitude of the Explosion When the Core of a Fast Reactor Collapses*, UKAEA-RHM (56)/113 (1956).
2. D. Okrent, J. M. Cook, D. Satkus, R. B. Lazarus, and M. B. Wells, *AX-1, A Computing Program for Coupled Neutronics-Hydrodynamics Calculations on the IBM-704*, ANL-5977 (May 1959).
3. R. B. Nicholson, *Methods for Determining the Energy Release in Hypothetical Reactor Meltdown Accidents*, APDA-150 (1962).
4. V. Z. Jankus, *A Theoretical Study of Destructive Nuclear Bursts in Fast Power Reactors*, ANL-6512 (Feb 1962).
5. N. Hirakawa, *MARS--A Two Dimensional Excursion Code*, APDA-198 (1967).
6. W. T. Sha and R. B. Nicholson, *Maximum Accident of Zoned Fast Reactors*, Trans. ANS 11, 696 (1968).
7. W. K. Ergen, *Self-limiting Power Excursions in Large Reactors*, Trans. ANS 8, 221 (1965).
8. G. L. Gyorey and C. A. Keck, *A Time-integrated Model for Reactor Excursion Calculations*, Trans. ANS 8, 498 (1965).
9. M. Becker, *The Principles and Applications of Variational Methods*, MIT Press (1964).
10. S. Kaplan, O. J. Marlowe, and J. Bewick, *Applications of Synthesis Techniques to Problems Involving Time Dependence*, Nucl. Sci. Eng. 18, 163 (1964).
11. R. Avery, *Proceedings of Sec. Int. Conf. on the Peaceful Uses of Atomic Energy*, Geneva, 1958, 12, 182 (1958).
12. A. F. Henry and N. J. Curlee, *Verification of a Method of Treating Neutron Space-Time Problems*, Nucl. Sci. Eng. 4, 727 (1958).
13. D. A. Meneley, G. K. Leaf, A. R. Lindeman, T. A. Daly, and W. T. Sha, *A Kinetics Model for Fast Reactor Analysis in Two Dimensions*, *The Symposium on Dynamics of Nuclear Systems*, sponsored by The University of Arizona, March 1970.
14. J. J. Kaganove, *Numerical Solution of the One-group Space-independent Reactor Kinetics Equations for Neutron Density Given the Excess Reactivity*, ANL-6132 (Feb 1960).
15. H. G. Kolsky, *A Method for the Numerical Solution of Transient Hydrodynamics Shock Problems in Two Space Dimensions*, LA-1867 (1955).
16. L. Amurud and R. S. Orr, *A Note on Inverted Centers of Pressure and Crossed Mass Points in a Two-dimensional Hydrodynamics Calculation*, LASL unpublished note (1963).
17. M. L. Wilkins and R. Giroux, *Calculation of Elastic Flow*, UCRL-7322 (1963).
18. H. G. Kolsky, *The Nearest Neighbor Hydrodynamic Calculation*, LASL-T5, unpublished note (1961).

19. R. S. Orr and F. Magee, LASL unpublished note (1961).
20. W. B. Goad, WAT--A Numerical Method for Two-dimensional Unsteady Fluid Flow, LAMS-2365 (1960).
21. W. Herrmann, Comparison of Finite Difference Expressions Used in Lagrangian Fluid Flow Calculations, MIT Technical Report WL-TR-64-104 (1964).
22. J. von Neumann and R. D. Richtmyer, J. Appl. Phys. 21, 232 (1950).
23. P. L. Brown and M. S. Hoyt, HAST1--A Numerical Calculation of Two-dimensional Lagrangian Hydrodynamics Utilizing the Concept of Space-dependent Time Steps, LA-3324 (1966).
24. J. F. Jackson, R. B. Nicholson, and W. T. Sha, "Numerical Stability Problems in the VENUS Disassembly Code," ANS National Topical Meeting On the New Developments in Reactor Mathematics and Applications (Mar 29-31, 1971).
25. O. A. Hough, K. M. Watson, and R. A. Ragatz, Chemical Process Principles, Vol. II, Thermodynamics, 2nd Ed. John Wiley & Sons, Inc., New York.
26. R. H. Brout, Equation of State and Heat Content of Uranium, APDA-118 (1957).
27. D. Miller, "A Critical-Review of the Properties of Materials at the High Temperatures and Pressures Significant for Fast Reactor Safety," Proceedings of the Conference on Safety, Fuels, and Core Design in Large Fast Power Reactors, October 11-14, 1965, ANL-7120, pp. 641-653.
28. E. J. Robbins, Limits for the Equation of State of Uranium Dioxide, TRG Report 1344, United Kingdom Atomic Energy Authority (1966).
29. D. C. Menzies, The Equation of State of Uranium Dioxide at High Temperatures and Pressures, TRG Report-1119, United Kingdom Atomic Energy Authority (1966).
30. R. A. Meyer et al., Fast Reactor Meltdown Accidents Using Bethe-Tait Analysis, GEAP-4809, General Electric Corporation (1967).
31. R. J. Ackermann et al., High Temperature Thermodynamic Properties of Uranium Dioxide, J. Chem. Phys. 25, 1089 (1956).
32. R. W. Ohse, High Temperature Vapor Pressure Studies of UO_2 by the Effusion Method, EUR-2166-E., European Atomic Energy Community (1964).
33. R. A. Harris, Preliminary Analysis of Postulated Maximum Accidents for the FFTF, Supplement 1--Additional Calculations for Sodium-in Conditions, BNWL-760, Supplement 1 (1969).
34. J. A. Christensen, Thermal Expansion and Change in Volume on Melting for Uranium Dioxide, HW-75148 (1962).
35. P. F. Wattlet and J. Graham, A Realistic Appraisal Containment Design Basis Accident, WARD-BDR-362-33 (1969).
36. G. F. Ball, R. B. Nicholson, and A. E. Flickman, Preliminary Hypothetical Accident Analysis for Fast Test Reactor Interim Reference Design Cores, APDA-194 (1966).
37. R. B. Nicholson and W. T. Sha, internal memorandum, Reactor Physics Division, ANL (1970).

38. Y. W. Chang, private communication (1970).
39. W. T. Sha and A. E. Waltar, *Fast Reactor Disassembly Calculation Utilizing a Temperature-density-dependent Equation of State*, Trans. ANS 12, 825 (1969).
40. A. E. Waltar, A. Padilla, Jr., and R. T. Shields, *MELT-II, A Two-dimensional Neutronics-Heat Transfer Computer Program for Fast Reactor Safety Analysis*, BNWL-1320 (to be published).
41. R. B. Nicholson and J. W. Stephesen, *Reactor Explosion Program*, ASTRA 417-3 (1960).
42. D. Basinger and J. Gvildys, *Three-dimensional Graphical Representation of Surface by Computer (Fast-reactor Containment Programs)*, ANL-7633 (to be published).
43. P. L. Browne, *REZONE--A Proposal for Accomplishing Rezoning in Two-Dimensional Lagrangian Hydrodynamics Problems*, LA-3455 (Sept 21, 1965).

ARGONNE NATIONAL LAB WEST



3 4444 00011454 6

